

## Magnetically Recoverable Nanocatalysts

Vivek Polshettiwar,<sup>\*,†</sup> Rafael Luque,<sup>‡</sup> Aziz Fihri,<sup>†</sup> Haibo Zhu,<sup>†</sup> Mohamed Bouhrara,<sup>†</sup> and Jean-Marie Basset<sup>\*,†</sup>

<sup>†</sup>KAUST Catalysis Center (KCC), King Abdullah University of Science and Technology (KAUST), Thuwal 23955, Saudi Arabia

<sup>‡</sup>Departamento de Química Orgánica, Universidad de Córdoba, Córdoba, Spain

### CONTENTS

1. Introduction	3036
1.1. Green and Sustainable Catalysis	3036
1.2. Homogeneous and Heterogeneous Catalysis	3037
1.3. Nanocatalysis and Magnetic Nanocatalysts	3037
1.4. Scope of This Review	3038
2. Synthesis of Magnetic Catalysts	3038
2.1. Carbonaceous Magnetic Materials	3038
2.2. Metal Oxide-Derived Magnetic Materials	3038
2.3. Polymer-Derived Magnetic Materials	3039
3. Characterization of Magnetic Catalysts	3039
4. Applications of Magnetic Nanocatalysts	3039
4.1. Hydrogenation Reactions	3039
4.1.1. Magnetically Recoverable Palladium (Pd)-Based Catalysts	3040
4.1.2. Magnetically Recoverable Platinum (Pt)-Based Catalysts	3042
4.1.3. Magnetically Recoverable Ruthenium (Ru)-Based Catalysts	3042
4.1.4. Magnetically Recoverable Rhodium (Rh)-Based Catalysts	3044
4.1.5. Magnetically Recoverable Gold (Au)-Based Catalysts	3044
4.2. Oxidation Reactions	3045
4.3. Carbon–Carbon Coupling Reactions	3047
4.3.1. Suzuki Reactions	3047
4.3.2. Heck Reactions	3052
4.3.3. Sonogashira Reactions	3053
4.3.4. Stille Reactions	3053
4.4. Magnetically Separable Organocatalysts	3054
4.5. Hydroformylation Reactions	3056
4.6. Olefin Metathesis	3057
4.7. Epoxidation Reactions	3059
4.8. Magnetically Recoverable Catalysts in Miscellaneous Reactions	3060
5. Focus on Environmental Applications	3064
5.1. Magnetic Photocatalysis	3065
5.2. Magnetic Biocatalysis	3065
5.2.1. Entrapment of Biocatalysts onto MSNPs	3066
5.2.2. Covalent Immobilization of Enzymes on MSNPs	3067

5.2.3. Binding of Macromolecules to Magnetic Nanoparticles	3069
5.3. Adsorption Using Magnetic Materials	3069
6. Conclusions and Perspectives	3070
Author Information	3070
Biographies	3070
Acknowledgment	3072
References	3072

### 1. INTRODUCTION

Catalysis is becoming a strategic field of science because it represents a new way to meet the challenges of energy and sustainability. These challenges are becoming the main concerns of the global vision of societal challenges and world economy. The societal pressure has been at the origin of the concept of green chemistry, which is becoming a leitmotiv in any important project dealing with this strategic domain of science. The concept of green chemistry, which makes catalysis science even more creative, has become an integral part of sustainability.

#### 1.1. Green and Sustainable Catalysis

Green chemistry, also called sustainable chemistry, is a philosophy of chemical research and engineering that encourages the design of products and processes that minimize the use and generation of hazardous substances. Green catalysis is a subchapter of green chemistry but probably the most important one. Greener and environmentally sound synthetic protocols and reaction conditions have played pivotal roles in recent years toward the goal of switching to increasingly efficient and benign processes that avoid the use of volatile organic solvents, toxic reagents, hazardous and/or harsh reaction conditions, as well as challenging and time-consuming wasteful separations.<sup>1–6</sup>

Among the various principles of green chemistry, the use of alternative energy sources (e.g., microwaves, solar), benign solvents (e.g., water, ionic liquids, supercritical CO<sub>2</sub>), and their combination,<sup>7,8</sup> as well as efficient and cleanly reusable catalytic materials,<sup>9–12</sup> contributed to the development of greener synthetic methods for a wide range of applications that are not only restricted to catalysis but that also include a variety of applications related to medicine, the environment, and nanoscience. In this sense, the search for environmentally benign, sustainable,

**Received:** July 21, 2010

**Published:** March 14, 2011

and efficiently reusable alternative catalytic systems has become critical.

## 1.2. Homogeneous and Heterogeneous Catalysis

Catalysis can be broadly divided into two branches, homogeneous and heterogeneous. In a homogeneous catalytic system, the active catalytic sites and the reactants are in the same phase; this system allows for easier interaction between the components, which in turn results in better activity. Homogeneous catalysts have several other advantages: high selectivities, high turn over numbers (TON), and effortless optimization of catalytic activity, for example, by simply tuning ligand and metals in the case of metal complex-catalyzed reactions. It is also possible to tune the chemo-, regio-, and enantioselectivity of the catalyst by modifying the active catalytic molecules.

Although these catalysts are widely used in a variety of industries, it is often difficult to isolate and separate the final product after the reaction has completed, making the overall process cumbersome. Even when it is possible to separate the catalyst from the reaction mixture, trace amounts of catalyst are likely to remain in the final product (at ppm or even the ppb level). It is essential to remove the catalyst because metal contamination is highly regulated, especially in the drug and pharmaceutical industry.

One efficient way to overcome the problem of isolation and separation with a homogeneous catalyst is the heterogenization of active catalytic molecules, thus creating a heterogeneous catalytic system.<sup>9–12</sup> Heterogenization is commonly achieved by entrapment or grafting of the active molecules on surfaces or inside the pores of a solid support, such as silica, alumina, or ceria. Although grafting can be achieved by covalent binding or by simple adsorption of the active catalytic molecules, covalent binding is preferred because it is generally sufficiently robust to survive the harsh reaction conditions; this binding and adsorption process minimizes catalyst leaching and allows the catalyst to be reused several times. However, the active sites in heterogeneous catalysts are not as accessible as in a homogeneous system, and thus the activity of the catalyst is usually reduced. Although attempts have been made to make all active sites on solid supports accessible to reactions, so as to achieve the same activity as the homogeneous counterpart, in most cases, only sites on the external surface of a porous solid support are available for reaction, and thus the overall reactivity of the catalyst system is decreased.

Consequently, we need a catalyst system that not only shows high activity and selectivity (like a homogeneous system) but also possesses the ease of catalyst separation and recovery (like a heterogeneous system). These goals can be achieved by nanocatalysis. Nanocatalysts bridge the gap between homogeneous and heterogeneous catalysis, preserving the desirable attributes of both systems.

## 1.3. Nanocatalysis and Magnetic Nanocatalysts

One of the most stimulating features of nanotechnology is its potential use in almost any field. The discovery of nanoparticles (NPs) with varied size, shape, and composition has stretched the limits of technology in ways that scientists would never have dreamt of a century ago. Nature makes and chemistry reshapes; huge varieties of nanoparticles have emerged in our daily life, in every field from drugs and electronics to paints and beauty care, and they are now emerging in the field of catalysis. The “nano” in nanocatalysis refers to very small particles in the nano scale range

of size. Because nanoparticles have a large surface-to-volume ratio relative to bulk materials, they offer an attractive alternative to conventional catalysts.<sup>13,14</sup>

The field of nanocatalysis (which involves a substance or material with catalytic properties that possesses at least one nanoscale dimension, either externally or in terms of internal structures) is undergoing an explosive development. Nanocatalysis can help design catalysts with excellent activity, greater selectivity, and high stability. These characteristics can easily be achieved by tailoring the size, shape, morphology, composition, electronic structure, and thermal and chemical stability of the particular nanomaterial. To understand the potential of nanocatalysis, we must clarify three key points:

- (1) For any chemical reaction to take place, the reactive species and the catalyst site need to come into contact with each other. Because of the nano size of the particles, the exposed surface area of the active component of the nanocatalyst is high, and this considerably enhances the contact between reactants and catalyst; in turn, this feature enables a heterogeneous catalytic system to achieve reaction rates close to its homogeneous counterpart.
- (2) Another key point is the ratio of surface area to volume during nanocatalysis. As an object gets smaller, its surface area-to-volume ratio increases; therefore, because of the extremely small size of nanocatalysts, they have a tremendous surface area-to-volume ratio. This in turn increases the catalyst accessibility and activity.
- (3) When materials are produced at the nanoscale particle size, they attain novel properties not found in their macroscopic counterparts, and these properties contribute to the performance and competence of nanocatalysts.

Thus, nanocatalysts enjoy several advantages over conventional catalyst systems; however, isolation and recovery of these tiny nanocatalysts from the reaction mixture is not easy. Conventional techniques (such as filtration) are not efficient because of the nano size of the catalyst particles. This limitation hampers the economics and sustainability of these nanocatalytic protocols. To overcome this issue, the use of magnetic nanoparticles has emerged as a viable solution; their insoluble and paramagnetic nature enables easy and efficient separation of the catalysts from the reaction mixture with an external magnet. Also, exhaustive control of their properties, including size, shape, morphology, and dispersity that somehow mimic nature, makes it possible for scientists to carefully design the materials that are specifically needed for a particular application. Other exciting properties of these magnetic materials include their highly active and specific centers of ultrasmall size coupled with their high specificities; these features serve to encourage this relatively novel but vastly expanding field.

The isolation and separation of nanocatalysts can be achieved using magnetically separable nanoparticles (MSNPs). They offer a promising option that can meet the requirements of high accessibility with improved reusability.<sup>15–17</sup> One of the most attractive features of MSNPs is their separation properties. Catalyst recovery and reuse are the two most important features for many catalytic processes, and most heterogeneous systems require a filtration or centrifugation step and/or a tedious workup of the final reaction mixture to recover the catalyst. However, magnetically supported catalysts can be recovered with an external magnet due to the paramagnetic character of the support,

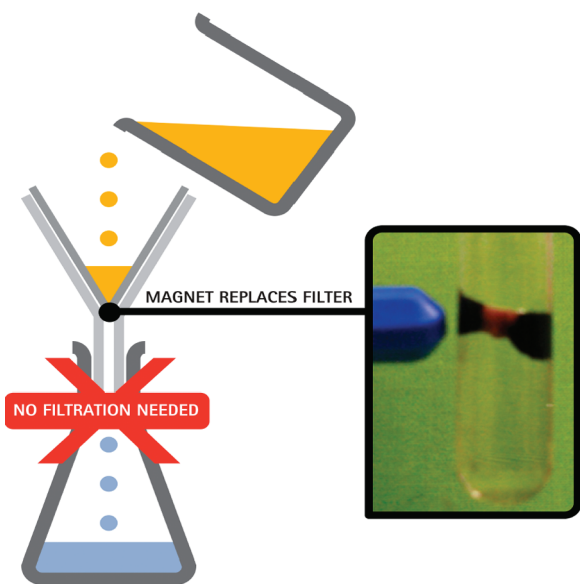


Figure 1. Catalyst separation by magnetic attraction.

resulting in remarkable catalyst recovery without the need for a filtration step (Figure 1); the catalysts can be subsequently reused in another cycle. Magnetically separable catalysts (MSC) also offer important activities in a wide range of reactions due to their potential for designed surface functionalities along with catalyst preparation.

#### 1.4. Scope of This Review

In this Review, we aim to present a broad overview on magnetically recoverable nanocatalysts. The main focus of this Review is on the use of magnetic nanomaterials as catalysts. We begin with an introductory discussion of the need of nanocatalysis, the nature of nanocatalysis, and the nature of magnetically recoverable nanocatalysis. Although a discussion of the synthesis and characterization of these magnetic nanomaterials is beyond the scope of this Review, we discuss these issues briefly to provide a basic outline to the reader. We then discuss the key focus of this Review, that is, an assortment of reactions and transformations using magnetic nanocatalysts. We start with hydrogenation reactions using various metal-based (Pd, Pt, Ru, Rh, Au) catalysts, followed by a discussion of oxidation reactions using magnetic nanocatalysts. Thereafter, we discuss the application of these catalysts for synthetically important carbon–carbon coupling reactions, such as Suzuki, Heck, Sonogashira, and Stille reactions. We then discuss the use of magnetic materials as organocatalysts and their application in other important reactions such as hydroformylation and olefin metathesis. Finally, we review the recently emerging area of using magnetic nanomaterials for environmental applications, in particular for photo- and biocatalysis. At the end of this Review, we summarize the advantages of magnetically recoverable nanocatalysts, discuss their impact on conventional catalysis, and offer perspectives for further development.

## 2. SYNTHESIS OF MAGNETIC CATALYSTS

There are several protocols reported in the literature for preparing a wide variety of catalytic magnetic materials, some of which are discussed below. It is important to note that the practicality and cost-effectiveness of these processes have a direct

effect on the sustainability of the catalytic protocols based on these materials.

### 2.1. Carbonaceous Magnetic Materials

Magnetic carbon nanoparticles were readily obtained from the carbonization of iron-doped polypyrrole nanoparticles.<sup>18,19</sup> Carbonization was performed at 800 °C and yielded microporous carbonaceous nanomaterials with approximately 4–5 wt % nitrogen. Palladium nanoparticles were subsequently deposited onto the surface of the microporous carbon using a conventional impregnation/deposition methodology and using  $\text{Pd}(\text{NO}_3)_2$  as a metal precursor in water. The synthesized material possesses a remarkably high palladium content (approximately 40 wt %) that is comprised of homogeneously and well-dispersed PdNP on the porous surface, with a reasonably narrow particle size distribution (around 4 nm). Related commercially available carbonaceous materials (e.g., Vulcan XC72R) and a carbon black, prepared by thermal decomposition of methane using dc thermal plasma processing, provided poorly dispersed Pd NP on the material surface (2–28 nm).<sup>18</sup>

Another example of this type of MSNP was recently reported by Zhu et al.<sup>19</sup> In that study, magnetic porous carbon microspheres were prepared via carbonization of chitosan (a cationic polymer) microspheres containing iron precursors (a negatively charged iron oxalate) that were absorbed due to the cationic and swelling properties of chitosan. In general, this biomass-derived material possessed large surface areas ( $>200 \text{ m}^2 \text{ g}^{-1}$ ) and good magnetic separation properties. Interestingly,  $^{57}\text{Fe}$  Mössbauer spectroscopic experiments indicated that the temperature of carbonization affected the type of Fe species observed in the sample. Thus, samples calcined at 700 °C contained  $\gamma\text{-Fe}_2\text{O}_3$ ,  $\text{Fe}_3\text{C}$ , and  $\alpha\text{-Fe}$ , whereas samples carbonized at 900 and 1000 °C exhibited peaks that indicated  $\text{Fe}_3\text{C}$  and  $\alpha\text{-Fe}$ . This phenomenon was claimed to result from the reaction of maghemite with carbon (to form  $\text{Fe}_3\text{C}$ ) and subsequent decomposition into metallic Fe. Because of these promising features and the potential adsorption properties of carbon, high temperature calcined materials (CSFe-1000) were tested for the adsorption of potential pollutants (e.g., phenol and nitrobenzene) in aqueous solutions.

A relatively similar magnetically ordered mesoporous carbon-containing super paramagnetic FePt NP (useful for the adsorption of pollutants<sup>20</sup>) was prepared via a simple nanocasting route, with polyfurfuryl alcohol (PFA, as the carbon source) formed after polymerization of furfural in the channels of a mesoporous silica employed as a hard template (KIT-6)<sup>21</sup> and FePt sources introduced in the framework of PFA through incipient wetness impregnation. Subsequent thermal treatment of the material in argon at 700 °C and extraction of the silica (by washing the solid with a 2 M solution of NaOH) rendered template-free mesoporous FePt/C materials with large surface areas ( $>1000 \text{ m}^2 \text{ g}^{-1}$ ) and important adsorption properties.

### 2.2. Metal Oxide-Derived Magnetic Materials

A range of novel materials based on titanium silicate mesoporous solids have been recently reported by Barmatova et al.<sup>22,23</sup> These materials were prepared following the so-called solid core–mesoporous shell morphology synthetic approach, originally developed by Yoon et al.<sup>24</sup> The novel materials were composed of quasi-spherical particles covered by a titanium silicate mesoporous shell containing isolated Ti atoms (denoted as Ti-SCMS) that could be elegantly modified by previously synthesized magnetic nanoparticles (MNPs). Up to

1.8 wt % Ti content was observed in the shell, with approximately 3 wt % Fe in the materials, mainly present as a blend of  $\text{Fe}_3\text{O}_4$  and maghemite ( $\gamma\text{-Fe}_2\text{O}_3$ ). According to physicochemical studies, these iron oxide NPs were stabilized within the particle core, and thus they did not interfere with the catalytic application of the materials, for example, the selective oxidation processes.

Another type of MSNP is magnetic  $\text{Fe}_2\text{O}_3/\text{SiO}_2/\text{TiO}_2$  composites. Wang et al. recently reported a facile chemical route to these interesting materials, which have photocatalytic applications. These hybrid nanoparticles have been reported to be spherical, 100 nm in diameter, and decorated with several  $\text{Fe}_2\text{O}_3$  particles (15 nm in diameter) as cores distributed within the titania matrix. The silica layers intercalated between magnetic cores and titania shells.<sup>25</sup>

Similarly, Xu et al. recently reported the preparation of a visible-light active  $\text{TiO}_2/\text{ZnFe}_2\text{O}_4$  photocatalyst via conventional liquid-phase transformation using the sol–gel method.<sup>26</sup> The formation of highly dispersed zinc ferrite nanoparticles (less than 5 nm in size, with imperfect crystallization) on the  $\text{TiO}_2$  material prevented the formation of the rutile phase to some extent. The advantage of this material was the coupling of the relatively narrow band gap for  $\text{ZnFe}_2\text{O}_4$  (light absorbing semiconductor) and the wide band gap of titania, which resulted in a semiconductor system with an enhanced primary charge separation and photocatalytic activity under visible light irradiation.

A magnetically recoverable material composed of palladium nanoparticles supported on hydroxyapatite-encapsulated maghemite nanocrystallites ( $\text{Pd-HAP-}\gamma\text{-Fe}_2\text{O}_3$ ) was also reported in the dehalogenation of organic compounds with molecular hydrogen.<sup>27</sup> Pd deposition on the magnetic support was achieved via simple impregnation with a solution of  $\text{PdCl}_2(\text{PhCN})_2$  in acetone. According to the authors, monomeric  $\text{PdCl}_2$  species were grafted by chemisorption onto the  $\text{P=O}$  groups of the support, which were subsequently reduced under  $\text{H}_2$  atmosphere to give Pd metallic MNP.<sup>28,29</sup> The materials were tested as catalysts in the dechlorination of 4-chlorophenol as a model compound, with quantitative yields to products obtained in 40 min for the optimum  $\text{Pd-HAP-}\gamma\text{-Fe}_2\text{O}_3$  catalyst.<sup>30</sup>

### 2.3. Polymer-Derived Magnetic Materials

Polymer-derived  $\text{Fe}_3\text{O}_4$ –polyaniline–Au magnetic nanocomposites have been prepared via a two-step process.<sup>31</sup> In the first step, a super paramagnetic  $\text{Fe}_3\text{O}_4$ –polyaniline (PANI) with a well-defined core–shell nanostructure was synthesized using an ultrasound-assisted in situ surface polymerization method. For this, aniline monomers were added to an aqueous solution of carboxylic acid-functionalized  $\text{Fe}_3\text{O}_4$  microspheres and partially reacted with the surface carboxylic groups to generate  $\text{COO}^-\text{H}_3\text{N}^+$  ion pairs, followed by aniline polymerization<sup>32</sup> on the particle's surface to form the monodispersed, well-defined  $\text{Fe}_3\text{O}_4$ –PANI core/shell structure.<sup>33</sup> Negatively charged discrete Au nanoparticles with particle sizes of approximately 4 nm were effectively loaded onto the positively charged magnetic support surface by electrostatic attraction. These materials were found to be catalytically active in the reduction of the dye Rhodamine B (RhB) using  $\text{NaBH}_4$  as a reducing agent.

## 3. CHARACTERIZATION OF MAGNETIC CATALYSTS

Magnetic materials have been characterized by electron microscopy (transmission electron microscopy (TEM) and scanning electron microscopy (SEM)) to determine the shape, size, and morphologies, X-ray diffraction (XRD) for elemental

composition, and gas adsorption technique for surface area of the materials. However, characterizing the functional groups grafted on the magnetic materials is often a challenging task due to the lack of data on the accessibility and chemical reactivity of the materials. Nuclear magnetic resonance (NMR) of these catalysts is difficult to record because the magnetic nature of the materials interferes with the magnetic field of the spectrometer. Fourier transform infrared spectroscopy (FT-IR) seems to be the best technique to characterize functionalized magnetic catalysts. To this end, Panella et al. developed a simple attenuated total reflection (ATR) infrared spectroscopy method in a specially designed in situ batch reactor-cell equipped with mechanical stirring to characterize the different groups (e.g., amino-propyl moieties) grafted onto the surface of a magnetically separable nanoparticle.<sup>34</sup> Using this novel approach, the authors determined that less than 40% of the grafted amino groups in a material composed of iron oxide nanoparticles embedded in a silica matrix was available for reaction (as observed in the transformation of the amine group to benzaldimine). This observation indicates that the theoretical loading of grafted groups exclusively provides an upper bound of active functional groups. Remarkable differences were observed between the estimated total amount of functional groups and the actual number of functional groups that were chemically available/accessible for the reaction. Advantages of the ATR methodology include the possibility to follow the formation of new bonds after/during the reaction and the great potential for further development using a range of more complex functional groups commonly employed in catalysis.<sup>35,36</sup>

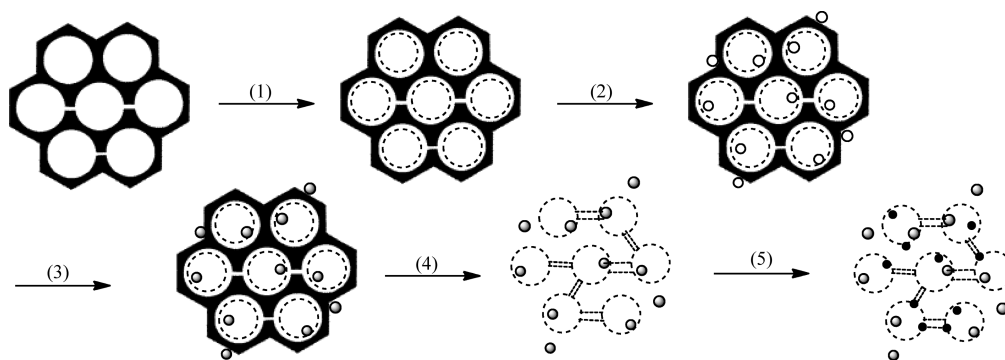
## 4. APPLICATIONS OF MAGNETIC NANOCATALYSTS

Catalysis is vitally important to the development of society, as it provides a sustainable way to convert raw materials into valuable chemicals and fuels in an economical, efficient, and environmentally benign manner.<sup>37–39</sup> Magnetically recoverable materials have been used in a wide range of catalytic reactions, including oxidations, hydrogenations, photocatalysis, and C–C bond formation, as well as in novel applications in asymmetric synthesis, hydration, Knoevenagel condensations, and  $\text{CO}_2$  cycloaddition reactions.<sup>15–17</sup> There has been an increasing trend toward the use of MSNPs in increasingly efficient green chemical synthesis. In addition to their facile separation, such materials also showed better selectivity, higher TOF, and enhanced stability as compared to their unsupported counterparts. In this section, we provide an overview of the applications of MSNPs in a wide range of catalytic processes and organic transformations.

### 4.1. Hydrogenation Reactions

Making bonds between hydrogen and other atoms is a primary method used to convert one functional group into another. Hydrogenation is a chemical reaction in which hydrogen atoms are added to other chemical bonds. These reactions are used in countless manufacturing processes and in basic research; they also occur in living systems. Important hydrogenation processes include the hydrogenation of carbon–carbon double or triple multiple bonds, the hydrogenation of carbonyls, and the hydrogenation of nitrogen-containing bonds. Homogeneous hydrogenation catalysts are generally more active than heterogeneous catalysts; however, the obstacle of recovery or reuse limits their use in industrial scale applications. Therefore, research has focused on heterogeneous catalysis systems for hydrogenation

Scheme 1. Nanocasting of the Magnetically Recoverable Pd/C Catalyst



reactions. Conventionally, heterogeneous hydrogenation catalysts have been based on Pt, Rh, Ru, and Pd materials and/or their nanoparticles (NPs) because of their excellent activities and selectivities. However, these metal nanoparticles (MNPs) must be protected by stabilizing agents to prevent aggregation to the thermodynamically favored bulk metal. In these scenarios, the immobilization of MNPs or homogeneous catalysts on magnetically separable solid supports tends to be a very appealing technique to furnish better handling properties and often possesses activities comparable to those of homogeneous and MNPs.

**4.1.1. Magnetically Recoverable Palladium (Pd)-Based Catalysts.** As the traditional and most-employed hydrogenation catalyst, much attention has been paid to homogeneous and heterogeneous Pd catalysts. Several materials, including pure  $\text{Fe}_2\text{O}_3$  nanospheres, silica-coated  $\text{Fe}_2\text{O}_3$  nanoparticles, and  $\text{Fe}_2\text{O}_3$  encapsulated in carbon, have been used as supports for Pd MNPs, thus forming magnetically recoverable Pd catalysts.

Palladium on carbon, often referred to as Pd/C, is a form of palladium that is commonly used for catalytic hydrogenation reactions in organic chemistry. Interestingly, this type of catalyst can be tailored to a magnetically separable catalyst using a simple nanocasting strategy.<sup>40</sup> Scheme 1 illustrates the nanocasting synthesis procedure, which includes the following steps: (1) synthesis of a carbon/SBA-15 composite using a mesostructured SBA-15 as the template, (2) selective loading of the cobalt nanoparticles on the outer surface of the composite particle, (3) coating of a nanometer-thick carbon layer on the cobalt particles for protection, (4) removal of the silica scaffold by an aqueous solution of hydrofluoric acid (HF) to create a porous system, and (5) deposition of a catalytically active noble metal on the now-accessible pore system by a conventional impregnation process. The as-synthesized catalyst prepared using this nanocasting protocol was active in the hydrogenation of octene, and this hydrogenation reaction was repeated by pipetting the reacted octane out (magnetic carbon had been separated from the solution by applying a magnetic field to the reactor) and refilling the reactor with fresh octene. The reaction rate of subsequent runs was almost identical to that of the initial run, indicating the stability and reusability of the catalyst.

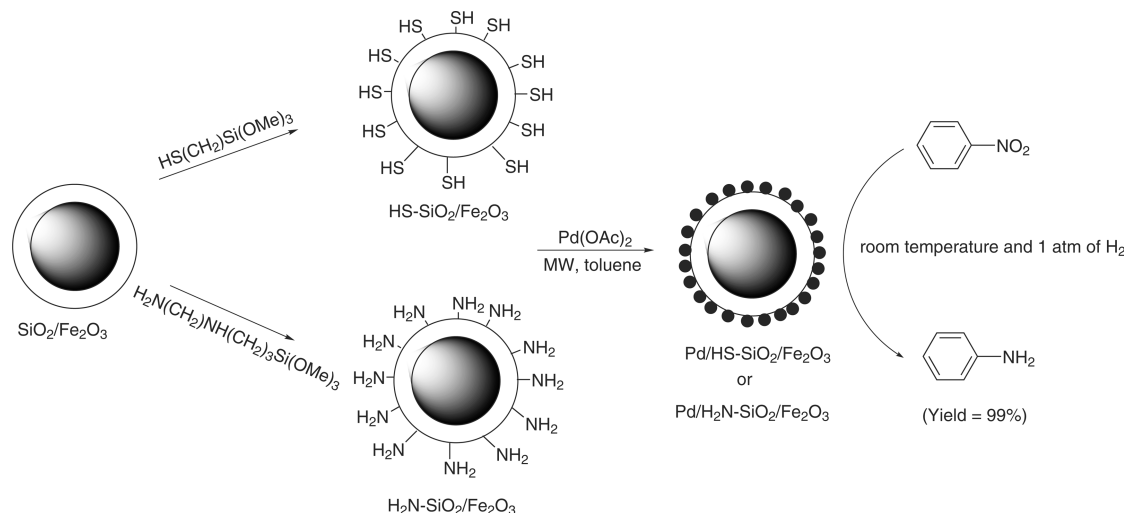
Moreover, it was possible to completely remove the catalyst after the reaction, and no leaching activity was observed in the reaction filtrate, as confirmed by the hot-filtration test. During the reaction (before its completion, to avoid complete consumption of the octene prior to the separation, fresh octene was also added), a magnetic field was applied to the bottom of the reactor

to immobilize the catalyst. Subsequently, the partially reacted solution was transferred to a new reactor and exposed to hydrogen to undergo another hydrogenation cycle. No hydrogen consumption was detected, confirming the truly heterogeneous nature of the protocol.

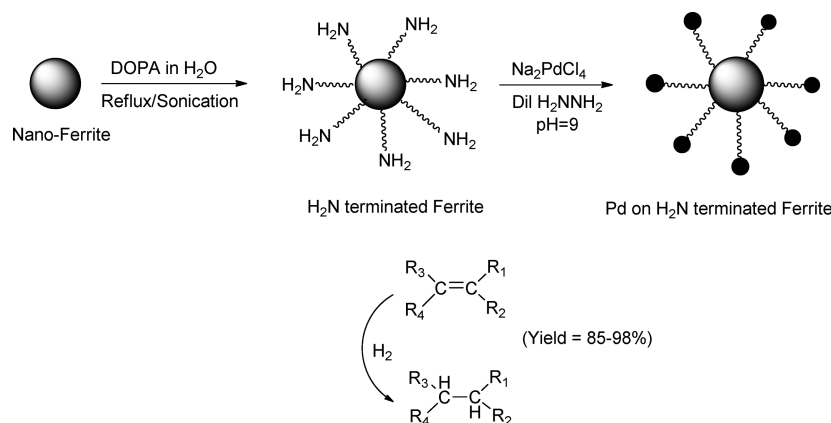
A similar magnetically recoverable Pd/C catalyst was also prepared by Tsang et al. using a simpler methodology.<sup>41</sup> First, a carbon-encapsulated nanomagnet carrier was synthesized using a sequential spraying, chemical precipitation, and controlled pyrolysis protocol. Nanometer-sized magnetic alloy particles enclosed in quasispherical graphitic shells were easily obtained in large quantities.  $[\text{Pd}(\text{acac})_2]$  in acetone was then deposited onto this carbon-protected nanomagnet by a wet impregnation method. The as-synthesized Pd/C catalyst, featuring a Fe–Ni magnetic core, showed higher activity in the hydrogenation of nitrobenzene as compared to the commercial carbon-supported catalysts. A unique advantage of this catalyst is that the external graphitic carbon surface can isolate and protect the magnetic core from destructive reactions with the environment, allowing for the use of a wide range of experimental conditions for various catalytic transformations.

Ying et al. also reported the preparation of Pd MNP supported on silica-coated  $\text{Fe}_2\text{O}_3$  nanoparticles that had surfaces that were modified with amino and thiol groups.<sup>42</sup> This Pd/ $\text{SiO}_2$ / $\text{Fe}_2\text{O}_3$  catalyst system was successfully employed in the hydrogenation of nitrobenzene (Scheme 2). Both Pd/HS– $\text{SiO}_2$ / $\text{Fe}_2\text{O}_3$  and Pd/ $\text{H}_2\text{NSiO}_2$ / $\text{Fe}_2\text{O}_3$  exhibited higher activities relative to those obtained with commercial Pd/C catalysts. However, Pd/ $\text{H}_2\text{NSiO}_2$ / $\text{Fe}_2\text{O}_3$  was more stable and less susceptible to deactivation than was Pd/HS– $\text{SiO}_2$ / $\text{Fe}_2\text{O}_3$ . After 14 runs of catalytic hydrogenation reactions, the Pd MNP in the Pd/HS– $\text{SiO}_2$ / $\text{Fe}_2\text{O}_3$  system became agglomerated and interconnected, whereas the Pd MNP on  $\text{H}_2\text{N–SiO}_2$ / $\text{Fe}_2\text{O}_3$  remained highly dispersed, with an average size of 4.8 nm. This result suggested that the *N*-(2-aminoethyl)-3-aminopropyltrimethoxysilane (AAPS) was a better affinity ligand than (3-mercaptopropyl)-trimethoxysilane (MPS), provided better Pd dispersion, and effectively suppressed the agglomeration, aggregation, and growth of Pd MNP during the hydrogenation of nitrobenzene.

In contrast to Ying's results, Rossi et al. found that MPS could stabilize Pd NPs on the surface of silica-coated magnetite nanoparticles<sup>43</sup> using a procedure similar to that described by Ying et al. (silica modification followed by attachment of the Pd NPs to the silica-coated magnetite nanoparticles). However, these silica-coated magnetite NPs were synthesized by

Scheme 2. Synthesis of Pd/SiO<sub>2</sub>/Fe<sub>2</sub>O<sub>3</sub> Magnetic Nanocomposites

Scheme 3. Pd on Amine-Terminated Ferrite Nanoparticles in Hydrogenation Reactions

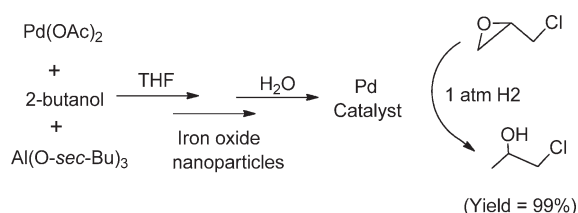


precoating the magnetic particle surfaces with soluble silicate and subsequently growing a silica layer by condensation of tetraethylorthosilicate, as compared to the water-in-cyclohexane reverse microemulsion process used by Ying. The difference in catalytic activity obtained for the same system (Pd/HS-SiO<sub>2</sub>/Fe<sub>2</sub>O<sub>3</sub>) may be due to the variations in the synthesis procedure. Pd/HS-SiO<sub>2</sub>/Fe<sub>2</sub>O<sub>3</sub> prepared by Rossi et al. was found to be well distributed on the magnetic support; it efficiently converted cyclohexene to cyclohexane under mild reaction conditions (75 °C and 6 atm) with TOF of 11 500 h<sup>-1</sup> and could be reused for up to 20 cycles (2500 TON each) without any significant loss in catalytic activity, demonstrating an efficient recycling process for hydrogenation reactions.

Interestingly, Pd can also be directly immobilized on the surface of amine-terminated iron nanoparticles without encapsulation in a silica sphere.<sup>44</sup> A facile route was developed for immobilizing Pd MNP on the surface of amine-terminated Fe<sub>3</sub>O<sub>4</sub> and NiFe<sub>2</sub>O<sub>4</sub> NPs; the system was then utilized in a series of hydrogenation reactions (Scheme 3). The key step in this route is the anchoring of dopamine molecules on the surface of NiFe<sub>2</sub>O<sub>4</sub> and Fe<sub>3</sub>O<sub>4</sub> using reflux and sonication. The dopamine on the surface of iron was considered as the linker between

the iron and Pd nanoparticles. The obtained NiFe<sub>2</sub>O<sub>4</sub>-DA-Pd and Fe<sub>3</sub>O<sub>4</sub>-DA-Pd catalysts exhibited high conversion and isolated yields for the hydrogenation of aromatic nitro and azide compounds to their respective amines and other unsaturated compounds. After five cycles, the catalysts were found to contain 8.49 wt % (NiFe<sub>2</sub>O<sub>4</sub>-DA-Pd) and 5.84 wt % (Fe<sub>3</sub>O<sub>4</sub>-DA-Pd) Pd, levels that are almost identical to the initial Pd content, 8.54% in NiFe<sub>2</sub>O<sub>4</sub>-DA-Pd and 5.87% in Fe<sub>3</sub>O<sub>4</sub>-DA-Pd. Furthermore, no deterioration in the catalytic efficiency was detected after 10 reuses. Therefore, dopamine seems to be an effective bridging molecule to stabilize Pd MNP on the surface of iron oxides, forming a highly efficient magnetic recoverable catalyst for hydrogenation reactions.

Multiple steps are usually required to prepare Pd MNP-based MS nanocatalysts. Promisingly, a simple one-pot sol-gel synthetic procedure for the preparation of such catalysts has been successfully developed, which significantly simplified the preparation procedure (Scheme 4).<sup>45</sup> A mixture of palladium acetate, Al(*O-sec-Bu*)<sub>3</sub>, 2-butanol, and THF was able to generate palladium NPs and iron oxide nanoparticles (dispersed in ethanol) that were subsequently added to the resulting black suspension. The resultant gel was isolated by filtration, washed with acetone,

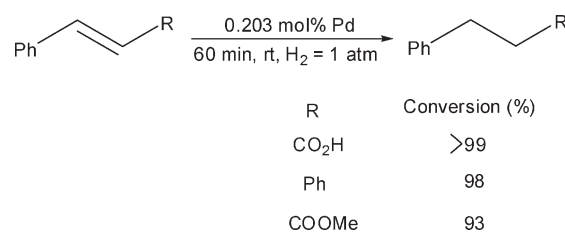
**Scheme 4. Magnetically Separable Palladium Catalyst in the Hydrogenolysis of Epoxides**

and dried at 120 °C for 5 h to yield a dark brown powder. As-synthesized iron oxide nanoparticles (60–90 nm) and palladium nanoparticles (2–3 nm) were entrapped in the fibrous aluminum oxyhydroxide matrix, and a magnetic  $\text{Pd}/\text{Fe}_2\text{O}_3/\text{Al}_2\text{O}_3$  catalytic system was obtained. This catalyst was highly active and selective for a wide range of epoxide hydrogenolysis at room temperature under 1 atm  $\text{H}_2$ , was highly recyclable (up to 25 times) without a loss of activity, and was easily recovered from the reaction mixture using an external magnet.

Rana and co-workers have described a new methodology to immobilize metallic Pd on surface-functionalized ferrite nanoparticles leading to a magnetically separable catalyst, which exhibits efficient catalytic activity in various hydrogenation reactions (Scheme 5).<sup>46</sup> The amine groups of branched polyethylenimine on the ferrite surface allow entrapping Pd nanoparticles and prevent metal leaching during the reaction. In addition, the environment provided by these groups leads to a structurally stable catalytic site, which makes them recyclable without any loss in activity.

**4.1.2. Magnetically Recoverable Platinum (Pt)-Based Catalysts.** Platinum is also widely employed as an active hydrogenation catalyst. Different Pt species can be supported on a series of magnetic materials to make them magnetically recoverable. Jaciento et al. have prepared Pt NPs on the surface of amino-modified silica-coated magnetite NPs ( $\text{Fe}_3\text{O}_4\text{--SiO}_2\text{--NH}_2$ ) using a microemulsion method.<sup>47</sup> These materials exhibited extraordinary catalytic activity in the hydrogenation of alkenes; a wide range of substrates reacted efficiently with full conversions and prominent TOF under mild conditions. Notably, all substrates were successfully converted to their completely saturated forms, even those containing aromatic rings. In the catalytic reduction of ketones to the corresponding alcohols, the reaction reached >99% conversion with a turnover number of 1200 for all substrates after a maximum reaction time of 2.2 h, with high TOF under mild conditions. This Pt catalyst could also be reused up to 7 and 14 times in the hydrogenation of benzene and 3-pentanone, respectively, without any significant loss in activity. These results account to a total accumulated TON of 8400 for benzene and 15 600 for the ketone. Meanwhile, the analysis of the product collected from all batches in the hydrogenation of 3-pentanone and benzene showed that only negligible Pt content was present in the organic phase ( $\text{Pt} < 0.01$  ppm) for both hydrogenation reactions, indicating that there was no leaching of the active species under the investigated reaction conditions. This stability found for these Pt-based materials may be due to the amine-binding sites anchored on the silica surface for metal retention.

A unique  $\gamma$ -CD ( $\gamma$ -cyclodextrin)-stabilized Fe-rich core and Pt-rich shell catalyst was developed by the Yamashita group (Scheme 6).<sup>48</sup> Fe–Pt NPs materials were prepared by thermal decomposition of an iron carbonyl complex ( $\text{Fe}(\text{CO})_5$ ), followed

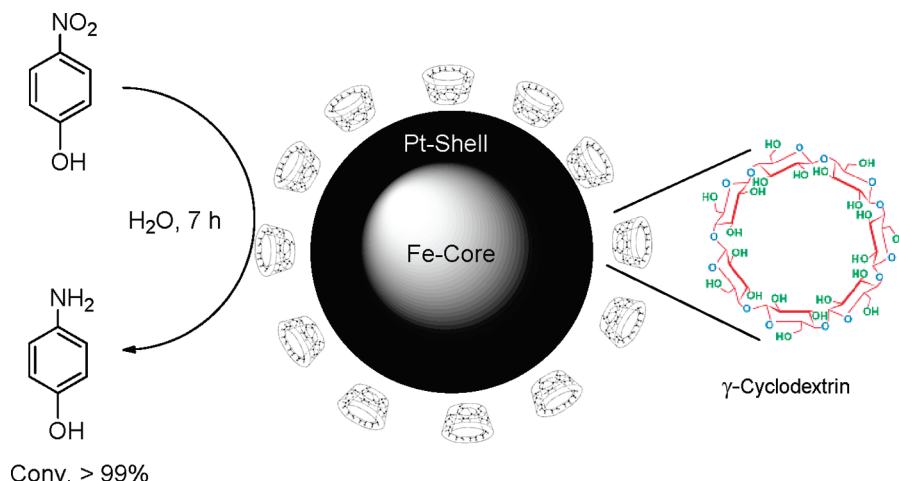
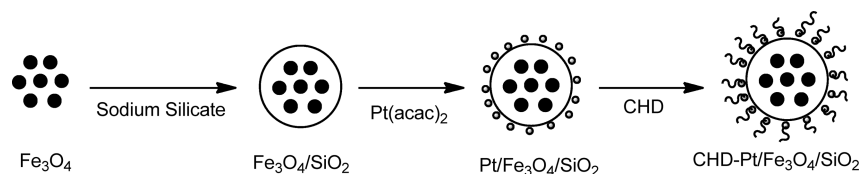
**Scheme 5. Selected Examples of Hydrogenation Reaction Using  $\text{Pd}/\text{Fe}_3\text{O}_4$  as Catalyst**

by reduction of platinum acetylacetonate ( $\text{Pt}(\text{acac})_2$ ) in the presence of oleic acid and oleylamine. To increase its hydrophilic performance, the NPs were subsequently treated with  $\gamma$ -cyclodextrin ( $\gamma$ -CD), which rendered them soluble in water rather than in organic solvents. The  $\text{Fe}_{\text{core}}\text{Pt}_{\text{shell}}$  NPs capped with  $\gamma$ -CD ( $\text{FePt-}\gamma\text{-CD}$ ) had a mean diameter of ca. 2.5 nm, which exhibited super paramagnetic behavior at 300 K with zero remanence and coercivity. The catalytic hydrogenation reaction with  $\text{FePt-}\gamma\text{-CD}$  as a catalyst can be conducted in water, which is an environmentally friendly and low-cost solvent. This catalyst was active for the reduction of *p*-nitrophenol, giving quantitative yields of *p*-aminophenol (conversion  $\geq 99\%$ ). The recovered catalyst could then be reused at least three times while maintaining activity identical to that of the initial run, and the TEM indicated that the size distribution of the recovered FePt NPs remained virtually unchanged. More significantly, the FePt NPs catalyst exhibited host–guest recognition properties to facilitate the reaction of less sterically hindered substrates. In the hydrogenation of an equimolar mixture of allyl alcohol and 3-cyclohexene-1-methanol under aqueous conditions, the FePt NPs showed a high product ratio of 10 for *n*-propanol and cyclohexane–methanol, whereas the  $\text{Pt}/\text{SiO}_2$  catalyst had a product ratio of 5.

Pt nanoparticle-based MSCs could also be extended to catalytic enantioselective hydrogenation reactions, providing an alternative for catalytic asymmetric synthesis. This chirally active catalytic system was derived from a  $\text{Pt}/\text{SiO}_2/\text{Fe}_3\text{O}_4$  matrix,<sup>49</sup> and Pt was supported on the surface of silica-coated  $\text{Fe}_3\text{O}_4$  nanoparticles through wet impregnation. The  $\text{Pt}/\text{SiO}_2/\text{Fe}_3\text{O}_4$  was eventually chirally modified using cinchonidine (CHD) (Scheme 7). This asymmetric catalytic system showed good catalytic performance in the hydrogenation of  $\alpha$ -ketoesters and fluorinated ketones (exhibiting results similar to the commercial  $\text{Pt}/\text{Al}_2\text{O}_3$  catalyst). In the hydrogenation of ketopantolactone, the catalyst was magnetically separated from the solution after each reaction cycle, washed twice with toluene, and reused without further activation. The enantioselectivity only slightly decreased from *ee* = 57% (first run) to a final value of *ee* = 52% (after the eighth reaction cycle). Pt and Fe species were not detectable in solution during the reaction.

A magnetically separable nanocatalyst consisting of Pt nanoparticles of 2–5 nm in sizes anchored on carbon-encapsulated nickel nanoparticles of about 30 nm in diameter has been artificially constructed. The construction process mainly includes two steps, that is, the nondestructive functionalization of the magnetic  $\text{Ni}(\text{C})$  nanocapsules with carboxylic acid end groups and the immobilization of Pt nanoparticles on the nanocapsules. The magnetically separable function of the nanocatalyst was well demonstrated for the hydrogenation of nitrobenzene to aniline.<sup>50</sup>

**4.1.3. Magnetically Recoverable Ruthenium (Ru)-Based Catalysts.** Supported Ru NPs on magnetic nanoparticles

Scheme 6. Schematic Illustration of the  $\gamma$ -CD ( $\gamma$ -Cyclodextrin)-Stabilized Fe-Rich Core and the Pt-Rich Shell CatalystScheme 7. Preparation of the Magnetic Cinchonidine-Modified Pt/SiO<sub>2</sub>/Fe<sub>3</sub>O<sub>4</sub>

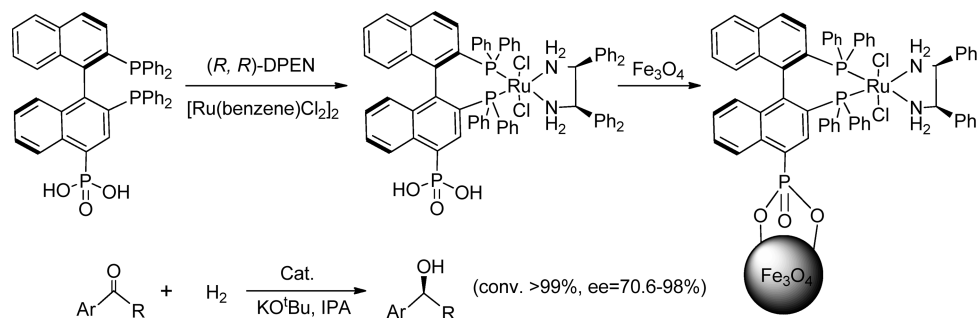
(NiFe<sub>2</sub>O<sub>4</sub>) modified by dopamine have also been recently synthesized, forming a magnetically recoverable Ru/NiFe<sub>2</sub>O<sub>4</sub> catalyst.<sup>51</sup> This Ru catalyst was employed in the chemoselective hydrogenation of alkynes to their respective alkanes at room temperature. Reactions proceeded smoothly at room temperature, producing the desired products at a yield greater than 90%. Moreover, the Ru/NiFe<sub>2</sub>O<sub>4</sub> catalyst could be used in microwave (MW)-assisted catalytic reactions. MW irradiation provides rapid and uniform heating of reagents, solvents, and intermediates, offering the advantage of short reaction times. Ru/NiFe<sub>2</sub>O<sub>4</sub> exhibited excellent conversions (above 90%) in the transfer hydrogenation of a series of carbonyl compounds under microwave (MW) irradiation. The catalyst was recoverable with an external magnetic field and remained highly active, even after five repeated uses. The Ru loading in the catalyst has been confirmed to be 3.89% (prior to the reaction) and 3.82% (after three uses). This result confirms the minimal loss of Ru during the reaction and explains its high efficiency in repeated applications, characteristics that are highly desirable from an economic point of view.

Some of the homogeneous chiral Ru complexes are very active in asymmetric hydrogenations. Interestingly, the chiral Ru complex-based catalyst can be rationally designed to create magnetically recoverable catalysts (Scheme 8).<sup>52</sup> The ruthenium(II) complex [Ru(BINAP)(DPEN)Cl<sub>2</sub>] was modified by phosphonic acids to link the complex to the magnetite NPs via a phosphorus group. This phosphonic acid-substituted BINAP [Ru(BINAP-PO<sub>3</sub>H<sub>2</sub>)(DPEN)Cl<sub>2</sub>] was synthesized by treating [Ru(benzene)Cl<sub>2</sub>]<sub>2</sub> with (R)-2,2'-bis(diphenylphosphino)-1,1'-binaphthyl-4-phosphonic acid (BINAPPO<sub>3</sub>H<sub>2</sub>), followed by (R,R)-1,2-diphenylethylenediamine (DPEN) in DMF at elevated temperatures. The treatment of this complex with Fe<sub>3</sub>O<sub>4</sub> by ultrasonication resulted in the [Ru(BINAP-PO<sub>3</sub>H<sub>2</sub>)(DPEN)Cl<sub>2</sub>]

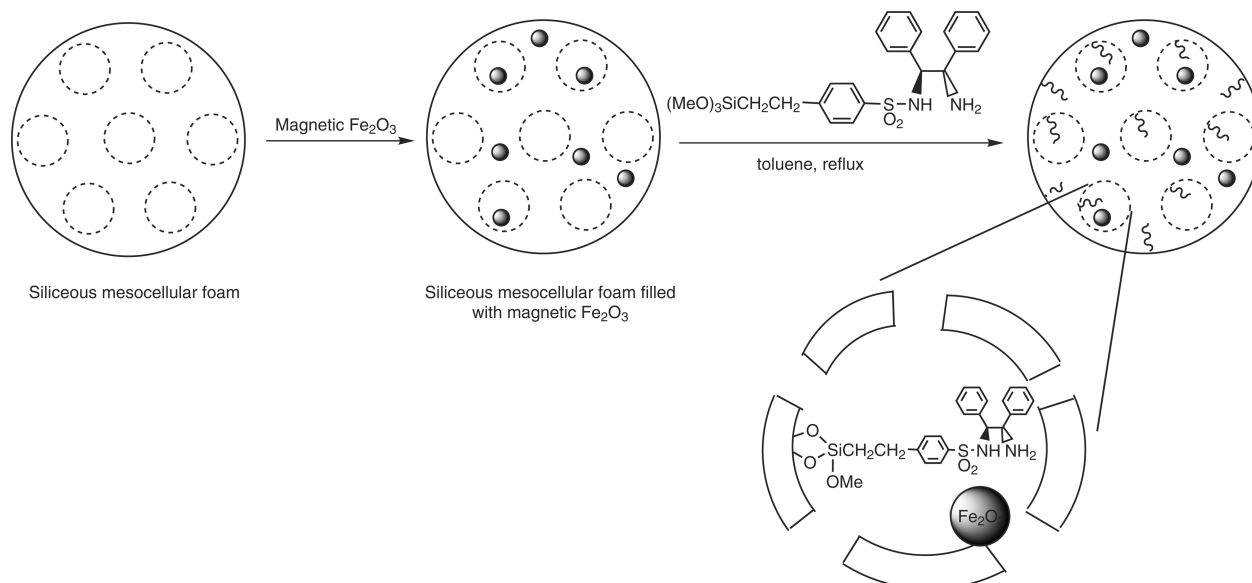
moieties being chemically bonded to Fe<sub>3</sub>O<sub>4</sub>. This catalyst was then used for the hydrogenation of a wide range of aromatic ketones to their corresponding secondary alcohols and exhibited high reactivity and enantioselectivity. The enantiomeric excess (ee) values were significantly higher than those of the parent homogeneous catalyst [Ru(BINAP)(DPEN)-Cl<sub>2</sub>] and were comparable to the values of its homogeneous counterpart. The stability of the recovered catalyst was investigated in the asymmetric hydrogenation of 1-acetonaphthone. In this reaction, the catalyst could be recycled 14 times with no decrease in conversion and/or enantiomeric excess. However, the MSCs tend to aggregate slightly, presumably because the [Ru(BINAP-PO<sub>3</sub>)(DPEN)Cl<sub>2</sub>] moieties on the MNP surfaces are less effective in preventing the aggregation of the MNPs than that of widespread coating agents such as oleic acid.

Another recoverable ruthenium catalyst for asymmetric hydrogenation was prepared by Li and colleagues.<sup>53</sup> This catalytic system was derived from a RuTsDPEN complex (TsDPEN = *N*-(*p*-toluenesulfonyl) 1,2-diphenylethylenediamine) that was immobilized onto a magnetic material (Scheme 9). To prevent aggregation of the magnetic NPs (due to their small particle size), a siliceous mesocellular foam filled with magnetic Fe<sub>2</sub>O<sub>3</sub> was used as a support for RuTsDPEN. RuTsDPEN was grafted to the support via SiCH<sub>2</sub>CH<sub>2</sub> links between the silica and the ligand. This heterogeneous catalyst afforded 97–99% conversion and an ee value of 94% in the asymmetric transfer hydrogenation of imines in a HCOOH–Et<sub>3</sub>N system (Scheme 10). Furthermore, this heterogeneous catalyst can be consecutively reused at least nine times, with ee values ranging from 94% to 90%. However, the reaction time had to be extended from 1.5 to 7 h to achieve comparable initial activities (99%) in subsequent runs. ICP analysis showed that an 11 mol % of ruthenium leached from the catalyst after nine runs, which indicated that the catalyst was

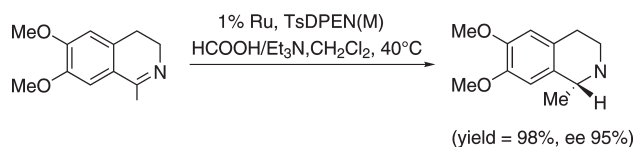
Scheme 8. Magnetite Chiral Ru Catalyst for Asymmetric Hydrogenation of Aromatic Ketones



Scheme 9. Schematic Representation of the Preparation of a Hybrid Ligand TsDPEN on Magnetic Material



Scheme 10. Magnetic TsDPEN Ligand in the Asymmetric Transfer Hydrogenation of Imines



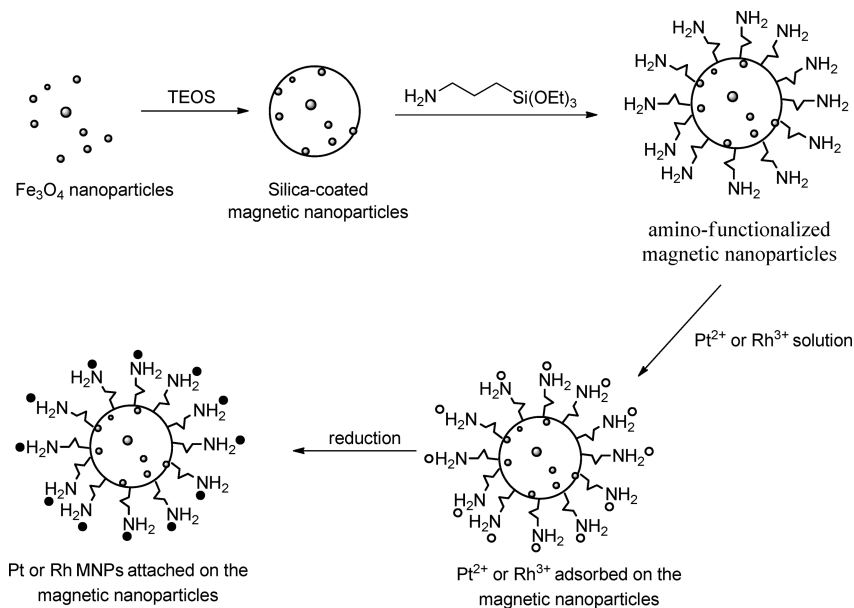
partly decomposed upon subsequent reuses. The scope of this protocol was also extended to the asymmetric transfer hydrogenation (ATH) of aromatic ketones, with  $\text{HCOOH}-\text{Et}_3\text{N}$  azeotrope as a hydrogen donor in  $\text{CH}_2\text{Cl}_2$  as a solvent. Different aromatic ketones were employed as substrates, and all the catalytic reactions had high catalytic activities with good ee values.

**4.1.4. Magnetically Recoverable Rhodium (Rh)-Based Catalysts.** Amino-functionalized silica-coated magnetic nanoparticles were also effective supports for the immobilization of Rh MNPs.<sup>54</sup> The general synthetic route is shown in Scheme 11. The preparation of these catalysts was based on the uptake of  $\text{Rh}^{3+}$  by amino-functionalized silica-coated magnetic nanoparticles, followed by metal reduction under controlled  $\text{H}_2$  conditions, leading to MNP formation. The 3-aminopropyltriethoxysilane on the silica spheres offers a substantial improvement in

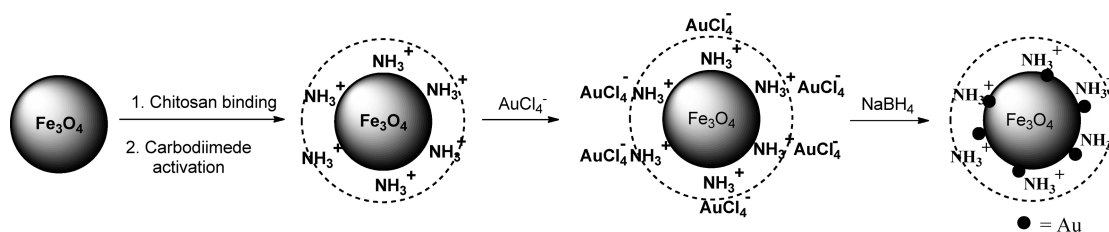
terms of  $\text{Rh}^{3+}$  uptake from  $\text{RhCl}_3$  solutions. The amino-functionalized silica can immobilize as much as 1.55% of Rh; by contrast, only 0.14% of Rh was adsorbed on the support without amino groups. The magnetically recoverable rhodium catalyst exhibited enhanced recovery/recycling properties in the hydrogenation of cyclohexene and benzene and was reusable for up to 20 successive batches without any significant loss in catalytic activity (TON of 180 000 and 11 550 for cyclohexene and benzene hydrogenation, respectively).

**4.1.5. Magnetically Recoverable Gold (Au)-Based Catalysts.** Gold (Au) catalysis has received considerable attention in recent years. Magnetically recoverable Au nanocatalysts can provide a novel approach for various applications of gold nanoparticles.<sup>55–57</sup> A magnetically recoverable Au nanocatalyst was fabricated through a simple adsorption–reduction of Au(III) ions on chitosan-coated iron oxide magnetic nanocarriers (Scheme 12).<sup>57</sup> Au(III) ions were adsorbed onto the magnetic nanocarrier and reduced by  $\text{NaBH}_4$  to produce the gold nanoparticles. Au nanoparticles (with a mean diameter of 3.1 nm) were found to be well dispersed on the surface of the support due to the stabilization of the Au nanoparticles by the chitosan layer. The catalytic performance of the resultant magnetically recoverable Au nanocatalyst was illustrated in the reduction of 4-nitrophenol to 4-aminophenol with  $\text{NaBH}_4$ . The reduction reaction

Scheme 11. Magnetically Recoverable Rh Catalysts on Amino-Functionalized Silica-Coated Nanoferrites



Scheme 12. Preparation of Magnetically Recoverable Au Nanocatalysts Using Chitosan-Coated Iron Oxides

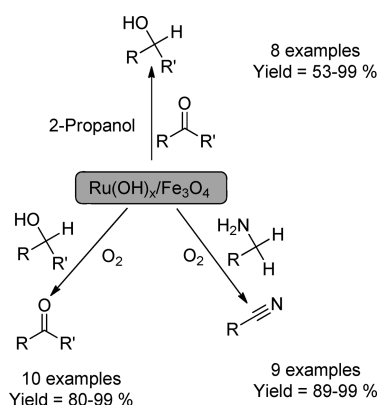


followed pseudo first-order kinetics and was diffusion controlled. The rate constant increased when the concentration of the Au nanocatalyst was increased, the initial concentration of 4-nitrophenol was decreased, or when the temperature was increased. Furthermore, the Au nanocatalyst was found to be highly stable with remarkable catalytic activities, even after 11 cycles.

#### 4.2. Oxidation Reactions

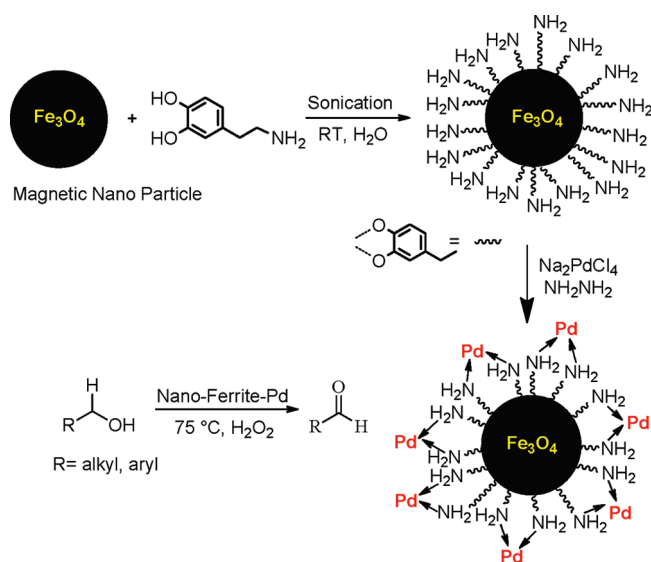
Oxidation reactions are vitally important to the chemical industry because of their potential for generating a variety of fine chemicals and drugs. Conventionally, oxidation has been achieved noncatalytically using stoichiometric quantities of oxidants (such as chromium and manganese oxides) in the presence of corrosive mineral acids, which in turn produces huge amounts of toxic waste. Because of growing environmental concerns, continuous efforts have been made to develop oxidation protocols using green chemistry principles with a focus on the development of easily recoverable and reusable heterogeneous catalysts. In light of these concerns, the use of magnetic nanomaterials as a solid support for heterogeneously catalyzed oxidation reactions has proven to be highly effective.

Mizuno and colleagues developed a heterogeneous ruthenium hydroxide (Ru(OH)<sub>x</sub>) catalyst supported on magnetic ferrites.<sup>58</sup> This catalyst system was able to catalyze the aerobic oxidation of alcohols and amines, as well as the reduction of carbonyl compounds to alcohols using 2-propanol as a hydrogen donor

Scheme 13. Ruthenium Hydroxide (Ru(OH)<sub>x</sub>) Catalyst Supported on Magnetic Ferrites

(Scheme 13). These systems are able to catalyze these reactions for a range of substrates, including aromatic, aliphatic, and heterocyclic molecules, in good yields and without requiring any additives and/or mediators. Importantly, product isolation was easily achieved using an external magnet, and the recovered catalyst was reused several times without any significant loss in catalytic performance.

Scheme 14. Pd Catalyst Supported on Dopamine-Functionalized Nanoferrite

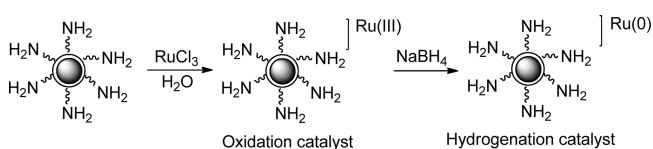


Polshettiwar and Varma developed a Pd catalyst supported on dopamine-functionalized nanoferrite (Scheme 14), another example of the use of magnetic catalytic systems in oxidation reactions.<sup>59</sup> Dopamine was chosen as a linker on the basis of its ability to change the uncoordinated Fe surface sites back to a bulk-like lattice structure with an octahedral geometry for oxygen-coordinated iron. This effect resulted in tight binding to iron oxide. Moreover, desorption of dopamine from metal oxides is less favorable than absorption, thus reducing the chances of leaching. These functionalized materials coated with Pd displayed high catalytic activity in the oxidation of alcohols and olefins with high turnover rates. The catalyst was easily separated using an external magnet (no filtration required), making the protocol practical and sustainable.

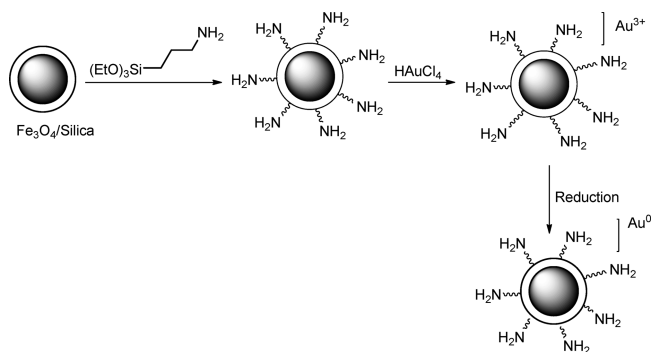
Similarly, Rossi and colleagues prepared magnetically separable Ru(III) and Ru(0) catalysts for oxidation and hydrogenation processes, respectively.<sup>60</sup> Both catalysts were prepared via the hydrolysis of ruthenium chloride to form a Ru(III) catalyst on amino-functionalized silica-coated magnetic nanoparticles, which was converted to Ru(0) upon further reduction by sodium borohydride (Scheme 15). Oxidized Ru(III) was found to be highly active in the oxidation of aryl and alkyl alcohols to aldehydes, as compared to the reduced Ru(0) form, which was active in hydrogenation reactions under mild conditions. The use of an amino-functionalized support stabilized the metal NPs and prevented metal leaching. Furthermore, the magnetic support enabled facile separation of the catalyst and product isolation from the reaction mixture.

Rossi and colleagues also prepared magnetically separable gold (Au) catalysts (Scheme 16).<sup>61</sup> The methodology employed for the reduction of metal nanoparticles was crucial in determining particle dispersion and distribution on the magnetic support, which in turn was able to significantly influence the catalytic activity. MNP reduction was conducted either by heating under air atmosphere or by hydrogen reduction at mild temperatures. Interestingly, the hydrogen reduction methodology seemed to afford an improved control over the particle dispersion, and the resulting Au catalyst was found to be highly active in the aerobic oxidation of alcohols. The catalysts were

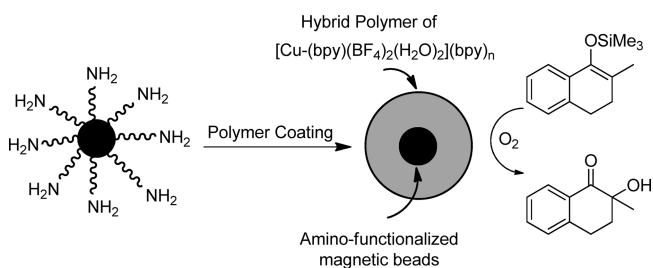
Scheme 15. Magnetically Separable Ru(III) and Ru(0) Catalysts



Scheme 16. Magnetically Separable Gold (Au) Catalyst



Scheme 17. Hybrid-Polymer-Encapsulated Bead Catalysts the Oxidation of Silyl Enolates



efficiently recovered by magnetic separation with negligible Au leaching.

Arai and his team developed a new strategy for the encapsulation of magnetic nanobeads by in situ self-assembly of an organic–inorganic hybrid polymer on the surface of amino-functionalized magnetic beads (Scheme 17).<sup>62</sup> The as-synthesized hybrid-polymer-encapsulated bead was used to catalyze the oxidation of silyl enolates to the corresponding  $\alpha$ -hydroxy carbonyl compounds, and this reaction provided good yields. Upon completion of the reaction, the catalyst was readily recovered by means of an external magnet and successfully reused several times.

Ko and Jang fabricated magnetic carboxylated polypyrrole nanotube (MCPy NTs)-supported Pd-catalysts.<sup>63</sup> These authors used vapor deposition polymerization (VDP), in which vaporized pyrrole-3-carboxylic acid monomers were polymerized by Fe cations adsorbed on an anodic aluminum oxide (AAO) membrane. During template removal, Fe salts in the polymer backbone were reduced to form magnetites, which made the as-synthesized material magnetic. These synthesized nanotubes contained active sites that were available for metal anchoring. As a result, no tedious surface functionalization was required.

The nanotubes were then coated with palladium chloride, which yielded a magnetic Pd-nanocatalyst upon reduction with hydrogen. The catalyst exhibited excellent catalytic activity and reusability in the Heck coupling of aryl iodides. However, challenging molecules (e.g., aryl chlorides) were not investigated here. Despite the good catalytic activity, the high cost of nanotubes may hinder their application as a catalyst support, especially because a simple magnetic nanoferrite can be utilized instead. For example, Baruwati and colleagues used a ferrite-supported Pd-catalyst for Heck and Suzuki coupling reactions and reported excellent yields (even for aryl chloride derivatives).<sup>64</sup>

Ti-silicate mesoporous materials with core-shell morphologies synthesized by Barmatova et al. were used in selective oxidation reactions using  $\text{H}_2\text{O}_2$  as a benign oxidation reagent.<sup>22</sup> Indeed, this novel material was able to combine the advantages of high activity and selectivity in these processes, with the added advantage of being easily separable from the reaction mixture by a simple magnet. Quantitative conversion and selectivity over 75% were observed for these magnetically separable catalysts (MSC) in the liquid-phase oxidations of 2,3,6-trimethylphenol (TMP) and methyl sulfide (MPS), under various conditions. Interestingly, hot filtration tests revealed the truly heterogeneous nature of the protocol, as there was no leached species in solution (no conversion increase in the filtrate after separation of the catalyst). Reusability of the catalysts was good, but the materials had to be filtered off and dried prior to reuse to obtain optimum activities.

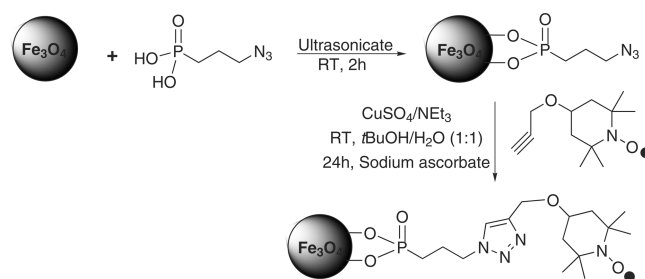
Similar titanium-containing mesoporous silica materials with encapsulated magnetic iron oxide nanoparticles were synthesized via a two-step coating method and utilized as catalysts in the oxidation of 2,6-di-*tert*-butylphenol with hydrogen peroxide.<sup>65</sup> The synthetic strategy (silica layer deposition on the surface of iron nanoparticles and formation of a Ti-HMS layer from subsequent sol-gel polymerization) allowed the preparation of catalytically active materials with iron oxide NPs (9.5 nm average particle size) in their structure. The oxidation of 2,6-di-*tert*-butylphenol with 30%  $\text{H}_2\text{O}_2$  led to the corresponding quinone in 97% yield with 99% selectivity, as compared to negligible conversion obtained for  $\text{TiO}_2$  and TS-1. The catalysts could be easily separated using a simple magnet and recycled up to five times without any appreciable loss in activity.

Garrell and co-workers immobilized the organic oxidant TEMPO (2,2,4,4-tetramethylpiperidine-1-oxyl) on iron oxide superparamagnetic nanoparticles by employing strong metal-oxide chelating phosphonates and azide-alkyne "click" chemistry (Scheme 18).<sup>66</sup> The obtained catalyst showed high catalytic activity and chemoselectivity in oxidation of alcohols (primary, secondary, and hindered ones substrates) to their carbonyl analogues, under both Minisci<sup>67</sup> and Anelli<sup>68</sup> conditions using low catalyst loadings. Catalyst was quickly recovered from solution using hand-held magnets. The authors also indicated that this catalyst was recovered and reused with over 20 times under the Minisci conditions and up to eight times under Anelli conditions without any decreases in activity. In addition, the leaching studies on this catalyst under Minisci conditions showed that the phosphonic acid-coated particles remain stable under the highly acidic oxidizing conditions and leaching was very small.

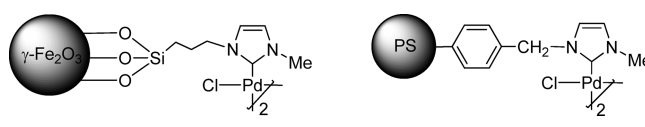
### 4.3. Carbon-Carbon Coupling Reactions

Cross-coupling reactions to form carbon-carbon bonds are among the most crucial transformations in synthetic chemistry.<sup>69</sup> Transition metal catalysts have been developed into excellent reagents in organic synthesis for the formation of carbon-carbon

**Scheme 18.** Synthesis of TEMPO-Coated Superparamagnetic Nanoparticles Catalyst



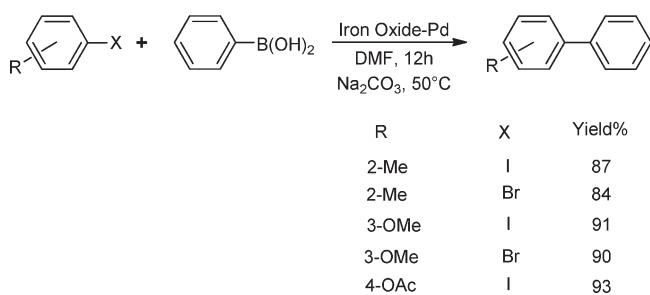
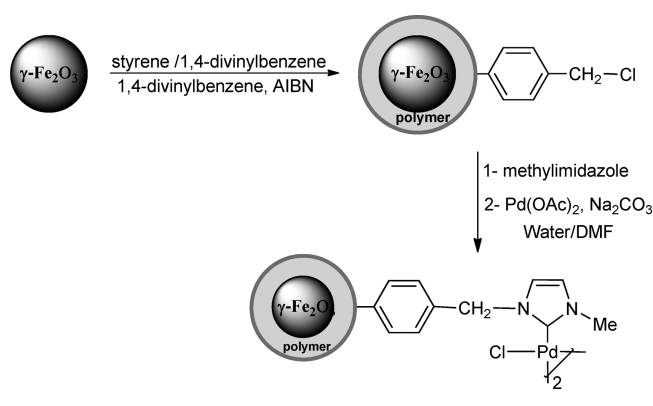
**Scheme 19.** Pd-N-Heterocyclic Carbene Immobilized on Magnetic Nanoparticles and on Polystyrene Resins



and carbon-heterocyclic bonds for simple and complex stereocontrolled reactions. These reactions are generally catalyzed by soluble palladium complexes with various ligands.<sup>69,70</sup> However, despite the remarkable progress achieved in this area to date, a number of challenges remain. The efficient separation and subsequent recycling of homogeneous transition metal catalysts continues to present a real scientific challenge. The development of heterogeneous catalysis seems particularly suitable for these reactions due to the wide accessibility and excellent stability of these solid supports.<sup>70,71</sup> Magnetite NPs are a recent and interesting alternative for these reactions.

**4.3.1. Suzuki Reactions.** The Suzuki coupling reaction is one of the most important synthetic transformations developed in the 20th century.<sup>72-75</sup> This reaction has arguably become one of the most powerful synthetic methods to prepare a wide range of biaryl compounds, which can then serve as building blocks and/or intermediates for various natural products, pharmaceuticals, and polymers.<sup>76-79</sup> There are several reasons for the development of this reaction at both the academic and the industrial levels. First, the scope of the protocol can be extended to many functional groups due to the mild reaction conditions, which makes this an attractive system for the total synthesis of complex drug molecules. Second, boron compounds are readily available, stable, and considered to be of low toxicity. Third (and importantly), the reaction works well with a wide range of substrates.

Gao and colleagues reported the preparation of a Pd N-heterocyclic carbene that could be immobilized onto the surface of oleate-stabilized soluble maghemite nanoparticles ( $\gamma\text{-Fe}_2\text{O}_3$ ) to form a stable and active magnetic nanocatalyst (Scheme 19).<sup>80,81</sup> The partial solubility of these NPs in various organic solvents is due to their small dimensions ( $11\text{ nm} \pm 10\%$ ) and organic coating. The superparamagnetism of the maghemite core allows the particles to be magnetically concentrated and redispersed using an externally positioned small permanent magnet. Using 7.3 mol % of catalyst and  $\text{Na}_2\text{CO}_3$  as the base in the presence of DMF, this catalyst provided nearly quantitative yields for electron-rich and electron-poor aryl iodides and bromides (Scheme 20).

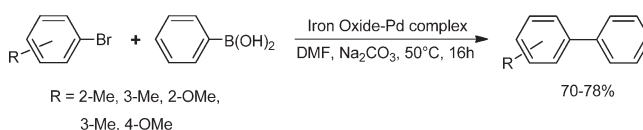
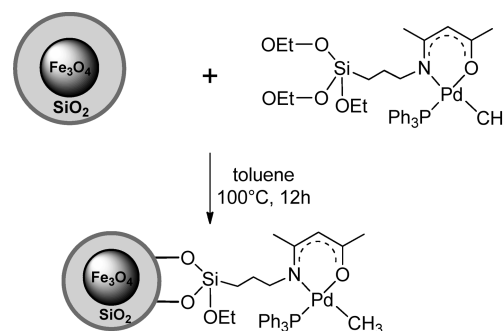
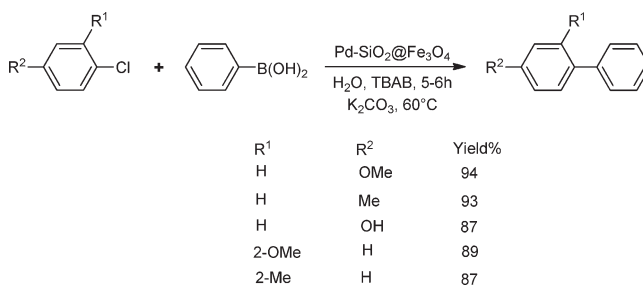
**Scheme 20. Maghemite Nanoparticle-Supported Suzuki Cross-Coupling Reactions****Scheme 21. Preparation of Iron Oxide Nanoparticle-Supported Pd–NHC Complexes**

The recycling of the materials was performed via magnetic concentration, washing and air-drying without further purification. No significant loss of catalytic activity of the immobilized catalyst was observed after several reaction cycles. This catalytic system was shown to be faster than an analogous polystyrene solid-phase system; the authors believe the increased rate is due to easier access to the surface active sites.

The research group led by Gao also examined an emulsion polymerization methodology as a novel route for the immobilization of a Pd–NHC catalyst on core/shell super paramagnetic nanoparticles that consisted of a highly crystalline  $\gamma$ -Fe<sub>2</sub>O<sub>3</sub> core and a very thin polymeric shell wall (Scheme 21).<sup>82</sup> These stable nanoparticle-supported catalysts were employed as soluble supports for immobilizing Pd catalysts to catalyze Suzuki cross-coupling reactions.

As-synthesized catalyst showed excellent activities in the Suzuki coupling of various aryl iodides and bromides with phenylboronic acid, using DMF as a solvent (Scheme 22). However, the coupling of aryl chlorides was not reported for this system. Recovery of the catalysts was easily achieved by applying an external permanent magnet, and recycling of the catalytic system was examined for five consecutive rounds in the synthesis of 4-phenyltoluene from 4-iodotoluene and phenylboronic acid. An isolation yield of  $88 \pm 3\%$  was obtained in each run. No significant loss of catalytic activity consequently observed during the five consecutive reactions.<sup>82</sup>

More recently, Jin et al. designed a magnetic nanoparticle-supported ( $\beta$ -oxoiminato) (phosphanyl) palladium catalyst via immobilization of a triethoxysilyl-functionalized palladium

**Scheme 22. Suzuki Cross-Couplings Using Magnetic Pd–NHC Complexes****Scheme 23. Synthesis of the MNP-Supported ( $\beta$ -Oxoiminato) (Phosphanyl) Palladium Complex****Scheme 24. Suzuki Cross-Coupling of Deactivated Aryl Chlorides and Phenylboronic Acid**

complex on the surface of robust SiO<sub>2</sub>/Fe<sub>3</sub>O<sub>4</sub> under refluxing toluene conditions (Scheme 23).<sup>83</sup>

The activity of this catalyst was evaluated in the Suzuki coupling of a series of aryl chlorides with arylboronic acid in water and in the presence of K<sub>2</sub>CO<sub>3</sub> as a base and tetrabutylammonium bromide as a phase-transfer agent. Reactions of phenylboronic acid with activated aryl chlorides (such as 4-chlorobenzonitrile, 1-chloro-4-nitrobenzene, and 1-chloro-2-nitrobenzene, using 0.5 mol % catalyst) led to the desired products with excellent yields after 3 h at 60 °C. The system was particularly efficient for the coupling of phenylboronic acid with deactivated aryl chlorides, including 4-chloroanisole, 4-chlorotoluene, 4-chlorophenol, 2-chloroanisole, and 2-chlorotoluene (Scheme 24). The activity of this catalyst was also evaluated in the coupling of sterically hindered substrates (such as 2-chloro-1,3-dimethylbenzene) with 4- and 2-methylphenylboronic acids, providing satisfactory results but at elevated temperatures and for extended reaction times.<sup>83</sup>

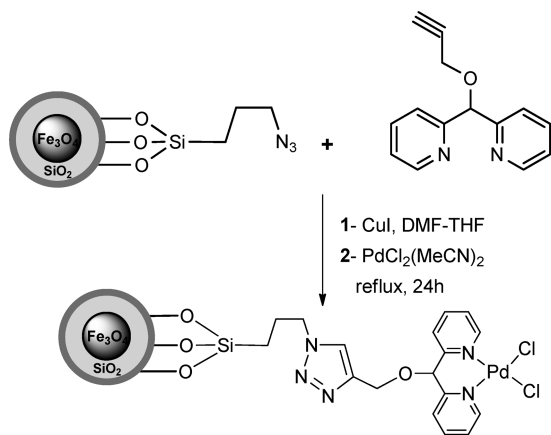
The catalyst could again be recovered by an external magnet, and reusability was further examined in the coupling of 4-chloroanisole with phenylboronic acid. These results revealed that the catalyst could be reused more than 10 consecutive times without

any significant loss of catalytic activity. After the reaction, less than 0.06% of the palladium content had leached out from the material into the solution.

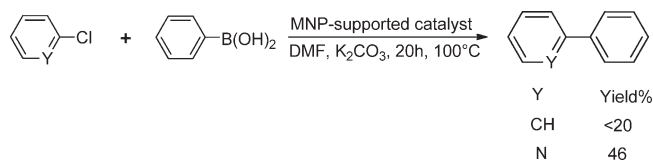
Gao and colleagues also reported the synthesis of a novel magnetic nanoparticle-supported di(2-pyridyl)methanol palladium dichloride complex via click chemistry (Scheme 25).<sup>84</sup>

Catalyst was then initially tested in the Suzuki coupling of phenylboronic acid with bromobenzene. Optimized results were achieved with a 0.2 mol % catalyst and the use of  $K_2CO_3$  as base in DMF at 100 °C. Under these conditions, fairly good to excellent yields were obtained in the coupling of aryl bromides containing electron-donating and electron-withdrawing substituents. Unfortunately, the catalytic system was less effective with more challenging substrates such as aryl chlorides and heterocyclic bromides, even when using larger quantities of catalyst (1 mol %) and extended reaction times (Scheme 26).<sup>84</sup>

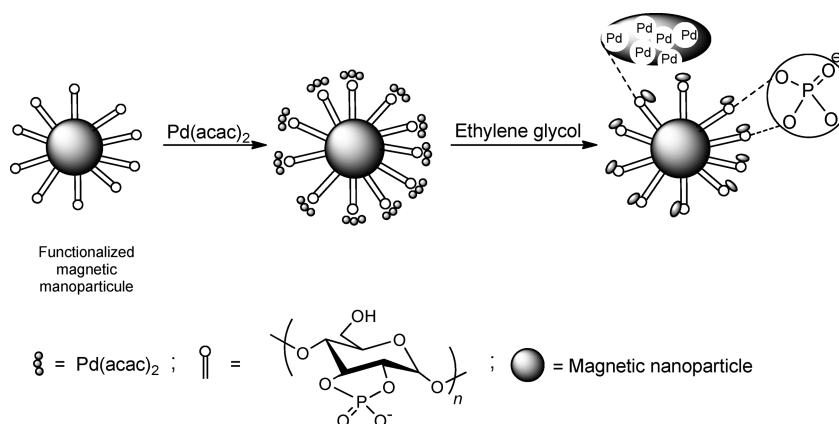
**Scheme 25.** Preparation of a MNP-Supported Di(2-pyridyl)-methanol–Pd Complex via Click Chemistry



**Scheme 26.** Coupling Reactions Using MSC-Supported Complexes



**Scheme 27.** Synthesis of Magnetic Nanoparticle-Supported Palladium Nanoparticles

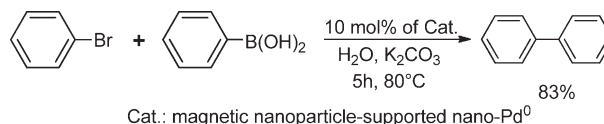


Upon completion of the reaction, the catalyst was recovered by an external magnet, washed with diethyl ether, further washed with water, dried under vacuum, and subsequently reused in another run. The coupling of 4-bromoacetophenone and phenylboronic acid could be maintained above 95% after five rounds of recycling. One noteworthy characteristic was the stability of this catalyst under a range of air and moisture conditions, thus allowing this reaction to be performed under air.

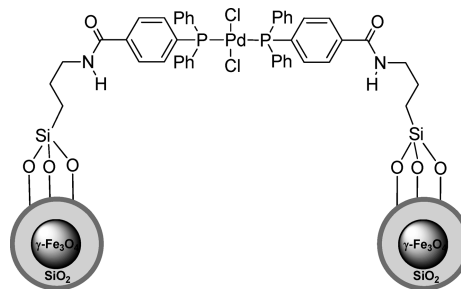
Yinghuai et al. have demonstrated that commercially available magnetic nanoparticles with a mean diameter of 100 nm can be enriched with phosphate functional groups and used as magnetic support for Pd-catalysts (Scheme 27).<sup>85</sup>

Material was then tested as a catalyst in the Suzuki coupling of phenylboronic acid with bromobenzene in the presence of  $K_2CO_3$ , using water as a solvent. The reaction led to the expected desired product at an excellent isolated yield after 5 h at 80 °C (Scheme 28). The authors indicated that, upon drying, the catalyst could be reused at least three times without any significant loss of activity. The material was able to be dispersed in both aqueous and organic solvents to produce a pseudohomogeneous catalyst system, but the scope of the reaction for a more diverse array of substrates was not discussed.<sup>85</sup>

**Scheme 28.** Suzuki Coupling Using Supported Ultrasmall Palladium on Magnetic Nanoparticles



**Scheme 29.** Pd(II)–Phosphine Complexes Supported on Magnetic Nanoparticles

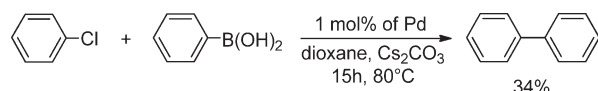


Thiel and his group anchored trimethoxysilyl-functionalized palladium(II)–phosphine complexes on magnetic nanoparticles and successfully employed them as heterogeneous catalysts in the Suzuki reaction of aryl bromides and iodides (Scheme 29).<sup>86</sup> In the presence of 1 mol % of this catalyst, the best results were obtained with  $\text{Cs}_2\text{CO}_3$  as the base in dioxane at 80 °C for 15 h. The heterogeneous catalyst can be readily recovered by magnetic separation, then subsequently washed with an  $\text{EtOH}/\text{CH}_2\text{Cl}_2$  mixture and gently dried under vacuum before being reused seven times in the coupling of bromobenzene and phenylboronic acid, without a marked loss of catalytic activity. However, under the same conditions, the catalyst provided moderate yields in the coupling of chlorobenzene and phenylboronic acid (Scheme 30).

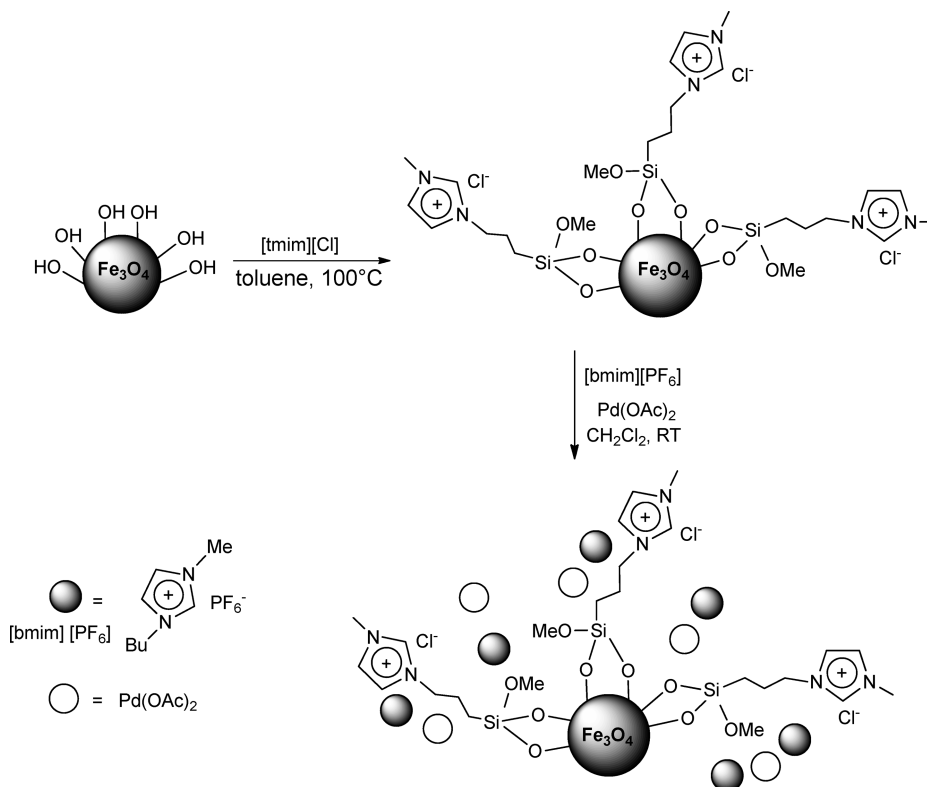
Jin and colleagues reported that  $\text{Pd}(\text{OAc})_2$  could be immobilized on a  $\text{Fe}_3\text{O}_4$ –ionic liquid hybrid material. The synthesis of this material comprises the treatment of  $\text{Fe}_3\text{O}_4$  with 1-(3-trimethoxysilylpropyl)-3-methylimidazolium chloride ( $[\text{tmim}][\text{Cl}]$ ) in refluxing toluene, followed by reaction with a solution of  $\text{Pd}(\text{OAc})_2$  and  $[\text{bmim}][\text{PF}_6]$  (Scheme 31).<sup>87</sup>

This catalyst was then tested for the Suzuki coupling of arylboronic acid with aryl bromides in neat water and in the presence of  $\text{K}_3\text{PO}_4$  as a base. This catalyst showed good activity in the coupling of aryl bromides, including sterically hindered and deactivated substrates. Its high efficiency may be attributed to the presence of well-dispersed  $\text{Pd}(\text{OAc})_2$  in the ionic liquid

**Scheme 30. Suzuki–Miyaura Coupling of Bromobenzene and Phenylboronic Acid**



**Scheme 31. Immobilization of  $\text{Pd}(\text{OAc})_2$  on the Surface of  $\text{Fe}_3\text{O}_4$ -Supported Ionic Liquid**

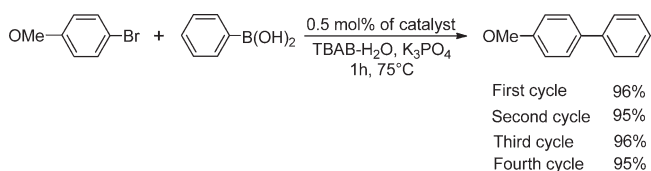


phase, which is more accessible to the reactants. The catalyst was recovered from the final reaction mixture using an external magnet, and its reusability was investigated in the coupling of 4-bromoanisole with phenylboronic acid in water. The recycled catalyst could be used in four consecutive runs without any noted loss of activity (Scheme 32).<sup>87</sup>

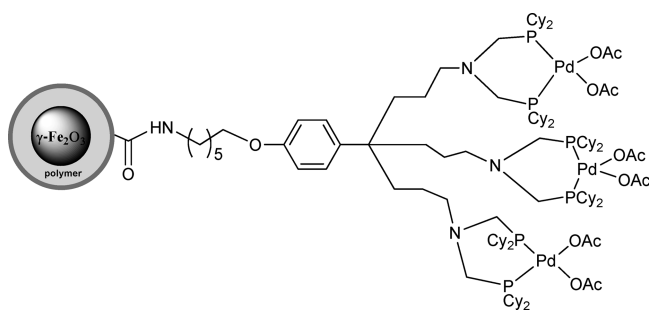
The authors believe that the excellent reusability and high stability of this catalyst could be correlated to the strong binding of  $\text{Pd}(\text{OAc})_2$  to the modified  $\text{Fe}_3\text{O}_4$ . Unfortunately, the coupling of readily available and low-cost aryl chlorides was not reported in this work.

Heuzé and colleagues synthesized a metallodendron functionalized with a dicyclohexyl–diphosphino palladium complex (Scheme 33).<sup>88</sup> The grafting of this dendron onto core–shell  $\gamma\text{-Fe}_2\text{O}_3/\text{polymer}$  300 nm MNPs was studied on the basis of the peptide reaction via covalent bond formation between the terminal primary amino group and the carboxyl group of the MNP polymer shell. The grafting efficiency was estimated from a Suzuki catalytic reaction of iodobenzene and phenylboronic acid and optimized by a convergent approach to give optimal catalytic reactivity in cross-coupling reactions. The formation of NP aggregates and consequently low catalytic activity in some

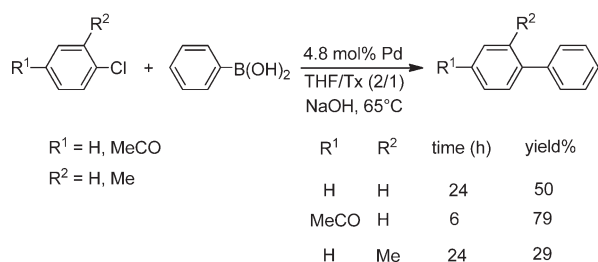
**Scheme 32. Reuse of the Catalyst in the Coupling of Phenylboronic Acid and 4-Bromoanisole**



**Scheme 33. Synthesis of Dendron-Functionalized Core–Shell Super Paramagnetic Nanoparticles**



**Scheme 34. Suzuki Cross-Couplings of Aryl Chlorides with Phenylboronic Acid Using Grafted MNPs**

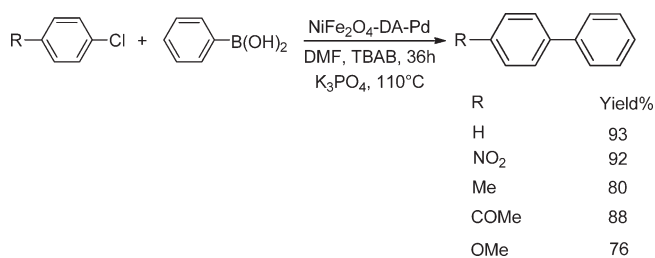


materials were observed in DMF and in aqueous medium with a nonionic surfactant. The optimum grafting efficiencies were obtained either in an aqueous medium (in the presence of a nonionic surfactant; e.g., triton X405, Tx) or in an organic/aqueous medium. After optimization of the grafting conditions, the activity of the MSC was investigated in the Suzuki coupling of a series of haloarenes with phenylboronic acid in THF/Tx using NaOH as a base.

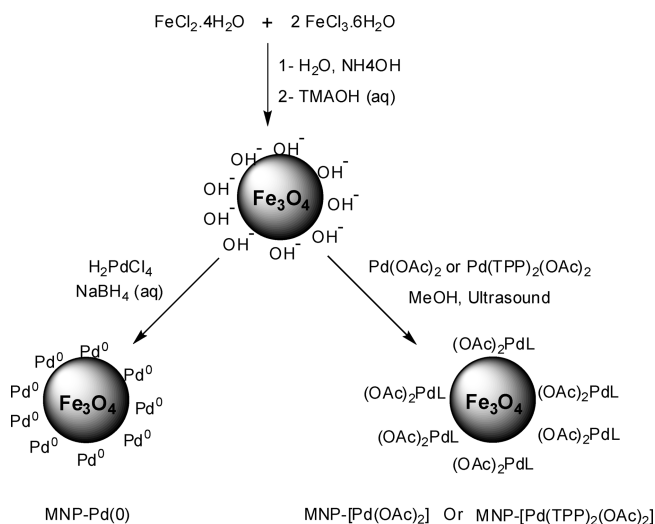
This catalyst showed excellent catalytic activities for the coupling of a range of iodo and aryl bromides, which were obtained in good to excellent yields. However, the coupling of aryl chlorides (such as chlorobenzene, 2-chlorotoluene, and 4-chloroacetophenone) with phenylboronic acid required higher catalyst loading, longer reaction times, and higher temperatures (Scheme 34). After reaction completion, the catalysts were readily recovered using a simple magnet to attract the super paramagnetic grafted nanoparticles. The recycling of the catalyst was briefly examined in the coupling of iodobenzene and phenylboronic acid. The results revealed that this catalyst could be reused for more than 25 consecutive runs without a loss of activity.<sup>88</sup>

He and colleagues synthesized a palladium catalyst that was based on magnetic nanoparticles by a “bottom-up” approach, and its catalytic behavior was investigated in the cross coupling of acrylic acid with iodobenzene.<sup>89</sup> The catalyst showed good performance on the first run relative to the traditional palladium catalysts supported on silica, alumina, and carbon. The authors indicated that upon recycling, the activity of the material was poor and heavily influenced by the choice of base in the reaction and by metal leaching, both of which contribute to the decrease in reactivity. More recently, Veinot and colleagues demonstrated that Fe–Fe<sub>x</sub>O<sub>y</sub> can be used as versatile supports to immobilize catalytic palladium species.<sup>90</sup> Immobilization is readily achieved

**Scheme 35. Suzuki–Miyaura Cross-Couplings of Aryl Chlorides with Phenyl Boronic Acid**

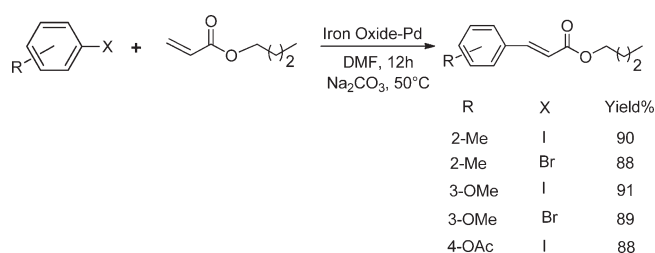


**Scheme 36. Preparation of MNP-Supported Palladium Catalysts**



via coordination of palladium to the iron oxide surface and subsequent reduction of these coordinated ions to their metallic state by the iron core. This material exhibited excellent activities in the Suzuki coupling of various aryl iodides and bromides, bearing either electron-withdrawing or -donating groups, in a mixture of water/ethanol (1:1) at room temperature under air. However, these conditions were not effective for widely available, low-cost aryl chlorides. The coupling of the activated 1-chloro-4-nitrobenzene with phenylboronic acid yielded only 25% of coupling product after 36 h at 80 °C. Negligible palladium leaching was observed, and the authors believe that Pd leaching might be promoted by the oxidative addition of bromobenzene to the Pd<sup>0</sup> surface. Recycling of the catalytic system was also studied in the synthesis of biphenyl from bromobenzene and phenylboronic acid; only a slight loss of activity was observed after three cycles.

Starting from NiFe<sub>2</sub>O<sub>4</sub>, Manorama and colleagues designed a novel catalyst system by anchoring Pd(0) nanoparticles on the surface of dopamine-modified NiFe<sub>2</sub>O<sub>4</sub> nanoparticles. These Pd(0) nanoparticles were anchored via reduction of Na<sub>2</sub>PdCl<sub>4</sub> with hydrazine monohydrate.<sup>64</sup> This material showed good activity in the Suzuki coupling of aryl bromides and iodides in the presence of K<sub>2</sub>CO<sub>3</sub> as a base and DMF as a solvent (temperatures ranging from 45 to 65 °C). For the reaction of aryl chlorides, this system gave satisfactory results in terms of yield; however, high temperatures and long reaction times were

**Scheme 37. Heck Cross-Coupling with Iron Oxide-Supported Palladium Nanoparticles**

needed in addition to the use of a phase-transfer agent (Scheme 35). The authors additionally indicated that the conversion of chlorobenzene with phenyl boronic acid could be maintained above 90% after three recycling steps. The presence of dopamine in the  $\text{NiFe}_2\text{O}_4$ -dopamine-Pd catalytic system enhances efficiency by acting as a ligand during the coupling processes.

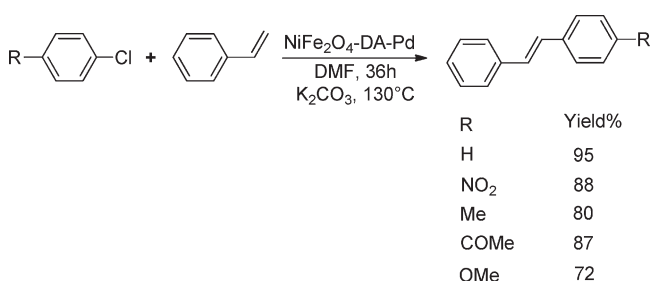
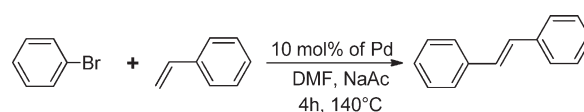
Rossi and co-workers also reported the preparation of supported palladium nanoparticles (NPs) stabilized by pendant phosphine groups by reacting a palladium complex containing the ligand 2(diphenylphosphino)-benzaldehyde with an amino-functionalized silica surface.<sup>91</sup> This catalyst showed good catalytic activity in the Suzuki reaction of several bromides with phenylboronic acid, but it was inactive for aryl chlorides. The catalyst could be recycled and reused for up to 10 recycles.

Along a similar line, Plucinski and co-workers also reported the synthesis of three MNP-supported palladium systems using a simple procedure (Scheme 36).<sup>92</sup> These nanoparticles loaded onto the magnetic supports have been used as catalysts for the Suzuki reaction between phenylboronic acid and bromobenzene as well as the Heck reaction between styrene and 4-bromonitrobenzene. On the basis of the kinetics of the reactions, it was determined that the reaction is not diffusion limited, but is influenced by the chemical nature of the aryl bromide. These supported nanoparticles have consistently resulted in very high yields of products of a variety of Suzuki and Heck cross-coupling reactions as well as other types of reactions such as hydrogenations. The results of palladium leaching investigations indicate that the catalyst instability was mainly caused by the presence of aryl bromide. The kinetic screening for catalyst reuse showed loss of activity over each subsequent cycle.

**4.3.2. Heck Reactions.** The Heck reaction is one of the most noteworthy and comprehensively employed reactions for the formation of carbon-carbon bonds, resulting in the arylation, alkylation, or vinylation of various alkenes by coupling with aryl halides.<sup>93-95</sup> Similar to the Suzuki cross-coupling, the development of efficient separable and recyclable catalysts remains a major scientific challenge and an aspect of economical relevance. This section focuses on some of the recent advances on the development of relevant MSCs to be utilized in Heck couplings.

Gao and colleagues reported that their Pd/N-heterocyclic carbene complex (highly active in Suzuki cross-coupling reactions) could also be applied to the Heck coupling of aryl halides with *n*-butyl acrylate (Scheme 37).<sup>81</sup> The recycling of this catalytic system was explored in the model coupling of 2-iodotoluene and *n*-butyl acrylate. Reported results indicated the catalyst could be recycled five times without any loss of activity.

Manorama and Baruwati also demonstrated that their  $\text{NiFe}_2\text{O}_4$ -dopamine(DA)-Pd catalytic system was highly active

**Scheme 38. Results of the Heck Cross-Coupling Reaction of Aryl Chlorides with Styrene****Scheme 39. MNP-Supported Catalyst as a Catalyst for Heck Coupling Reactions**

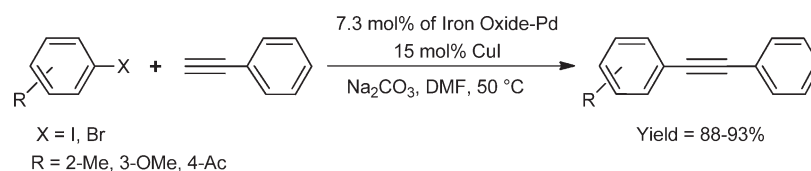
and selective in Heck couplings, showing good conversions and selectivity for coupling products in the reaction of aryl iodides and bromides with styrene at mild temperatures (45 or 65 °C), using  $\text{K}_2\text{CO}_3$  as a base and DMF as a solvent.<sup>64</sup> However, the coupling of aryl chlorides required significantly longer times and higher temperatures and provided lower yields as compared to aryl iodides and bromides (Scheme 38). No significant loss in catalytic activity was observed for the immobilized catalyst after three reaction cycles; recycling of the nanoparticles was achieved by magnetic concentration followed by washing with chloroform and drying at room temperature under vacuum before reuse in another run.

Yinghuai and colleagues also demonstrated the use of supported ultrasmall (less than 1 nm) palladium on magnetic nanoparticles in the Heck coupling of bromobenzene with styrene.<sup>85</sup> In the presence of 10 mol % Pd and sodium acetate as the base, the catalyst produced the desired products at moderate yields (Scheme 39). The MNP could be recovered via magnetic attraction and, upon washing with an organic phase and water, could be recycled at least five times without a significant decrease in activity.

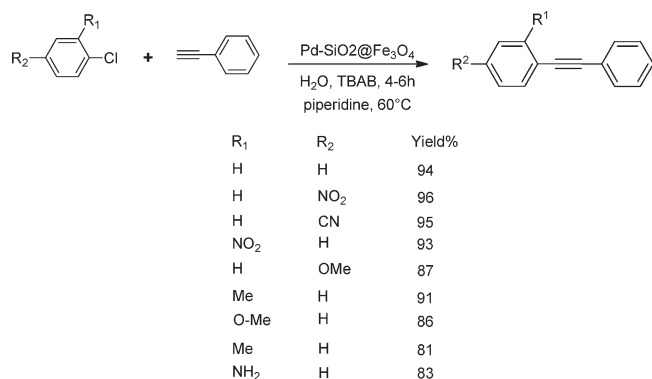
In 2006, Jang et al. prepared magnetic carboxylated polypyrrole nanotubes (MCPPyNTs) as supports for Pd-nanoparticles.<sup>96</sup> The resulting catalyst showed excellent activities in the Heck coupling of a range of aryl iodides with *n*-butylacrylate and/or styrene, with yields over 97%. In addition, the catalyst was more active than its carbon-supported analogues. The authors believe that the observed increase in yields may be due to the higher available surface area of the Pd nanoparticles. Importantly, there was no loss of catalytic activity in the conversion of the nonactivated aryl iodides and no morphological changes in the catalyst upon recycling and continuous reuse of the MSC (up to five times). However, the coupling of aryl bromides and chlorides was not reported for this system, and a study on a more diverse array of substrates is necessary to determine the scope of this catalyst in Heck coupling reactions.

Zhang prepared magnetic composite microsphere-supported palladium complex catalysts by immobilizing Pd nanoparticles on the surface of magnetic composite microspheres and demonstrated

Scheme 40. Sonogashira Cross-Coupling with Iron Oxide-Supported Palladium Particles



Scheme 41. Sonogashira Cross-Coupling of Aryl Chlorides and Phenylacetylene



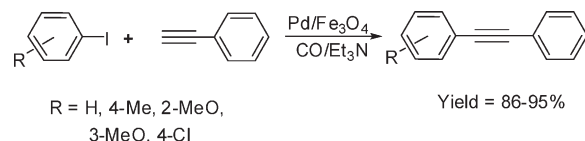
their use as heterogeneous catalysts in the Heck reaction.<sup>97</sup> Good-to-excellent yields of coupling products were obtained from iodides with acrylic acid at 95 °C for 3 h (using DMF as a solvent and tributylamine as a base). In addition, no *cis*-product was observed. However, the coupling of aryl bromides required longer times and higher reaction temperatures and gave significantly lower yields relative to aryl iodides. The novel catalyst can be easily recovered using a permanent magnet and can be reused at least six times without any loss of catalytic activity in the coupling of acrylic acid and iodobenzene.

**4.3.3. Sonogashira Reactions.** Pd-catalyzed alkynylation has emerged as an important method for the synthesis of alkynes over the last quarter century. The preparation of conjugated aryl alkynes is likewise of great interest in materials science because of their widespread presence in many bioactive natural products.<sup>98–100</sup> In contrast to Suzuki reactions, there are relatively few examples of the use of MSNP systems in Sonogashira couplings.

Encouraged by the results obtained in the Suzuki and Heck coupling reactions, the group of Gao also tested their MNP-supported NHC-coordinated Pd system in the Sonogashira cross-coupling reaction of aryl halides and phenyl acetylene.<sup>81</sup> A variety of electron-rich and -poor aryl iodides and bromides were successfully alkynylated at good yields with 7.3 mol % of catalyst in the presence of sodium carbonate as a base and 15 mol % of copper cocatalyst, but a study of a more diverse array of substrates is necessary to more fully determine the scope of this catalyst (Scheme 40). The recyclability of this catalyst was also explored in the coupling of 2-iodotoluene and phenyl acetylene; the catalyst could be recycled at least five times with no detectable deactivation.

Jin and colleagues also demonstrated that their MNP-supported catalyst was highly active in the Sonogashira coupling of aryl halides in the absence of a copper cocatalyst.<sup>83</sup> In addition, this catalyst provided the first successful example of a heterogeneous Sonogashira protocol that used aryl chlorides as

Scheme 42. Sonogashira Carbonylative Coupling of Alkynes and Aryl Iodides



substrates in aqueous media. This catalyst successfully coupled a wide array of chlorides, including electron-rich substrates in the presence of only 0.5 mol % catalyst (Scheme 41), whereas hindered chlorides (including 2-chloro-1,3-dimethylbenzene) required higher temperatures (80 °C) and longer reaction times to achieve comparable results. The recycling of the catalyst was also examined in the coupling of 4-chloroanisole with phenyl acetylene. The conversion in the systems could be maintained above 95% after 10 recycling steps.

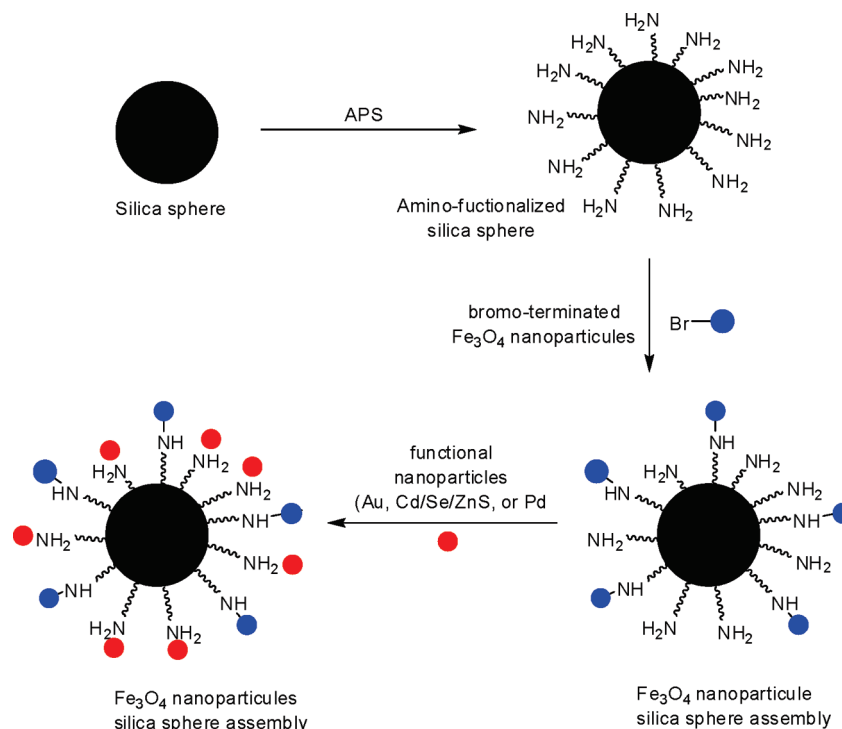
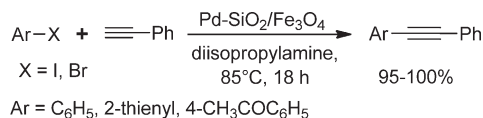
Xia and co-workers also developed a highly efficient Pd(0) catalyst immobilized on Fe<sub>3</sub>O<sub>4</sub> nanoparticles for the carbonylative Sonogashira coupling reaction of aryl iodides with terminal alkynes under phosphine-free conditions (Scheme 42).<sup>101</sup> This magnetic catalyst was synthesized through a wet impregnation incorporating palladium nanoparticles and superparamagnetic Fe<sub>3</sub>O<sub>4</sub> nanoparticles in KBH<sub>4</sub> solution. The catalyst showed high activity and could be recovered and reused seven times without significant loss in catalytic activity and selectivity. However, the coupling of aryl bromides and chlorides was not reported for this system.

Hyeon and co-workers reported a nice method of preparing multifunctional nanoparticles assemblies on silica spheres.<sup>102</sup> Uniform silica spheres synthesized by the Stöber method were first functionalized with amino groups by reaction with 3-aminopropyltrimethoxysilane (APS). To assemble the magnetic nanoparticles on the silica spheres, Fe<sub>3</sub>O<sub>4</sub> nanoparticles were treated with 2-bromo-2-methylpropionic acid and coupled with the amino groups. The subsequent functionalization of the remaining amino groups with Au, CdSe/ZnS, and Pd afforded multifunctionalized silica spheres (Scheme 43).

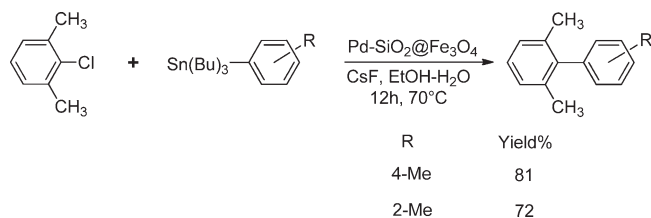
The performances of one of these catalyst, Pd/SiO<sub>2</sub>-Fe<sub>3</sub>O<sub>4</sub>, have been evaluated in cross-coupling Sonogashira reactions of aryl iodides and bromides (Scheme 44). The recycling studies have shown that the catalyst can be readily recovered and reused several times. However, the catalyst showed a constant decrease in activity over four recycling processes.<sup>102</sup>

**4.3.4. Stille Reactions.** The cross-coupling reaction using organostannane compounds, known as the Stille reaction, has widespread use in organic synthesis due to the growing availability of organostannanes, their stability in moisture and air, and their excellent compatibility with a large variety of functional groups.<sup>103–105</sup> Stille cross-coupling has played a pivotal role in a number of syntheses, including those of rapamycin and

Scheme 43. Synthetic Procedure To Obtain Multifunctional Nanoparticle/Silica Sphere Assemblies

Scheme 44. Sonogashira Coupling Reactions with Magnetic Pd–SiO<sub>2</sub>/Fe<sub>3</sub>O<sub>4</sub> Catalyst

Scheme 45. Sonogashira Coupling of 2-Chloro-1,3-dimethylbenzene



dynemicin.<sup>106–108</sup> Unfortunately, no remarkable progress has been made toward developing nanoparticle-supported palladium to accomplish Stille couplings. The first example of such a process was provided by Jin and colleagues, who reported a heterogeneous Pd–SiO<sub>2</sub>/Fe<sub>3</sub>O<sub>4</sub> catalyst in the cross-coupling of aryl chlorides with organostannanes.<sup>83</sup> Electron-deficient and electron-rich aryl chlorides reacted with allyltributyltin to give the cross-coupling products in excellent yields in the presence of 0.5 mol % of catalyst at 50 °C. In addition, 1-chloronaphthalene and 9-chloroanthracene were successfully coupled with tributylphenylstannane in good yields (91% and 92%, respectively). Sterically hindered substrates, such as 2-chloro-1,3-dimethylbenzene,

could also be coupled under the investigated conditions (Scheme 45). Most importantly, the catalyst was found to be active for the coupling reactions of unprotected 4-chlorophenol and 2-chloroaniline. Unfortunately, the reusability of the catalysts in the Stille reaction was not reported for these systems.

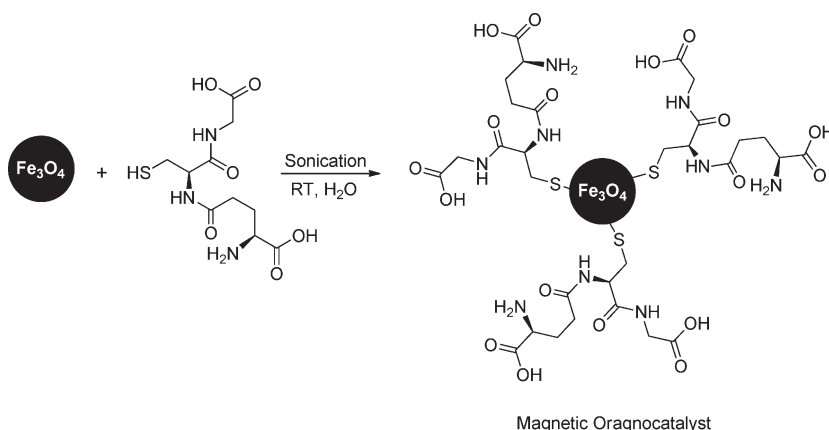
#### 4.4. Magnetically Separable Organocatalysts

Organocatalysis, catalysis using organic molecules without any metals, has become a very significant area of research, and this metal-free approach has attracted worldwide attention.<sup>109</sup> A range of important reactions have benefited from developments in this area.<sup>110–112</sup> This environmentally benign approach has been made even greener by grafting the organocatalysts onto solid supports<sup>113,114</sup> and by using alternative energy sources.<sup>115</sup> The first magnetically separable nano-organocatalysts were developed by Polshettiwar et al. using glutathione, which is a tripeptide consisting of glutamic acid, cysteine, and glycine units and is a ubiquitous antioxidant present in human and plant cells. Sonochemical covalent anchoring of glutathione molecules via coupling of its thiol group with the free hydroxyl groups of ferrite surfaces rendered an interesting nano-organocatalyst (Scheme 46).<sup>116,117</sup>

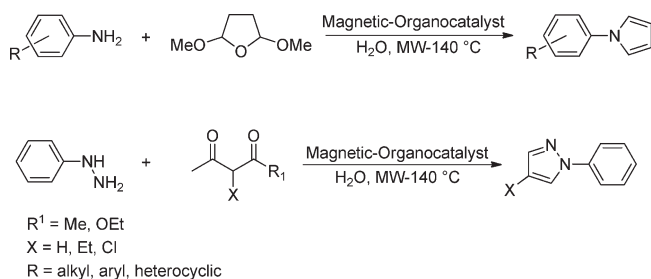
This glutathione-based magnetic nano-organocatalyst showed remarkable efficiency in the Paal–Knorr synthesis of a series of pyrrole heterocycles under aqueous microwave (MW) conditions.<sup>116</sup> Notably, this aqueous reaction protocol proceeded in the absence of a phase-transfer catalyst due to the selective absorption of microwaves by the reactants, nano-organocatalyst, and aqueous medium. A series of hydrazines and hydrazides also reacted with 1,3-diketones, providing the corresponding pyrazoles in good yields (Scheme 47).<sup>117</sup>

Because of the magnetic nature of the catalyst, it could be recovered within a few seconds using an external magnet. Most importantly, the product phase naturally separated from the

## Scheme 46. Magnetically Separable Glutathione-Based Organocatalyst



## Scheme 47. Paal–Knorr Reactions and Pyrazole Synthesis Using Nano-organocatalysts



aqueous medium after completion of the reaction, which in turn enabled the isolation of the final product by simple decantation (Figure 2).<sup>116,117</sup>

Afterward, Luque and Varma extended this technique, for the catalytic activity in homocoupling of arylboronic acids under microwave irradiation using a magnetically separable glutathione-based organocatalyst.<sup>118</sup> This catalyst provided good yields for a range of substrates, which incorporate electron-donating or -withdrawing substituents at the ortho or para position (Scheme 48); however, it was less active toward pyridyl and pyrazole boronic acids. The recycling of the nanoferrite-anchored glutathione catalyst has been examined in the homocoupling of phenylboronic acid. Recycled catalyst was used in a repeat reaction without any appreciable loss of activity.

Another nano-organocatalyst was prepared by grafting stable nitroxyl radical 2,2,6,6-tetramethylpiperidine-1-oxyl (TEMPO) onto graphene-coated nanobeads with a magnetic cobalt core using “click” chemistry (Scheme 49). The as-synthesized CoNP–TEMPO showed high catalytic activity in the chemoselective oxidation of primary and secondary alcohols (bleach was used as a terminal oxidant). The catalyst could be reused for several reaction cycles without any considerable loss in activity. In addition, the magnetic nature of catalyst enabled its facile isolation and recycling by magnetic decantation.<sup>119</sup>

Another interesting example of a magnetic organocatalyst is a chiral 4-*N,N*-dimethylaminopyridine (DMAP) analogue supported on magnetic NPs.<sup>120</sup> This catalyst exhibited high enantioselectivity and excellent recyclability in the kinetic resolution of sec-alcohols (Scheme 50). The enhanced enantioselectivity of

## NO USE OF SINGLE DROP OF ORGANIC SOLVENTS

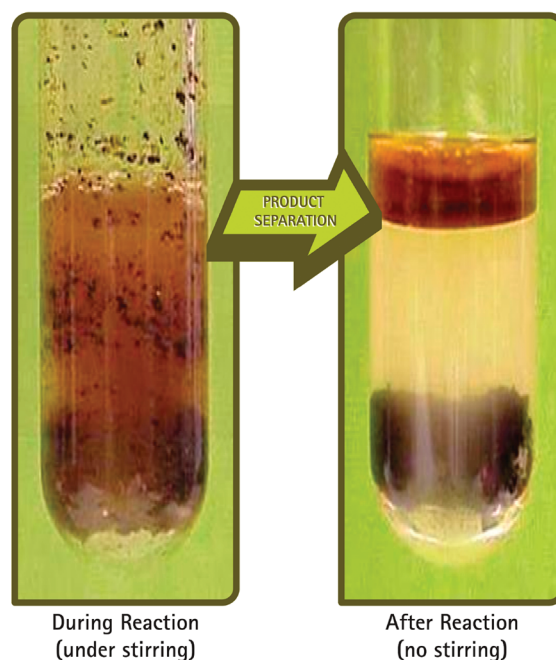
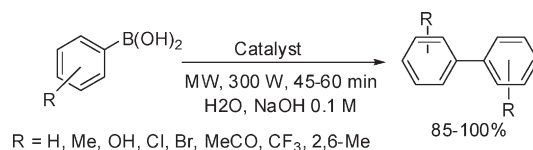


Figure 2. Product isolation in pure aqueous medium without using organic solvents.

## Scheme 48. MW-Assisted Aqueous Homocoupling of Substituted Arylboronic Acids Using Nanoferrite Glutathione as Catalyst



this chiral organocatalyst relies on a confluence of weak, easily perturbed van der Waals and hydrogen-bonding interactions that seem to promote enantioselective reactions. The synthesis of the immobilized catalyst was based on supporting a stable, easily synthesized chiral DMAP analogue onto a robust NP support.

The resultant material was insensitive to air/moisture, easily recoverable using an external magnetic field, and highly effective in the acylation of a range of sec-alcohols with variable steric and electronic characteristics under process-scale friendly conditions (room temperature, low catalyst loading, and acetic anhydride as the acylating agent). The level of enantio-discrimination in the reaction was comparable to that obtained with the corresponding homogeneous catalyst, and thus the resolved alcohols could be isolated with excellent enantiomeric excess. The catalyst was recyclable to an unprecedented extent, and the high activity and selectivity profiles were well retained even after a minimum of 32 consecutive cycles.

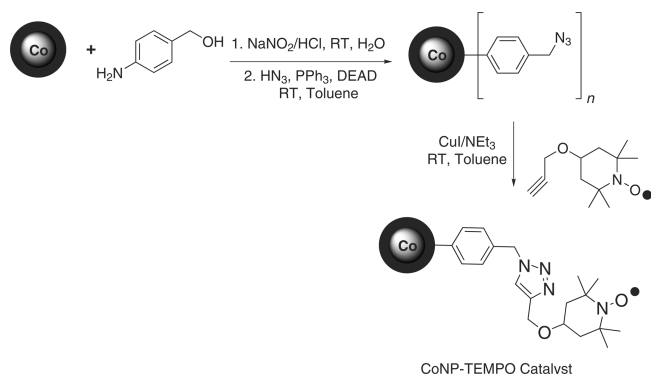
#### 4.5. Hydroformylation Reactions

Hydroformylations are one of the most important synthetic transformations developed in the 20th century with large-scale industrial applications.<sup>121–123</sup> The amount of hydroformylation products produced per year reflects its importance. Separation of the expensive Rh-based catalyst was first achieved by Kuntz, using the now well-known TPPTS ligand.<sup>121</sup> Magnetic nanocomposite

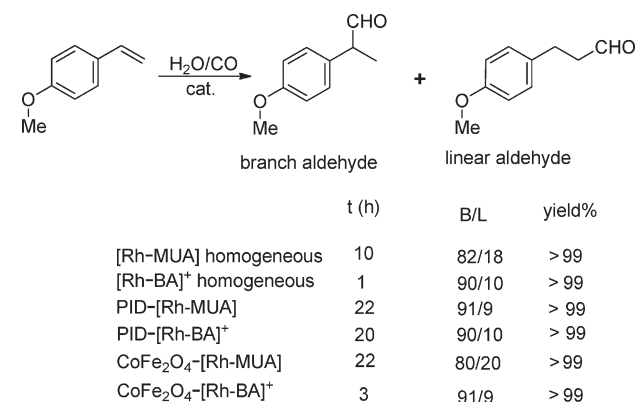
systems could also be helpful in this process, although relatively few reports have dealt with their application in the hydroformylation of olefins.

A research group led by Yoon immobilized neutral and cationic Rh complexes  $[\{\text{Rh}(1,5\text{-COD})(\mu\text{-S}(\text{CH}_2)_{10}\text{CO}_2\text{H})\}_2]$  ( $[\text{Rh-MUA}]$ ; MUA = 11-mercaptoundecanoic acid) and  $[\text{Rh}(1,5\text{-cod})(\eta^6\text{-benzoic acid})]\text{BF}_4$  ( $[\text{Rh-BA}]^+$  (BA = benzoic acid) on various supports, including poly(iodomethylstyrene-co-divinylbenzene) (PID) and magnetic cobalt nanoferrite ( $\text{CoFe}_2\text{O}_4$ ) as micrometer-sized supports.<sup>124,125</sup> The carboxylic acid functional group in the cationic rhodium complex was able to bind to the surface of the magnetic Co-ferrite nanoparticles through  $\pi$ - $\pi$  interactions.<sup>126</sup> Furthermore, the cationic nature of the complex generated several cationic sites around the nanomagnet, which in turn led to the formation of stable magnetic nanoparticles without any aggregation in organic solution (not even in dilute systems). The cationic catalyst  $[\text{Rh-BA}]^+$  showed much higher activity than the neutral  $[\text{Rh-MUA}]$ . As expected, both catalysts exhibited inferior activities upon immobilization on the micrometer-size support,

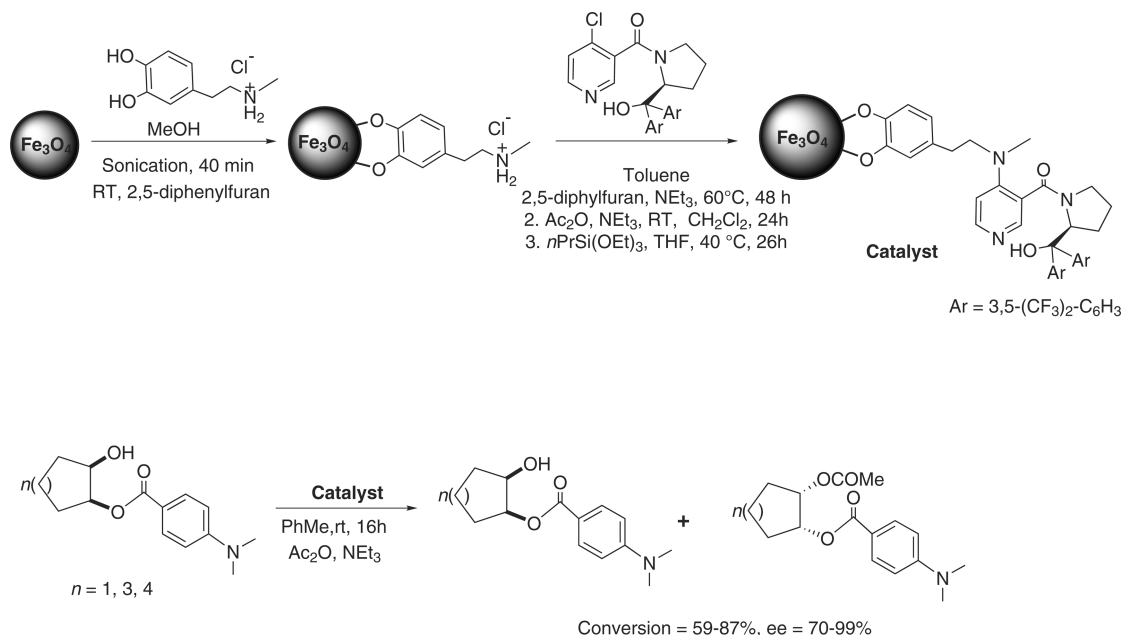
**Scheme 49.** Synthesis of the Magnetic CoNP-TEMPO Catalyst System



**Scheme 51.** Hydroformylation of 4-Vinylanisole



**Scheme 50.** Preparation of Immobilized Chiral 4-*N,N*-Dimethylaminopyridine (DMAP) Analogues for Asymmetric Acylations

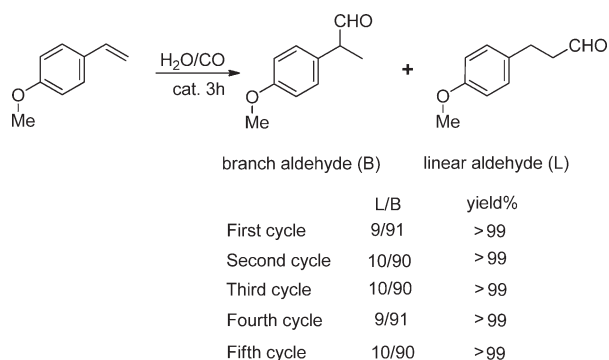


mostly due to steric and diffusion effects (Scheme 51). However, despite a reduction in activity by two-thirds as compared to its homogeneous counterpart, the MNP-supported catalyst ( $\text{CoFe}_2\text{O}_4\text{--}[\text{Rh--BA}]^+$ ) can be considered an interesting alternative to catalysts immobilized on other support materials.

The recycling of  $\text{CoFe}_2\text{O}_4\text{--}[\text{Rh--BA}]^+$  was also investigated in the hydroformylation of 4-vinylanisole; the catalyst was able to be recycled at least five times without loss of activity (Scheme 52).

Dendritic catalysts largely rely on the supramolecular properties of the molecules.<sup>127</sup> An important contribution in the development of efficient MSCs for hydroformylation chemistry was reported by Alper and colleagues in 2006.<sup>128</sup> In this study, they developed a methodology to heterogenize active Rh-catalysts by growing polyaminoamido dendrons on silica-coated nanoferrites. Up to three generations, G0, G1, and G2, were

**Scheme 52. Recycling of  $\text{CoFe}_2\text{O}_4\text{--}[\text{Rh--BA}]^+$  Catalyst over Five Cycles**

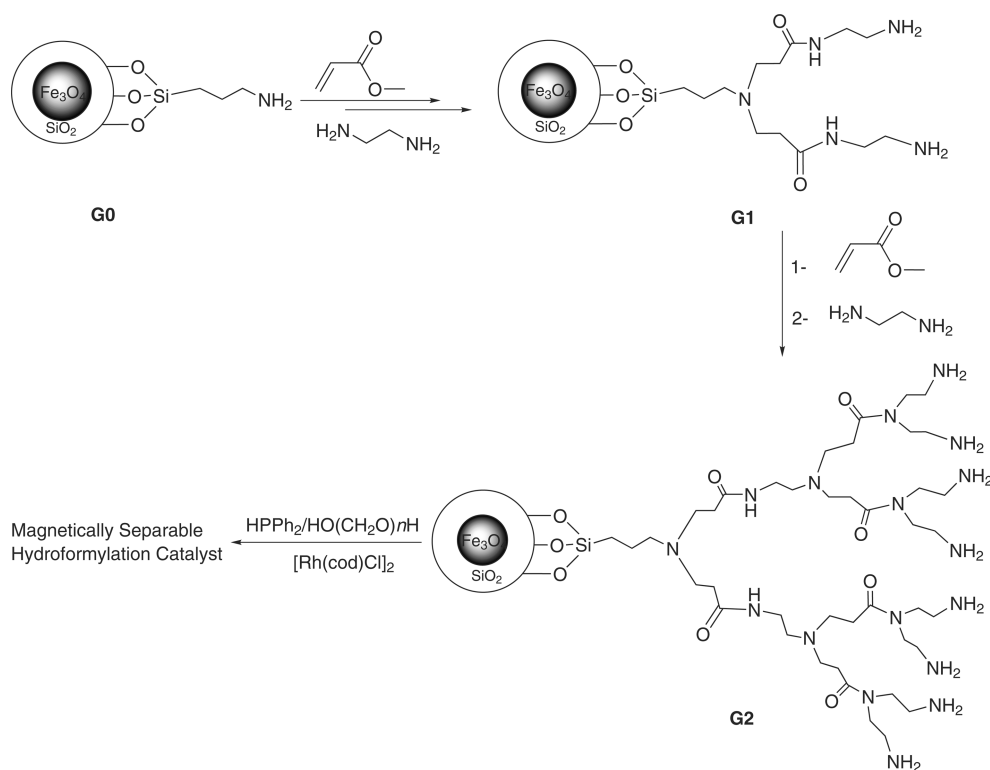


constructed through two subsequent steps of Michael-type addition of methyl acrylate followed by amidation with ethylenediamine (Scheme 53). After phosphination of each generation followed by complexation with  $[\text{Rh}(\text{cod})\text{Cl}_2]$ , these materials were employed as catalysts in hydroformylation reactions. The ensuing catalysts were reported to be stable and increased solubility in organic solvents; they were able to catalyze the reaction with an excellent reactivity and selectivity. These systems were recovered using an external magnet, followed by washing with dichloromethane, flushing with nitrogen, and subsequent reuse in the hydroformylation of styrene. The catalyst could be recycled up to five times without significant loss in activity or selectivity. However, the G(0) catalyst was far less reactive in the fifth run (from 99% to 69% yield after five cycles). This interesting concept (of using dendronized MNPs as supports) may be extended to other catalyst systems for various organic reactions.

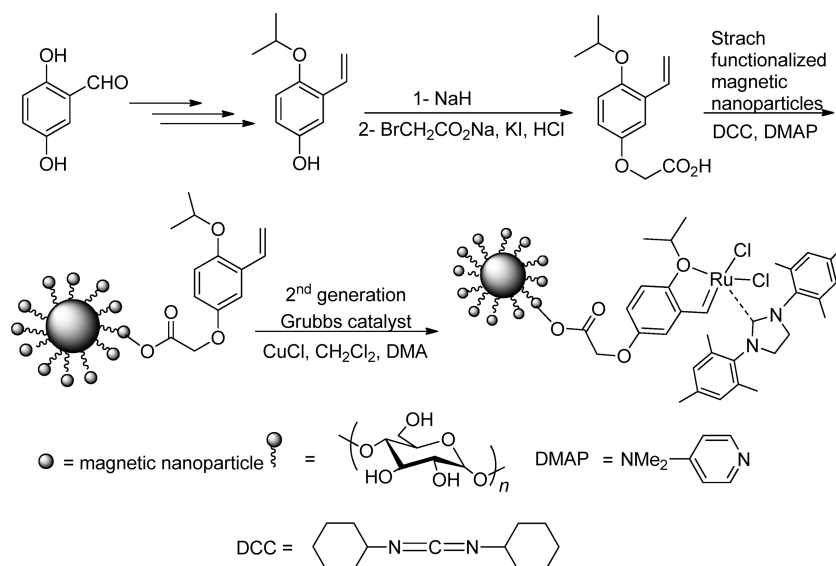
#### 4.6. Olefin Metathesis

Olefin metathesis, discovered in the 1960s by Banks and Bailey,<sup>129</sup> including ring-closing, ring-opening, and cross metathesis reactions, opened new industrial routes to important petrochemicals, polymers, and specialty chemicals.<sup>130,131</sup> Recently, Grubbs and Hoveyda catalysts are widely used in homogeneous conditions for these types of reactions in particularly for functionalized olefins.<sup>132–138</sup> However, homogeneous metathesis catalysts present inherent drawbacks, including decomposition via bimolecular pathways and the need to use complex processes to separate the reactants/products from the catalysts. Overall, these issues can lead to ruthenium contamination of the products, which is not acceptable for the pharmaceutical or to some extent the polymer industry and also hinders the recycling and regeneration

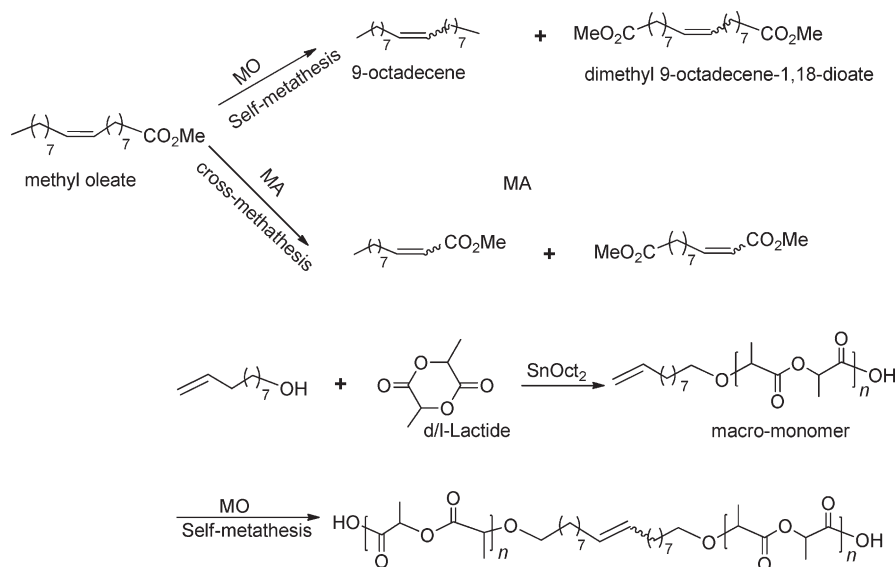
**Scheme 53. Synthesis of a Magnetically Separable Hydroformylation Catalyst**



Scheme 54. Immobilized MS Hoveyda–Grubbs Catalyst



Scheme 55. Metathesis Reactions of Methyl Oleate and Macro-monomer



of active catalysts. To overcome these problems, the heterogenization of ruthenium-based Grubbs and Hoveyda catalysts on magnetic supports offers an interesting alternative to improve the separation and recyclability properties of the catalysts.<sup>139,140</sup>

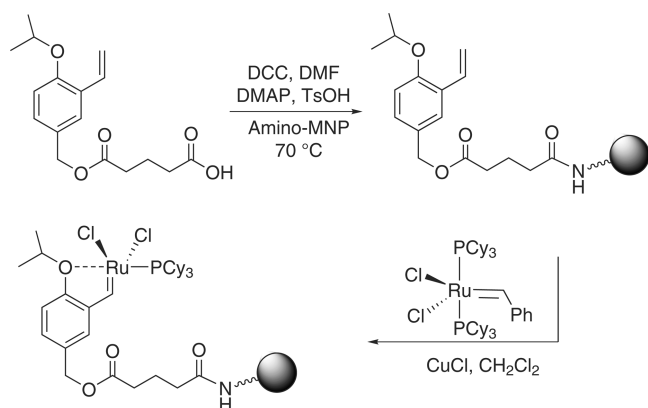
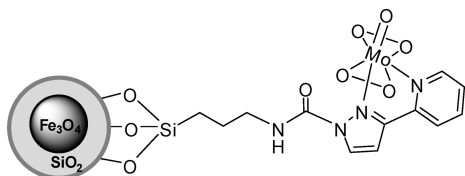
Yinghuai and colleagues successfully immobilized a second-generation Hoveyda–Grubbs catalyst on an MNP support with a mean diameter of 100 nm.<sup>141</sup> The catalyst was prepared via the immobilization of orthoisopropoxystyrene ligands on commercially available MNPs through covalent bonding followed by treatment with a second-generation Hoveyda–Grubbs catalyst to generate its magnetic version (Scheme 54).

This catalyst showed good activity for both self- and cross-metathesis reactions of methyl oleate (Scheme 55). In addition, the catalyst was found to be more active than the second-generation Grubbs catalyst and comparable to an unsupported second-generation Hoveyda–Grubbs catalyst in a cross-metathesis

reaction between methyl oleate (MO) and methyl acrylate (MA). Recycling studies have indicated that the catalyst can be readily recovered and reused several times with sustained activity.<sup>141</sup>

Interestingly, the group of Che also developed a novel type of Hoveyda–Grubbs catalyst by assembling magnetic nanoparticles with a Grubbs I catalyst.<sup>142</sup> Scheme 56 describes the synthesis of the magnetic nanoparticle-supported Hoveyda–Grubbs catalyst. The isopropoxystyrene derivative was first treated with glutaric anhydride in the presence of Et<sub>3</sub>N and DMAP to create 5-(4-isopropoxy-3-vinylbenzyloxy)-5-oxopentanoic acid, which was further reacted with amino-functionalized ferrite. The as-synthesized material was then coupled with a first-generation Grubbs catalyst in the presence of CuCl to produce the desired magnetic Hoveyda–Grubbs catalyst.

This catalyst exhibited excellent activity in ring-closing metathesis (RCM) reactions, comparable to homogeneous and

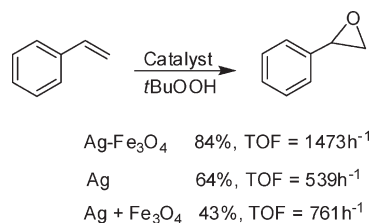
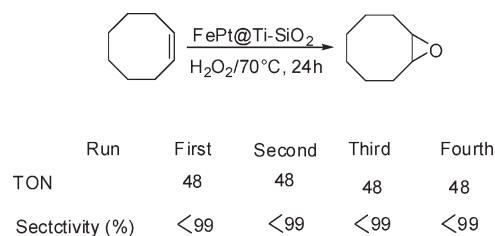
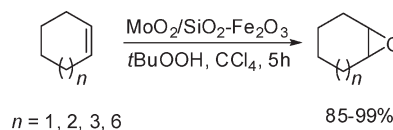
**Scheme 56.** Preparation of the Magnetic Hoveyda–Grubbs Catalyst**Scheme 57.** Molybdenumperoxo Catalyst for Olefin Epoxidation on Silica-Coated MNPs

other supported catalytic systems. Furthermore, the material could be readily recovered and reused 22 times in the RCM of *N*, *N*-diallyl-4-methylbenzenesulfonamide and 18 times in the RCM of *N*-allyl-*N*-(pent-4-enyl)-4-methylbenzenesulfonamide without any significant loss of activity.<sup>142</sup>

#### 4.7. Epoxidation Reactions

Epoxides, for example, ethylene- and propylene-oxide are important intermediates in industrial production of various chemicals, which is generally carried out through heterogeneous catalyst. Considering the economical importance of these oxides, new sustainable methods are needed. In this regard, Thiel and co-workers have demonstrated that organic–inorganic hybrid nanocatalysts synthesized by covalently anchoring [(*L*–*L*)-MoO(O<sub>2</sub>)<sub>2</sub>] (*L*–*L* = (3-triethoxysilylpropyl)[3-(2-pyridyl)-1-pyrazolyl]acetamide) on silica-coated MNPs were efficient catalysts for selective olefin epoxidation (Scheme 57).<sup>143</sup> The reaction worked well with series of substrates cyclooctene, cycloheptene, cyclohexene, styrene, and 1-octene in chloroform as a solvent and *tert*-butylhydroperoxide (*t*-BuOOH) as oxidant under reflux condition. Recycling studies have shown that the catalyst can be readily recovered and reused six times in the epoxidation of cyclooctene without significant loss of activity. The catalyst also showed significantly enhanced catalytic activity and recyclability as compared to similar molybdenum catalysts supported on mesoporous MCM-41 or silica nanospheres. The high activity and stability of this catalyst system are attributed to the uniform dispersion of the catalytically active sites on the surface and the strong interaction between the chelating ligand and the molybdenum center.

Zhang and co-workers also reported the preparation of a magnetically recoverable Ag/Fe<sub>3</sub>O<sub>4</sub> nanocomposite for the catalytic epoxidation of styrene.<sup>144</sup> The synthesis was performed

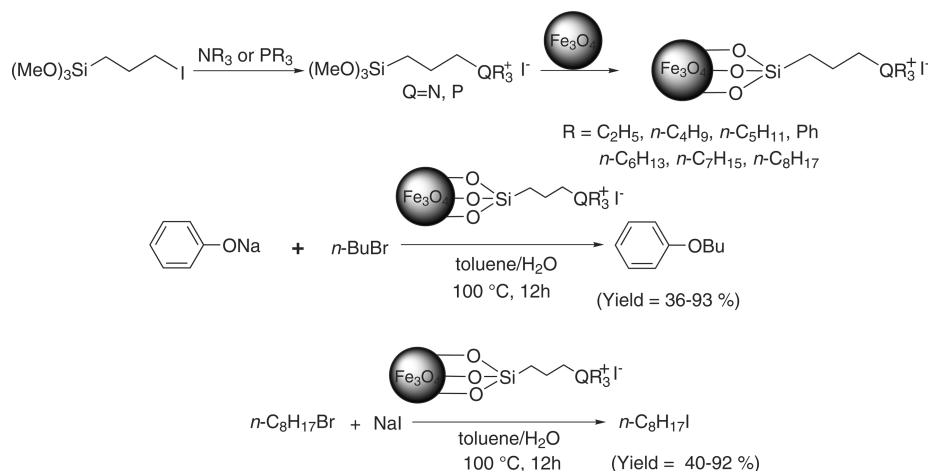
**Scheme 58.** Epoxidation of Styrene Using Magnetic Catalyst**Scheme 59.** Oxidation of Cyclo-octene Using FePt–Ti–SiO<sub>2</sub> and Recycling Experiment**Scheme 60.** Epoxidation of Olefins with *t*-BuOOH Catalyzed by the Magnetic-Mo Nano Catalyst

in one pot by the addition of AgNO<sub>3</sub> and FeCl<sub>3</sub> to a solution of ethylene glycol and polyvinylpyrrolidone, leading to a suspension of AgCl with Fe<sup>III</sup> cations in ethylene glycol. The Ag<sup>0</sup> was generated through reduction of Ag<sup>+</sup> by ethylene glycol, whereas Fe<sup>2+</sup> species were formed via reduction of a fraction of the Fe<sup>3+</sup> cations. The catalytic performance of the Ag–Fe<sub>3</sub>O<sub>4</sub> nanocomposite for the epoxidation of styrene has been evaluated in presence of *t*-BuOOH as the oxidant (Scheme 58). The obtained results showed that styrene oxide was formed in 84% yield after 13 h with a TOF of 1473 h<sup>-1</sup>. In addition, no deactivation is observed after the catalyst was recycled at least five times. The high catalytic activity as compared to other systems was explained by a synergetic interaction between the Fe<sub>3</sub>O<sub>4</sub> nanoparticles and the Ag nanocrystals.

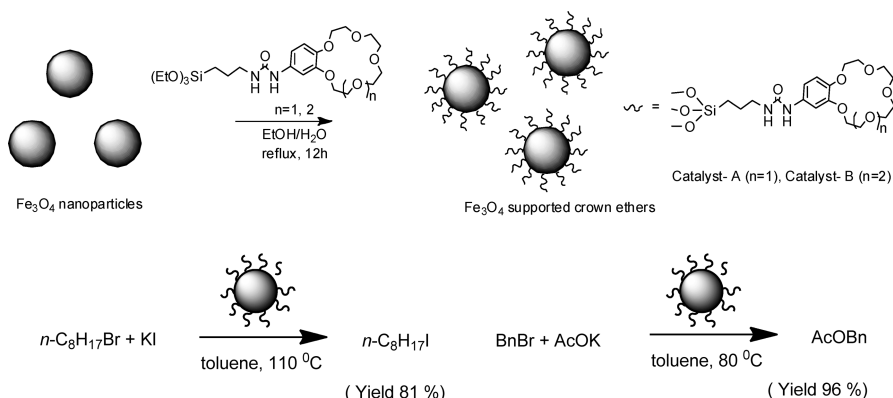
Mori and co-workers have synthesized a new spherical nanocatalyst, FePt/Ti–SiO<sub>2</sub>, by adopting a two-step coating method including a ligand-exchange step with (3-mercaptopropyl)-triethoxysilane and a sol–gel process using tetraethyl orthosilicate and tetrapropyl orthotitanate.<sup>145</sup> The Ti–oxide moiety was proven to exist in the isolated and tetrahedral form. This new nanocatalyst has been used four times with consistent activity in the liquid phase for selective epoxidation using hydrogen peroxide (Scheme 59). Recovery from the reaction mixture was readily achieved by applying an external permanent magnet, and the used catalyst could be recycled without any appreciable loss in activity.

Hyeon and co-workers also reported a new magnetically recyclable nanocomposite catalyst for the epoxidation of olefins

Scheme 61. Magnetically Heterogenized Phase-Transfer Catalyst



Scheme 62. Preparation of Magnetic Nanoparticle-Supported Crown Ethers and Their Corresponding Catalytic Application

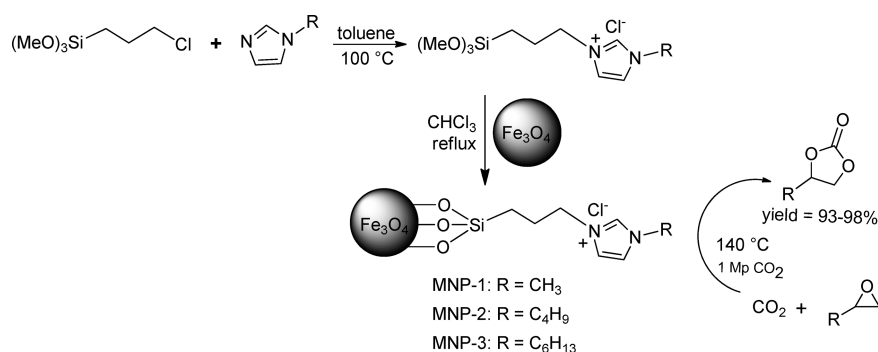


based on molybdenum oxide nanoparticles incorporated into a mesoporous silica shell that was coated on dense silica-coated magnetite nanoparticles (Scheme 60).<sup>146</sup> Haematite ( $\alpha\text{-Fe}_2\text{O}_3$ ) particles of about 400 nm in diameter obtained from a hydrothermal reaction were first stabilized with poly(vinylpyrrolidone) in water and then with a dense silica layer with the desired thickness ( $d = 50$  nm). An additional mesoporous silica shell was then generated on the surface of these particles by condensation of TEOS and *n*-octadecyltrimethoxysilane (C18-TMS).  $\text{MoO}_2$  was then introduced into the mesoporous silica shell by impregnation with ammonium molybdate followed by reduction with  $\text{H}_2$ . Recycling studies have shown that the catalyst can be readily recovered and reused six times without significant loss of activity.

#### 4.8. Magnetically Recoverable Catalysts in Miscellaneous Reactions

Apart from the previously discussed typical catalytic processes, magnetically recoverable materials have been reported to catalyze a wide range of related reactions with appreciable catalytic performance. Because of their robust nature, MSNPs can be modified with various functional groups. Functionalized magnetic materials are able to generate different types of catalytically active sites that can be employed in various reactions.

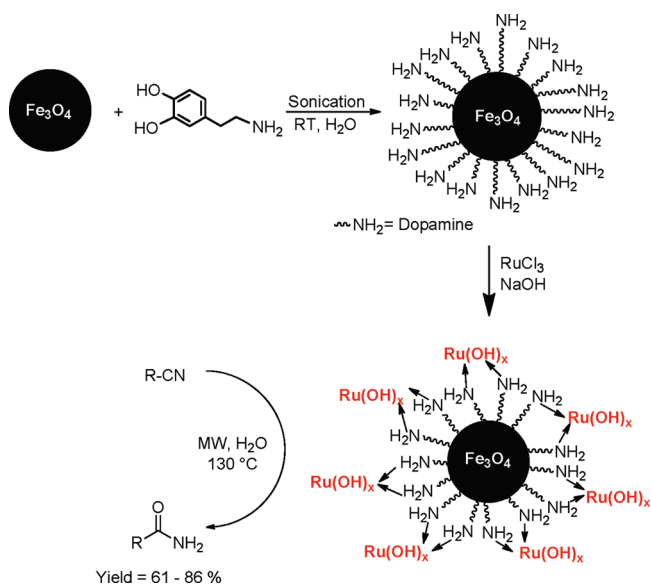
Catalytic phase-transfer processes have been recognized as environmentally benign alternatives to many homogeneous reactions. Phase-transfer catalysts (including quaternary ammonium and phosphonium salts, as well as crown ethers) have been utilized as versatile phase-transfer catalysts. Nevertheless, a practical problem related to phase-transfer catalysis is the difficulty of separating the products and starting materials from the catalysts in the final reaction mixture. The heterogenization of phase-transfer catalysts on MSNPs has shown some advantages in terms of stability and activity relative to other supports. The first example of MNP-supported quaternary ammonium and phosphonium salts and their catalytic activity in phase-transfer reactions was reported by Sato.<sup>147</sup> (3-Iodopropyl) trimethoxysilane was used as the bridge for tethering quaternary ammonium and phosphonium salts on magnetite (Scheme 61). The catalyst loading on magnetite was in the range of  $0.10\text{--}0.25 \text{ mmol g}^{-1}$ , and the catalysts were composed of nanometer-sized particles. These materials were investigated in the *O*-alkylation reaction of  $\text{PhONa}$  with *n*-BuBr and tetra-*n*-butylammonium iodide (TBAI), as well as with a PS resin-supported counterpart employed as a reference. The catalyst immobilized on magnetite-NPs possessed a conversion that was comparable to that of tetra-*n*-butylammonium iodide, relative to the much less effective PS resin-supported catalyst under identical reaction conditions.

**Scheme 63.** Fabrication of Magnetically Recoverable Ionic Liquid Catalysts and Their Application in the Reaction of CO<sub>2</sub> with Epoxides

Facile and rapid separation of the catalyst could be achieved by applying a simple magnet, and the catalyst was reusable without any significant loss of activity up to four times. Furthermore, the halogen exchange reaction of 1-bromooctane was investigated. The activity of the supported catalyst for this reaction was also almost identical to that of TBAI, although the yield was slightly reduced as compared to that of TBAI under the same reaction conditions.

Later, magnetic nanoparticle-supported crown ethers for catalytic solid–liquid (S–L) phase-transfer catalysis (PTC) were also developed by the same group (Scheme 62).<sup>148</sup> A silanization protocol was employed for the covalent attachment of crown ethers to magnetite NPs. The loading of crown ethers onto the magnetite nanoparticles ranged from 0.23 to 0.27 mmol g<sup>−1</sup>. A halogen exchange reaction of 1-bromooctane with KI was studied, and the MNP-supported crown ethers showed catalytic activity almost identical to the nonsupported system. The catalytic performance of these magnetically recoverable crown catalysts was strongly dependent on the ring size of the crown (the 18-membered crown ethers were generally more suitable to capture K<sup>+</sup> than were 15-membered crowns; thus, the 18-membered crown material provided superior activity). The MNP-supported catalyst B was much more efficient (96% conversion) than were the benzo crown ethers (3% conversion). Furthermore, catalyst A showed good catalytic activity (78% conversion), which was slightly superior to that of benzo-18-crown-6 (71% conversion), whereas benzo-15-crown-5 did not promote the reaction at all. The MNP-supported crown ether (catalyst B) was rapidly concentrated by placing an external magnet close to the sidewall of the reaction vessel, and it could be recycled at least eight times without any loss of catalytic activity.

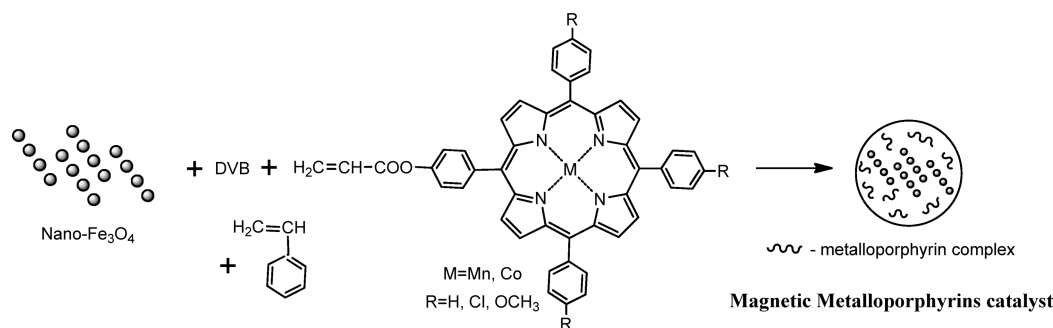
In addition to phase-transfer catalysts and crown ethers, ionic liquids can also be anchored to MNPs. Ionic liquids have been reported to act both as a reaction medium and as catalysts; they are increasingly being explored for targeted chemical tasks due to their modular and tunable structures and properties. MNP-supported ionic liquid materials were prepared following the procedure depicted in Scheme 63.<sup>149</sup> The ionic liquid precursors were prepared by quarternization of *N*-alkyl imidazole with 3-chloropropyl-trimethoxysilane and then attached to the MNPs (8–10 nm particle size), which were protected by a layer of silica (1–2 nm thickness) to prevent aggregation. The activity of these ionic liquid-coated magnetic Fe<sub>3</sub>O<sub>4</sub> NPs was then evaluated in the reaction of CO<sub>2</sub> and epoxides, which is an important and atom-economic transformation for the generation of valuable

**Scheme 64.** Synthesis of Nanoferrite–[Ru(OH)]<sub>x</sub> for the Hydration of Nitriles to Amides

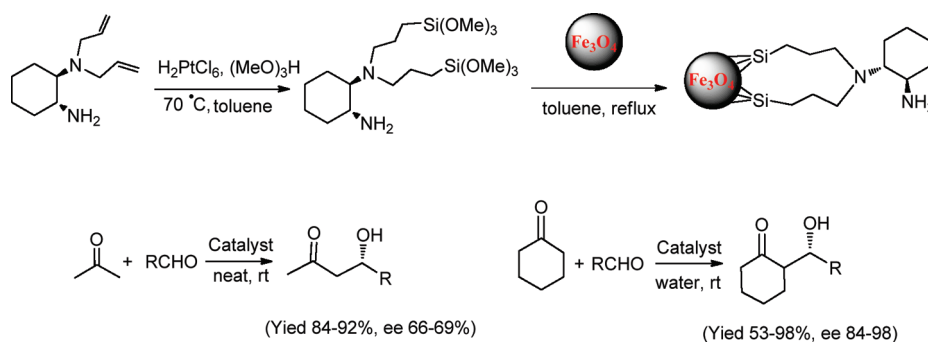
cyclic carbonates from CO<sub>2</sub>. Among the three catalytic systems tested, the MNP-1 catalyst demonstrated the highest activity in CO<sub>2</sub> cycloaddition reactions at a lower CO<sub>2</sub> pressure. The activity of the supported MNP-1 catalyst (87% yield for styrene carbonate) was comparable to that of the free [BMIM]Br catalyst (94% yield for styrene carbonate) for this reaction. Moreover, the recyclability of MNP-1 (which was evaluated using epichlorohydrin as the substrate) was excellent, and the material could be reused up to 11 times with essentially no activity loss. The reused catalyst had virtually unchanged morphology, even after 11 runs (as observed by TEM), and only a slight decrease in ionic liquid loading (from 0.60 to 0.58 mmol g<sup>−1</sup>) was observed.

The hydration of nitriles has great synthetic significance in the large-scale preparation of the corresponding amides because amides are a very important group of compounds in the chemical and pharmaceutical industry. Polshettiwar and Varma successfully conducted this reaction using nanoferrite-supported magnetically recyclable ruthenium hydroxide [Ru(OH)]<sub>x</sub> catalysts under benign aqueous conditions (Scheme 64).<sup>150</sup> The catalyst was prepared by surface reaction of ruthenium chloride with single-phase Fe<sub>3</sub>O<sub>4</sub> nanoparticles at a basic pH. However, the

Scheme 65. Synthetic Route for Magnetic Metalloporphyrin Catalysts



Scheme 66. Preparation of MNP-Supported Chiral Primary Amine Catalysts for Aldol Condensation



$\text{Fe}_3\text{O}_4$  nanoparticles (with a size range of 11–16 nm) had to be pretreated with dopamine in water for 2 h to avoid  $[\text{Ru}(\text{OH})]_x$  leaching from the support. This synthesis yielded  $[\text{Ru}(\text{OH})]_x$  (3.22 wt % Ru loading) supported on the amine-functionalized nanoferrite catalyst in excellent yields. The nanoferrite– $[\text{Ru}(\text{OH})]_x$  catalyst also showed high catalytic activity in the hydration of activated, inactivated, and heterocyclic nitriles in pure water under MW irradiation conditions. Meanwhile, the hydration of benzonitrile was evaluated to clarify the lifetime of the catalyst and its level of reusability, both of which are important factors in the application of heterogeneous systems. During the hot filtration test, when the reaction reached 25% conversion, one-half of the liquid reaction mixture (the half that was under hot conditions, this was the portion that was free of catalyst) was separated into another reaction tube. After an additional 20 min of MW exposure to both portions of the reaction mixture, the portion containing the nanocatalyst had proceeded to 85% conversion, and the catalyst-free portion had reached 32% conversion, indicating the heterogeneity of the system. Moreover, the amount of Ru in the catalyst remained almost unchanged (3.16 wt %) after three reaction cycles, indicating almost negligible Ru leaching during the reaction. This remarkable stability is believed to be due to a well-defined amine-binding site located on the surface of nanoferrite, which acts as a pseudoligand by noncovalently binding to  $[\text{Ru}(\text{OH})]_x$  through metal–ligand interactions.

Metalloporphyrins have been extensively investigated recently as catalysts for alkene epoxidation and alkane hydroxylation under mild conditions. Despite the widespread use of homogeneous metalloporphyrins as catalytic systems (despite their inherent drawbacks, mostly catalytic stability and recovery), the immobilization of metalloporphyrins on magnetic supports has

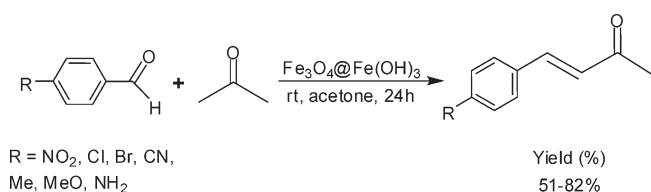
become a popular and useful approach for creating highly active and reusable catalysts. A series of Co(II) porphyrin and Mn(III) porphyrin (with different phenyl–substituent complexes supported on magnetic polymer nanospheres) were prepared and employed in the hydroxylation of cyclohexane with molecular oxygen (Scheme 65).<sup>151,152</sup> As compared to their unsupported homogeneous catalyst counterpart, metalloporphyrins immobilized on magnetic polymer nanospheres possessed significantly improved catalytic activities with turnover numbers (TON) 215–308 times greater than those of the nonsupported metalloporphyrin catalysts. The increased activity in the supported systems was probably due to the suitable nanosphere micro-environment for the “accommodation” of porphyrin catalytic centers. Importantly, the high turnover numbers of these catalysts are well retained after five reuses, and no loss of magnetic responsiveness or morphological change was detectable after each reuse. Thus, the catalytic performance and chemical properties of these catalysts were found to be very stable and were well retained, even after several reuses.

A magnetically recyclable chiral heterogeneous primary aminocatalyst was also developed for the asymmetric aldol reaction (Scheme 66).<sup>153</sup> Chiral cyclohexanediamines linked to trimethoxysilane were immobilized onto MNPs. Prior to immobilization, the MNP was protected with a layer of silica to prevent aggregation. The resultant catalyst was reported to efficiently promote aldol condensations of acetone and cyclohexanone, affording the desired aldol products in high yields and levels of stereoselectivity. The catalysts could also be easily recycled and reused up to 11 times with essentially no loss in activity and/or stereoselectivity. TEM images of the catalyst showed slight aggregation after 11 uses; however, it maintained its nanospheric dimensions and the silica coating structure.

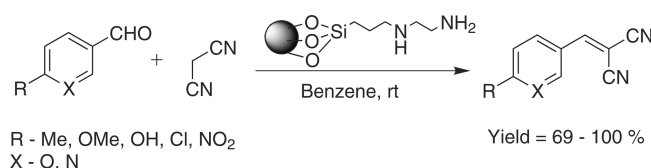
Another magnetically recoverable catalyst utilized in the aldol condensation of benzaldehyde and methyl isocyanoacetate was prepared by Claesson et al.<sup>154</sup> The support employed in this study was composed of monodisperse particles with silica cores, which were covered with maghemite nanoparticles and another outer silica shell; the PCP–pincer palladium complex was immobilized on this support to give a heterogeneous catalyst. The catalyst worked efficiently in the condensation of benzaldehyde and methyl isocyanoacetate.

Recently, the group of Song reported the preparation of a magnetic  $\text{Fe}_3\text{O}_4\text{--Fe}(\text{OH})_3$  composite microsphere by depositing  $\text{Fe}(\text{OH})_3$  gel on the  $\text{Fe}_3\text{O}_4$ .<sup>155</sup> The performance of this catalyst has been evaluated in aldol reactions of acetone with aromatic aldehydes, and it showed good yields except when 4-hydroxybenzaldehyde was used (Scheme 67). This catalyst was also

**Scheme 67. Aldol Reaction between Acetone and Aromatic Aldehydes Catalyzed by  $\text{Fe}_3\text{O}_4\text{--Fe}(\text{OH})_3$**



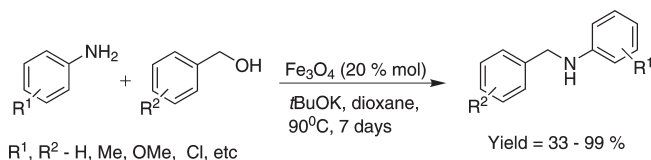
**Scheme 68. Diaminosilane-Functionalized Cobalt as a Catalyst in the Knoevenagel Condensation Reaction<sup>156</sup>**



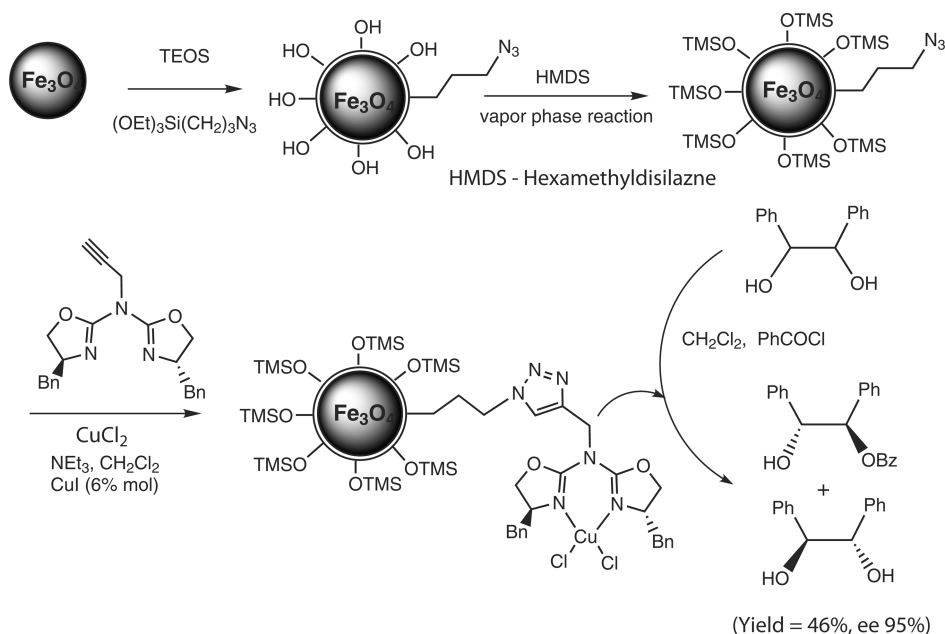
tested in several aldol reactions between various ketones and 4-chlorobenzaldehyde. The yields of the reactions were moderate when the reaction was conducted at room temperature. The recycling of the catalyst has been examined in the aldol reaction between acetone and 4-chlorobenzaldehyde, and the recycled catalyst was reused five times with a constant yield.

The Knoevenagel condensation is a classical general route for the preparation of valuable synthetic intermediates. For example, it is a key step in the commercial production of antimalarial drugs. This catalytic reaction can also be performed using recyclable organosilane-functionalized magnetic nanoparticle catalysts. The magnetically recoverable catalyst was prepared by reacting the surface hydroxyl on  $\text{CoFe}_2\text{O}_4$  nanoparticles with *N*-[3-(trimethoxysilyl)propyl] ethylenediamine (Scheme 68).<sup>156</sup> The resulting nanoparticles were functionalized via silane chemistry with diamine, creating basic surface sites. The basic MNPs were reported to be efficient heterogeneous catalysts for the Knoevenagel condensation of several aromatic aldehydes with malononitrile. Quantitative conversion of the reactants was achieved under mild reaction conditions. The reaction rates were comparable to those of diamine-functionalized large-pore mesoporous silica materials SBA-15 and were faster than those obtained with small-pore (2.2 nm diameter) MCM-48. This magnetically recoverable catalyst could be reused five times without any significant decrease in its catalytic activity, and no leaching of amine species from the support was detected upon ICP analysis of the reaction mixture.

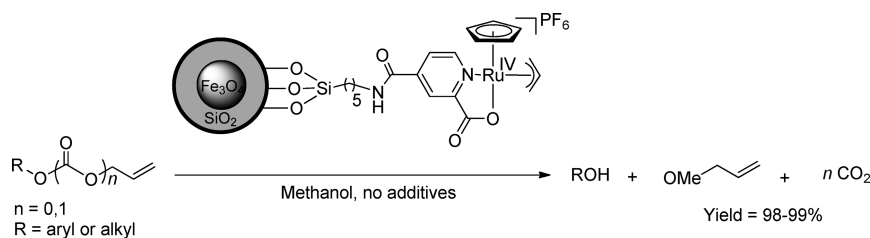
**Scheme 70. Magnetite Catalyzes the *N*-Alkylation Reaction of Aromatic Amines and Benzyl Alcohols**



**Scheme 69. Magnetic Catalyst Prepared Using “Click Chemistry” for the Kinetic Resolution of Racemic Mixtures**



Scheme 71. Magnetically Separable Deallylation Catalyst

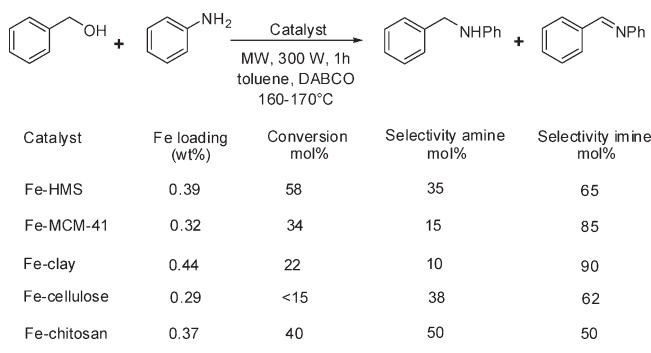


Remarkably, MSCs offered a potential advantage in the kinetic resolution of racemic mixtures, by which a pure enantiomer can be separated from two diastereoisomers. Copper(II)–azabis(oxazoline) complexes grafted on silica-coated magnetite nanoparticles were reported to be highly selective and recyclable in the kinetic resolution of 1,2-diols.<sup>187</sup> As indicated by Scheme 69, the magnetite–silica nanoparticles were treated with 3-azidopropyltriethoxysilane to functionalize the particles with azide end groups, which acted as a convenient building block for grafting the catalysts. Subsequently, a copper(I)-catalyzed azide/alkyne cycloaddition reaction was conducted using click chemistry and the above Cu-complexes with an azide-functionalized surface of magnetite–silica nanoparticles. The as-synthesized catalysts were employed in the desymmetrization of racemic 1,2-diols (hydrobenzoin) through an asymmetric benzylation reaction. As compared to azabis(oxazolines) that have been “clicked” to common polymeric supports such as MeO–PEG or a Merrifield resin, Fe<sub>3</sub>O<sub>4</sub>–SiO<sub>2</sub> proved to be a superior support with respect to activity (48% conversion) and selectivity (96% ee); the catalyst was also able to be employed in up to five runs with consistently high activity and selectivity. Recycling of the catalysts was also quantitatively achieved by magnetic separation.

As mentioned above, magnetite has the potential to be modified with numerous types of functional groups to create active environments for catalytic applications; however, these magnetites are not intrinsically catalytically inactive. Unmodified magnetite was found to be an excellent catalyst for the selective *N*-alkylation of aromatic amines with benzylic alcohols via a hydrogen autotransfer process (Scheme 70).<sup>158</sup> In addition to high yields, high selectivity was also observed in the reaction. The reactions selectively took place with aromatic amines and benzylic alcohols only, due to the ability of magnetite to discriminate between aromatic and aliphatic amines, as well as between benzylic and aliphatic alcohols. This readily available catalyst could be reused up to eight times in the reaction without losing effectiveness.

Kitamura and colleagues prepared a heterogeneous deallylation catalyst by immobilizing [CpRu( $\eta^3$ -C<sub>3</sub>H<sub>5</sub>)(2-pyridinecarboxylato)]PF<sub>6</sub> onto silica-coated nanoferrite particles.<sup>159</sup> The obtained materials showed high saturation magnetization and high levels of dispersibility with weak coercive forces. The catalyst was highly active for deallylation reactions and could operate in alcoholic solvents in the absence of any extra additives to complete the reaction (Scheme 71). The only coproducts were volatile allyl ethers. The catalyst was recycled by simple magnetic separation and reused 10 times with only a slight loss of activity, indicating that the protocol was economical.

Like the deallylation process, Xu and co-workers have developed dehydrogenation catalyst by synthesis of Au–Co magnetic core–shell structured NPs through a one-step seeding-growth

Scheme 72. Microwave-Assisted Selective *N*-Alkylation of Aniline with Benzyl Alcohol

method at room temperature under ambient atmosphere.<sup>160</sup> In addition to possessing good thermal stability and easy recovery properties, the resultant Au–Co NPs showed high catalytic activity and long-term stability for the hydrolytic dehydrogenation of aqueous ammonia borane. Moreover, this rational and general method was also extended to the other metallic systems, which can be used as optical, magnetic, and electrical materials as well as for heterogeneous catalysts.

Luque and co-workers reported the preparation of highly active, selective, and reusable supported iron and iron oxide nanoparticles on a variety of porous materials in microwave-assisted *N*-alkylations of benzyl alcohol with aniline.<sup>161</sup> Among the reported catalysts, Fe–HMS (HMS: hexagonal mesoporous silica) was found to be highly active (Scheme 72). The catalyst was then evaluated for *N*-alkylation of a range of substituted benzyl alcohols with aniline and provided good yields. In addition, this catalyst was also found to be reusable, preserving >90% of their initial activity and selectivity after three reuses. No Fe-leaching was detected in the final reaction mixture upon recycling of the catalyst.

## 5. FOCUS ON ENVIRONMENTAL APPLICATIONS

The use of MSNPs has also been extended to a range of environmental challenges (including photodegradation and/or adsorption of pollutants and biocatalysis) due to their excellent separation properties and their ability to be functionalized in many different ways. Furthermore, the use of magnetic iron oxides has the added advantage of low toxicity and biocompatibility.<sup>162,163</sup> In this section, we aim to provide an overview of the applications of various MSCs in environmental challenges, including photocatalysis and photodegradation of pollutants in water, biocatalysis, immunoassay, and the adsorption of toxic organic compounds from aqueous solutions.

### 5.1. Magnetic Photocatalysis

The photodegradation of pollutants in air or water is currently a major challenge of efforts to ensure clean water and air for legislations worldwide. The inherent advantages of MSNPs discussed before make them attractive candidates for wastewater treatment.<sup>164,165</sup> A great deal of work has therefore been devoted to the preparation of a wide range of photocatalysts that possess magnetic properties for the degradation of various organic chemicals from solution, including dyes, herbicides, and related pollutants. Upon efficient degradation of the various compounds, the photocatalysts are then easily recoverable from solution using a simple magnet.

The photocatalytic properties of magnetic  $\text{Fe}_2\text{O}_3/\text{SiO}_2/\text{TiO}_2$  composites were examined using the photodegradation of methylene blue (MB) solutions under UV light. MB was decomposed (80%) after 80 min in the presence of the catalysts under the investigated reaction conditions. The reaction was followed by monitoring the absorbance at 660 nm. Coating the magnetic cores with silica enhanced the photocatalytic activity of the hybrid nanoparticles by preventing the transfer of the photogenerated electrons into the lower-lying conduction band of the iron oxide core, thus eliminating photodissolution.<sup>166</sup> These materials with high photocatalytic efficiency may find applications in the photodegradation of organic pollutants in solution.

Similarly, the previously described zinc ferrite-doped  $\text{TiO}_2$  system exhibited excellent activity in the photocatalytic degradation of methyl orange (MO) under visible light irradiation.<sup>167</sup> Although little or no degradation of MO was observed in the absence of the photocatalyst and/or while using  $\text{TiO}_2$  or  $\text{ZnFe}_2\text{O}_4$  as photocatalysts (despite the good visible light absorptivity of the latter), remarkable degradation of MO was observed for the  $\text{TiO}_2/\text{ZnFe}_2\text{O}_4$  material (up to 35%). The maximum photocatalytic activity was obtained for a material calcined at 500 °C for 2 h, containing 3 wt % of zinc ferrite.

Magnetically separable titania photocatalysts have also been recently reported in the degradation of a chloroacetanilide herbicide (propachlor) in water.<sup>168</sup> The materials were prepared by modifying titania NPs (Degussa P25) with nanocrystalline  $\gamma\text{-Fe}_2\text{O}_3$  NPs with a protective lining made up of two oppositely charged polyelectrolytes, each with various  $\gamma\text{-Fe}_2\text{O}_3$  loadings (3, 8, 13, 20, and 30 wt %). Catalysts containing a 20 wt %  $\gamma\text{-Fe}_2\text{O}_3$  had activity fairly similar to that of P25 (the most active catalyst), with decreased activities observed for the other loadings. This effect has been extensively reported in the literature and is due to induced photodissolution (injection of charges from titania into  $\gamma\text{-Fe}_2\text{O}_3$ ).<sup>169,170</sup> Nevertheless, the superior activity of 20 wt %  $\gamma\text{-Fe}_2\text{O}_3\text{-TiO}_2$  seemed to be correlated to an increase in adsorption of propachlor (20%) as compared to the other photocatalysts (19% or less). Most importantly, the catalyst was easily separable from the reaction mixture by an external magnet and could be reused at least three consecutive times under UV-vis irradiation ( $\lambda > 290$  nm) without any noticeable change in activity. The observed photocatalytic degradation behavior is a compendium of factors: complex partition equilibria, particle dispersibility, light adsorption, and charge transfer processes, in which the degradation of the polyelectrolyte can also influence the photocatalytic activity of materials at longer irradiation times.

Among the reported photocatalysts for the degradation of organic pollutants, dyes, and related compounds, those exhibiting high photocatalytic activities under sunlight irradiation are

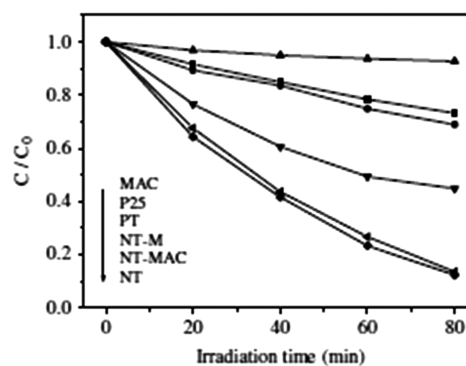


**Figure 3.** Activity of various photocatalysts (P25, PT, NT-MAC and their respective supports MAC, NT-M, and NT) in the photodegradation of X-3B dye.<sup>172</sup> Reprinted with permission from ref 172. Copyright 2008 Elsevier B.V.

highly desirable.<sup>171</sup> Two general strategies have been developed to increase the photocatalytic activity of  $\text{TiO}_2$  for visible light irradiation: the use of an organic dye as a photosensitizer and doping  $\text{TiO}_2$  with metallic and nonmetallic elements. Several approaches have been reported with this aim.

A novel magnetically separable composite photocatalyst, composed of a nitrogen-doped titania-coated  $\gamma\text{-Fe}_2\text{O}_3$  magnetic activated carbon (NT-MAC), has been synthesized by a simple coating method and employed in the degradation of a dye (Reactive Brilliant Red X-3B) in aqueous solution under solar light irradiation, using P25 and pure  $\text{TiO}_2$  (PT) as references for comparison.<sup>172,173</sup> The MSC, denoted as NT-MAC, possessed activity (86.5% degraded X-3B) comparable to that of N-doped  $\text{TiO}_2$  (87%) and higher activity than both P25 (26.8%) and pure  $\text{TiO}_2$  (31.1%) (Figure 3).

Nitrogen-doping seemed to be critical to achieve high photocatalytic activities in these systems. Photodissolution effects were investigated by ICP analysis of the processed water. The concentration of Fe ions was ca. 0.70  $\text{mg L}^{-1}$  at different irradiation times; this concentration is insufficient to degrade organic compounds (e.g., phenol) by processes other than photocatalysis. The material was also highly recyclable under the investigated reaction conditions, maintaining over 90% of its initial photocatalytic activity (85% X-3B degradation) after six uses.

Yin and co-workers have prepared core-shell structured  $\text{Fe}_3\text{O}_4/\text{SiO}_2/\text{TiO}_2$  nanophotocatalysts by combining two steps of a sol-gel process with calcination.<sup>174</sup> The as-obtained core-shell structure is composed of a central magnetite core with a strong response to external fields, an interlayer of  $\text{SiO}_2$ , and an outer layer of  $\text{TiO}_2$  nanocrystals with a tunable average size. In addition, the control over the size and crystallinity of the  $\text{TiO}_2$  nanocatalysts made it possible to achieve higher photocatalytic efficiency than that of commercial photocatalyst Degussa P25. The photocatalytic activity was increased as the thickness of the  $\text{TiO}_2$  nanocrystal shell decreases. Photocatalyst was recovered by applying an external magnetic field while maintaining their photocatalytic activity during at least 18 cycles of use.

### 5.2. Magnetic Biocatalysis

Enzymes are versatile macromolecules with major advantages as biocatalysts: high stability, ultrahigh reaction selectivity, and specificity under mild conditions; these compounds are currently finding increasing applications in various processes, such as redox reactions, (trans)esterification processes, and enantioselective

synthesis.<sup>175</sup> However, their widespread application in many of these processes is hampered by inherent drawbacks, including cost, availability, and difficulties in recovery and recycling. For the recovery and recycling of enzymes, several methodologies have been reported as alternatives to the use of free/crude enzymes in biocatalyzed reactions.<sup>176</sup> These methodologies include the entrapment of biocatalysts on porous materials (such as ion-exchange resins), the adsorption of enzymes on the surface of a material, and the immobilization of enzymes on different supports via functionalization and/or covalent binding.<sup>177</sup> The use of supports to improve the reusability properties of enzymatic systems has been extended to a wide range of inorganic materials; of these materials, magnetic NPs have the additional advantage of stability and easy separation.<sup>178</sup> In this section, we will describe various methods for the preparation of magnetically separable enzymatic catalysts and their applications in biocatalysis and immunoassays.

**5.2.1. Entrapment of Biocatalysts onto MSNPs.** Magnetically separable nanoparticles are particularly useful for imaging and separation techniques.<sup>179,180</sup> However, they need to be functionalized and/or coated with various agents (e.g., metal catalysts, antibodies, or enzymes) due to their intrinsic chemical and biological inertness. The entrapment/encapsulation of enzymes into magnetic materials is a particularly interesting approach to obtain easily recyclable biocatalysts.

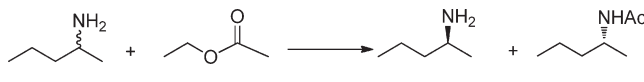
One of the first examples of the entrapment of enzymes in magnetite-containing sol–gel materials for heterogeneous biocatalysis was described by Reetz et al. in 1998.<sup>181</sup> These authors utilized a previously reported methodology to simultaneously entrap lipases (such as *Pseudomonas cepacia* and *Candida antarctica*) and nanostructured super paramagnetic magnetite into hydrophobic sol–gel materials derived from methyl/ethyl/propyl/butyltrimethoxyorthosilane (R-TMOS).<sup>182</sup> The activity of the biocatalyst was investigated for the esterification of lauric acid with *n*-octanol. In general, the lipase/magnetite-containing gels exhibited remarkable enzymatic activities (3 times more active than the nonentrapped free enzymes). One of the catalysts was also tested as an enantioselective catalyst in the kinetic resolution of racemic 2-pentylamine, using ethyl acetate as an acylating agent and *t*-butylmethyl ether as a solvent (Scheme 73).

The ee obtained in the resolution was 97–99%; similar values were obtained for a comparable gel without magnetite.<sup>183,184</sup> Also, the material of this system had the additional advantage of simple separation by a magnet.

Sen and co-workers have reported the synthesis of hierarchically ordered porous functionalized magnetic nanocomposites as biocatalysis for the hydrolysis reaction (Scheme 74).<sup>185</sup> The catalyst exhibited a catalytic conversion value of  $5.9 \times 10^{-3} \mu\text{mol min}^{-1} \text{mg}^{-1}$  for the hydrolysis of *p*-nitrophenyl palmitate to *p*-nitrophenol and palmitic acid. However, this value was found to be nearly one-half ( $3.9 \times 10^{-3} \mu\text{mol min}^{-1} \text{mg}^{-1}$  of enzyme) when the lipase immobilized on nonfunctionalized support. The catalytic efficiency was unaffected upon the second cycle on the lipase immobilized functionalized nanocomposite, whereas a dramatic reduction in catalytic activity was observed when the nonfunctionalized support was used.

$\text{Fe}_3\text{O}_4$  NPs have, in theory, an intrinsic enzyme mimetic activity (similar to that found in peroxidases), with the ability to oxidize organic substrates, combined with facile separation from the reaction mixtures using a simple magnet. Inspired by this concept, Gao et al. developed a novel immunoassay in which antibody-modified magnetite NPs are able to perform three

**Scheme 73. Racemic Resolution of 2-Pentylamine Using a Biocatalyst Based on *Candida antarctica* Entrapped on Magnetite Containing a Methyl-/Propyltrimethoxyorthosilane Gel**

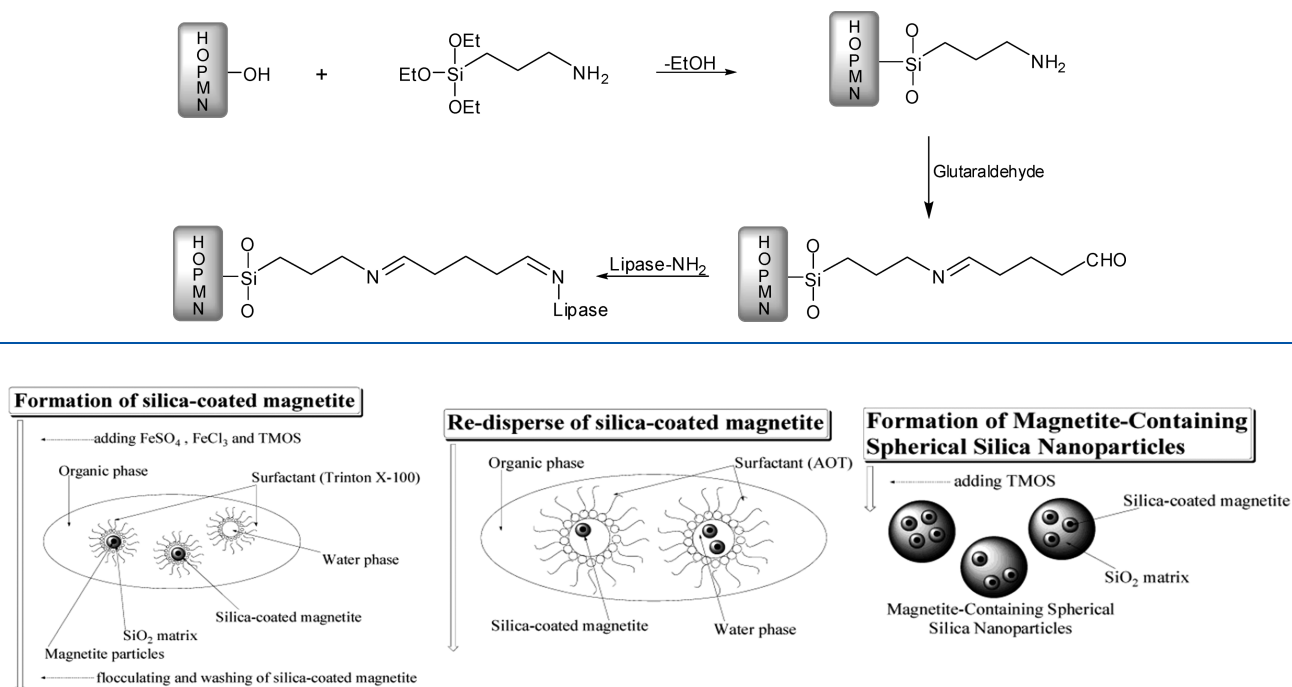


functions: capture, separation, and detection.<sup>186</sup> Magnetite NPs of three different nanoparticle sizes (30, 150, and 300 nm) were prepared and tested in a series of oxidation reactions of typical peroxidase organic substrates (e.g., 3,3',5,5'-tetramethylbenzidine, diazoaminobenzene, *o*-phenylenediamine) using hydrogen peroxide as a green oxidant.  $\text{Fe}_3\text{O}_4$  NP was robust, active, and highly reusable under the investigated reaction conditions; the activity was dependent on pH (optimal 3.5–4.5), temperature (30–40 °C),  $\text{H}_2\text{O}_2$  concentration (higher than that used with peroxidases), and NP size (small NP, 30 nm, exhibited higher oxidation activities).  $\text{Fe}_3\text{O}_4$  NPs (30 nm particle size) were then functionalized with different reagents, including silica, 3-aminopropyltriethoxysilane (APTES), polyethylene glycol (PEG), or dextran to make them biocompatible for subsequent antibody immobilization. With this purpose, an antibody to cardiac troponin I (TnI, a well-known biomarker for myocardial infarction) was immobilized on the  $\text{Fe}_3\text{O}_4$  NPs. The  $\text{Fe}_3\text{O}_4$ –antibody hybrid material was mixed with serum, which allowed for the capture of the target TnI in the sample, and the captured TnI material was simply separated from the mixture by a magnet. The TnI–antibody– $\text{Fe}_3\text{O}_4$  complex was then transferred onto a plate coated with another anti-TnI antibody, and 3,3',5,5'-tetramethylbenzidine was added in the presence of  $\text{H}_2\text{O}_2$  to give a colored product, which was evaluated by measuring the absorbance at 652 nm. The concentration of TnI in the sample correlated with the quantity of colored product, demonstrating the multifunctionality of  $\text{Fe}_3\text{O}_4$  NPs as an alternative for standard magnetic enzyme-linked immunosorbent assays (ELISA).

With similar bioseparation and biocatalytic applications in mind, the simultaneous entrapment and/or immobilization of biological macromolecules (e.g., enzymes) and/or magnetite/magnetic carbons in sol–gel materials is a promising methodology to obtain bioactive, mechanically stable, and magnetically separable materials. An example of this approach is the preparation of horseradish peroxidase entrapped on magnetite-containing spherical silica NPs, reported by Yang et al.<sup>187</sup> The authors synthesized these hybrids using a reverse-micelle technique, as described in Figure 4.

Next, following the prehydrolysis of the silica precursor, horseradish peroxidase (HRP) was simply encapsulated in the magnetite-containing silica material by mixing and stirring a diluted solution of the protein in a phosphate buffer (PBS) to preserve the enzyme from denaturation. The maximum entrapment efficiency was 85–90%, with HRP highly stabilized on the MSC (unleachable even in PBS for over 60 days). The activity of the HRP–magnetite silica material was then studied in the oxidation of 2–2'-azino-bis(3-ethyl)benzothiazoline-6-sulfonic acid (ABTS) with  $\text{H}_2\text{O}_2$  and compared to that of the crude/free enzyme. As expected, the entrapped HRP had lower activity than did the free enzyme (78% of the activity of the free HRP), which may be related to conformational changes of the partially denatured enzyme and/or to the diffusion constraints of the substrate through the NP pores. In any case, the hybrid nanobiocatalyst was reusable under the investigated reaction conditions, preserving 81.4% of the initial activity after five cycles.

Scheme 74. Immobilization of Lipase on the Novel Hierarchically Ordered Porous Magnetic Nanocomposites

Figure 4. Preparation of enzyme entrapped on magnetite-containing spherical silica NPs.<sup>187</sup> Reprinted with permission from ref 187. Copyright 2004 American Chemical Society.

Furthermore, this material could be employed in a novel magnetic separation immunoassay system (using an antibody instead of an enzyme) for the quantitative determination of gentamicin. The entrapped antibody retained its capacity to bind gentamicin, behaving similarly to the free antibody. The detection limit for gentamicin was  $160 \text{ ng mL}^{-1}$ .

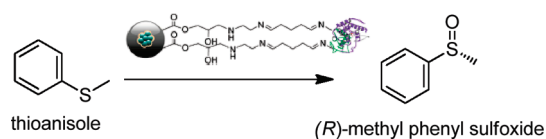
Magnetic single-enzyme NPs encapsulated within a composite inorganic/organic polymeric network have also been recently synthesized by Yang et al. following a surface modification/in situ aqueous polymerization methodology.<sup>188</sup> The enzyme chosen for the study was glucose oxidase (GOD), which is widely utilized in the food industry and in clinical and chemical analysis.<sup>189</sup> The activity of the bionanocatalyst was investigated in the production of quinoneimine, which was followed spectrometrically at 505 nm to detect solution color changes generated from quinoneimine, then compared to that of free GOD. Significant differences in activity and stability were observed for free and encapsulated GOD. The maximum activity of both biocatalysts was highly dependent on the pH, temperature, and type of solvent. Both free and encapsulated GOD were maximally active at pH 5.8. Nevertheless, the latter was found to have a remarkably improved stability at higher pH (9.0); about 85% of its maximum activity was retained at that pH, whereas the activity of free GOD lowered significantly (20–25%). The encapsulated GOD also appeared to be less sensitive to temperature changes (residual activity over 80% at temperatures ranging from 50 to 70 °C) than was free GOD, for which the activity decreased dramatically from 87% at 50 °C to 9% at 70 °C. The exposure of enzymes to organic solvents, even at low quantities, can also affect the denaturation of the biocatalysts. Interestingly, while free GOD loses most of its activity upon exposure for 20 min at 30 °C to an aqueous solution containing 10% (v/v) of a polar organic solvent

(e.g., methanol, THF, or dioxane), the encapsulated GOD preserved over 80% of its initial activity. The storage stability and the durability of the encapsulated GOD also proved to be excellent, with nearly 95% of its initial activity retained after nine uses in the course of 1 month (free GOD preserved less than 31% of its original activity). These results indicate that the developed nano biocatalyst was significantly more stable than the free enzyme.

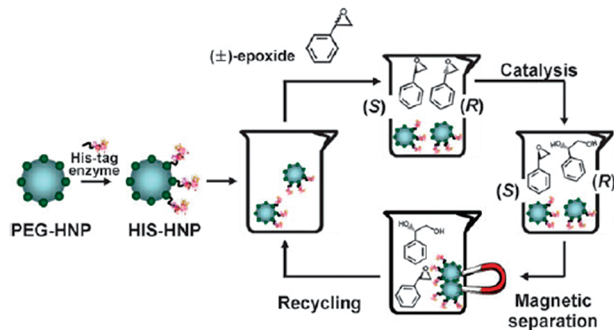
A magnetically switchable bioelectrocatalytic system also based on GOD has been developed by employing cross-linked enzyme aggregates in a magnetic mesocellular carbon foam.<sup>190</sup> The GOD in the pores were stabilized via cross-linking with glutaraldehyde. As a result of the cross-linking and the small pores present within the mesocellular material (ca. 10 nm), the bionanocatalyst retained over 90% of its initial activity in the oxidation of glucose after 12 washings (as well as after continuous incubation with vigorous stirring for 22 days), while immobilized GOD without any cross-linking retained less than 50% of its activity. The specific activity of the GOD cross-linked aggregates was 29% of that obtained for free GOD in buffer solution. The developed material was also a proof of concept to prepare a magnetically switchable bioelectrocatalyst. Changes in the anodic current were observed when the material was brought into contact with the electrode by a magnetic field, whereas no current was detected when the biocatalyst was pulled up (above the electrochemical cell) by the magnet, even in the presence of glucose. Most interestingly, anodic currents could also be switched on and off, and a constant signal was maintained in the on state. These findings may pave the way for bioelectrocatalysts in related areas, including bioconversion, switchable biofuel cells and regeneration of enzyme electrodes.

**5.2.2. Covalent Immobilization of Enzymes on MSNPs.** A magnetically separable nanobiocatalyst was designed, which

**Scheme 75. Enantioselective Sulfoxidation of Thioanisole Catalyzed by an MSC<sup>191</sup>**



**Scheme 76. Immobilization of His-Tagged Epoxide Hydrolases on PEG–HNP and Their Application in the Resolution of Racemic Styrene Epoxide<sup>198a</sup>**



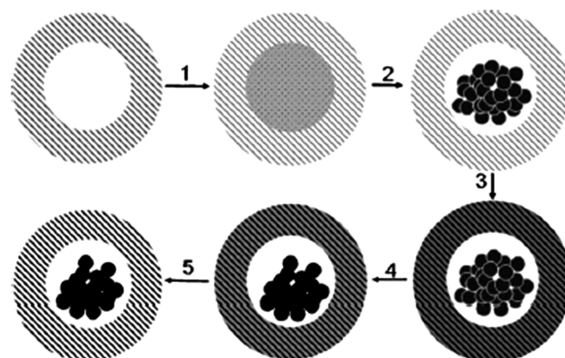
<sup>a</sup> Reprinted with permission from ref 198. Copyright 2009 Royal Society of Chemistry.

was composed of a covalently immobilized enzyme (chloroperoxidase, CPO) on MNPs with iron oxides and thick polymer shell core.<sup>191</sup> The biocatalyst was utilized in the enantioselective sulfoxidation of thioanisole to (*R*)-methyl phenyl sulfoxide (Scheme 75).

Product concentration increased linearly within 100 min, and the catalyst had a total turnover number (TON) of 25 000, similar to that reported for free CPO.<sup>192</sup> The product ee was >99% (*R*), and the enzyme was also stable upon immobilization and reusable for at least 12 cycles. Interestingly, a remarkable decrease in enzymatic activity has been reported for immobilized CPO on other supports.<sup>193,194</sup>

Similarly prepared immobilized lipases (including porcine pancreatic lipase, *Candida rugosa*, and *Pseudomonas cepacia* on amino-functionalized Fe<sub>3</sub>O<sub>4</sub> NPs) have also been employed in the transesterification of soybean oil with methanol for fatty acid methyl ester (biodiesel) production.<sup>195</sup> The biocatalysts had a >80% lipase loading, with residual activities greater than 70% as compared to the respective free lipases. They were also highly stable and could be reused many times under the investigated conditions, with an appreciable decrease in activities observed only after five cycles. Among the selected lipases, ferrite immobilized *Pseudomonas cepacia* was further investigated in the enzymatic transesterification of soybean to biodiesel and compared to the free enzyme; this particular lipase strain was chosen due to its higher tolerance to methanol as compared to the others.<sup>196</sup> Despite the fact that low conversions were obtained for both free (47.6%) and immobilized (55%) *Pseudomonas cepacia* in reactions performed under conventional heating (40 °C) in 100 mL flasks, a remarkable quantitative yield was obtained when the transesterification reaction was performed in a reactor (yields >99% after the first three cycles, 44.3% conversion after nine cycles). These differences were attributed to the improved mixing of the stirring systems with impellers in the reactor.

**Scheme 77. Synthetic Procedure of HMCSMCs Materials<sup>a</sup>**

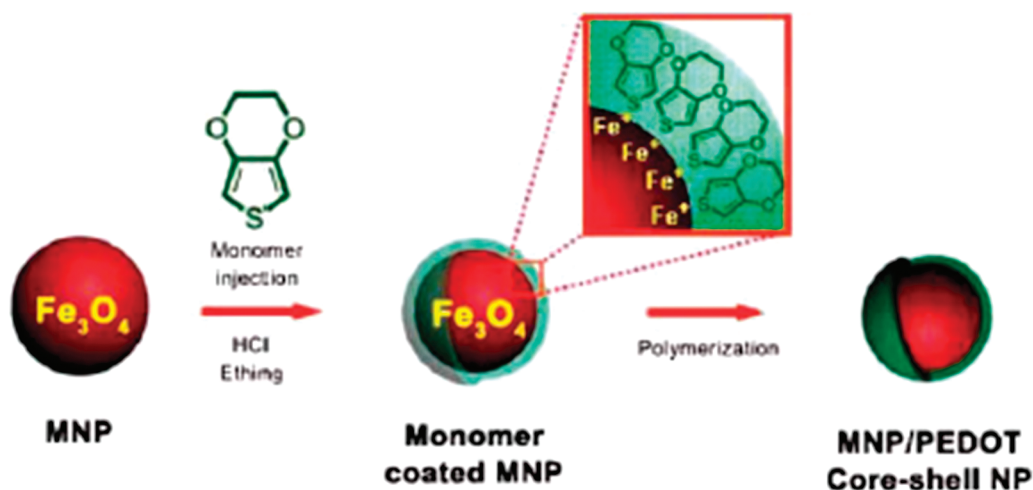


<sup>a</sup> Reprinted with permission from ref 200. Copyright 2009 Wiley-VCH Verlag GmbH & Co. KGaA.

Chen et al. have recently demonstrated that zirconia NPs (ca. 20 nm diameter) modified by a carboxylic surfactant of a long alkyl chain (e.g., tween 85 or erucic acid) as supports were able to remarkably improve the activity of immobilized lipases in asymmetric reactions in organic media.<sup>197</sup> The NP surface was successfully changed from hydrophilic to hydrophobic upon grating of the organic moieties, and two lipases (*Candida rugosa* and *Pseudomonas cepacia*) were entrapped into the modified zirconia through adsorption in aqueous solution. Various *Candida rugosa*-based biocatalysts (CRL) were utilized in the resolution of (*R,S*)-ibuprofen. The results showed that the activity of the biocatalysts was strongly dependent on the surface properties of the zirconia NPs, with good activities and ee (96.3%) obtained for the CRL–erucic acid–ZrO<sub>2</sub> material after 3 days (a maximum of 80% ee was obtained with crude CRL). These biocatalysts were also found to be highly recyclable; no activity loss was observed after eight uses.

A different biocatalytic application demonstrated by Lee et al.<sup>198</sup> synthesized hybrid Fe<sub>3</sub>O<sub>4</sub>–silica–NiO superstructures by the assembly of NiO at the surface of magnetic silica and subsequent functionalization with polyethylene glycol (PEG) to minimize the nonspecific binding of molecules to the surface and interference of the solid surface on the activity of the immobilized enzymes. These MS materials, denoted as PEG–HNP, were designed as supports for His-tagged epoxide hydrolases. The immobilized enzymes were subsequently employed in the enantioselective resolution of racemic styrene oxide, as indicated by Scheme 76. Results obtained for the His–HNP material show that a 98% ee of enantiopure (*S*)-styrene oxide could be obtained after 25 min, with almost 60% conversion. Comparing the activities of free and immobilized enzymes, it was observed that more than 70% of the enzymatic activity was preserved after immobilization, and the catalyst was easily removed by placing a small magnet at the bottom of the reaction vessel. The material was also highly reusable under the investigated reaction conditions. (*S*)-Styrene oxide was obtained with ee >98% with reaction times of 25–105 min after the sixth cycle; an almost negligible quantity of detached enzyme (<5%) was observed after each reuse.

A variety of other enzymes have also been immobilized on amine-functionalized magnetic NPs and employed in biocatalytic protocols. For example, glycolate oxidase (GO) was isolated and partially purified from *Medicago falcata* Linn. and subsequently immobilized onto hydrothermally synthesized amine-functionalized magnetic NPs via physical adsorption.<sup>199</sup> The maximum loading of GO onto the material was 56 mg per gram

Scheme 78. Preparation of  $\text{Fe}_3\text{O}_4$ –PEDOT NPs via Seeded Polymerization Mediated by Acidic Etching<sup>202a</sup>

<sup>a</sup> Reprinted with permission from ref 202. Copyright 2007 Royal Society of Chemistry.

of support, and the activity recovery was 45%. However, a support with enzyme concentration  $20 \text{ mg mL}^{-1}$  (36.1% activity recovery) was selected for experimental purposes.<sup>200</sup> Both free and immobilized GPO were tested in the oxidation of glycolic to glyoxylic acid. Several factors were screened in the reaction, including the effects of the pH, temperature, and kinetic parameters, as well as the reusability of the systems. The optimum pH for the reaction was 9 at  $30^\circ\text{C}$  for both the free and the immobilized enzyme. However, the activity of the free GO was remarkably affected by variations in pH, unlike that of the immobilized GO (71.5% vs 96.4%, respectively, of their initial activities preserved after incubation at  $4^\circ\text{C}$  for 24 h). For temperature, the optimum temperature for free GO was  $15^\circ\text{C}$ , whereas the immobilized GO had a significantly higher optimum temperature ( $40^\circ\text{C}$ ). Finally, the immobilized GO was only slightly reusable under the investigated reaction conditions, as only 70% of its initial activity was retained after four cycles (reuses taking over 17 h after the first 12 h reaction run), with an estimated half-life of 117 h. However, the selectivity to glyoxylic acid did not change after reuse and was as high as 98.9%.

**5.2.3. Binding of Macromolecules to Magnetic Nanoparticles.** An interesting approach for the preparation of mesoporous silica–magnetite nanocomposites (via a one-step coating method) for the binding and elution of salmon sperm DNA has been recently reported by Sen and Bruce.<sup>201</sup> The binding of sheared denatured salmon sperm DNA is dependent on the nature and properties of the materials. Pure magnetite and various silica–magnetite nanocomposites (prepared at various pH values) partially uncovered with the silica coating exhibited very high DNA binding (>90%) as compared to commercial materials and to fully silica-coated magnetite NPs (60–80%). The optimum material for salmon sperm DNA binding was obtained when the pH of the solution in the magnetite-coating step was adjusted to 7.

### 5.3. Adsorption Using Magnetic Materials

Porous materials and/or nanocomposites with embedded magnetic particles also show great potential for drug delivery and adsorption due to their high surface area and porosity.

Medical adsorbents that feature ease of separation, high adsorption capacity, and reusability (upon recovery and/or restoration of their adsorption properties) are highly desirable and will become increasingly important in the future. A range of magnetically separable materials and biochemical compounds have been reported. Guo et al. have recently reported the preparation of hollow mesoporous carbon spheres with magnetic cores (HMCSMCs) as easily separable adsorbents of pigments as endogenous toxins (e.g., bilirubin). The synthesis of these materials is fairly straightforward, as indicated in Scheme 77.<sup>200</sup>

In the first step, an iron nitrate solution was introduced into the hollow core of as-prepared hollow mesoporous aluminosilicates, using a previously described methodology that involves a vacuum nanocasting technique followed by calcination of the core into hematite particles (step 2).<sup>200</sup> Next, furfuryl alcohol was introduced into the mesoporous channels and polymerized under in situ catalysis by the aluminosilicate template (step 3). Finally, the polyfurfuryl alcohol generated was carbonized under  $\text{N}_2$  at  $600$ – $700^\circ\text{C}$ , while hematite particles were simultaneously reduced to magnetite/maghemite (step 4). The silica template was then removed using an aqueous solution of NaOH (step 5) to give the HMCSMCs materials. The quantity of magnetic core and the saturation magnetization values could easily be tuned by changing the concentration of iron nitrate solution in the synthesis. The size of nanoparticles in the core ranged from 18 to 42 nm, depending on the iron species. The adsorption properties of these materials were investigated by measuring the removal of bilirubin from bilirubin phosphate buffer solutions. The characteristic 438 nm UV absorption band of bilirubin was used to measure the concentration of bilirubin. HMCSMC materials exhibited good adsorption capacities with respect to bilirubin, typically between 85 and 146 mg bilirubin per gram of adsorbent.

Thiol-containing polymer-encapsulated magnetic nanoparticles (denoted as  $\text{Fe}_3\text{O}_4$ –PEDOT) have also been employed as reusable adsorbents of heavy metal ions.<sup>202</sup> These materials were prepared by inducing ferric cations onto the magnetic nanoparticles with a partial etching process followed by seed polymerization, as illustrated in Scheme 78. The resultant spherical-shaped  $\text{Fe}_3\text{O}_4$ –PEDOT NPs had a core diameter of ca. 9 nm and a shell thickness of ca. 2 nm.

The adsorption capacities of these MSNPs for heavy metal ions (including  $\text{Ag}^+$ ,  $\text{Hg}^{2+}$ , and  $\text{Pb}^{2+}$ ) were subsequently investigated in aqueous solutions. Uptake saturation occurred within 2 h of contact time, with an initial heavy metal ion concentration of ca. 15 ppm. The observed uptakes were 27.96, 16.02, and 14.99 ppm for  $\text{Ag}^+$ ,  $\text{Hg}^{2+}$ , and  $\text{Pb}^{2+}$ , respectively, with a maximum adsorption capacity of  $437 \text{ mg g}^{-1}$ . Up to 95% of the heavy metals could be removed after 24 h, with the adsorption rates following the order  $\text{Ag}^+ > \text{Hg}^{2+} > \text{Pb}^{2+}$ . Most importantly, the ease of separation of the materials (using a simple magnet) and recyclability (no loss of adsorption capacity after 10 uses) indicate that these materials would make excellent candidates for heavy metal adsorption in solution.<sup>202</sup>

There are also several examples of using MSNPs for wastewater and sludge treatment or for other advanced hazardous waste treatment technologies. For further information, readers are kindly referred to the recently published work of Brar et al.<sup>203</sup> and Li et al.<sup>204</sup>

## 6. CONCLUSIONS AND PERSPECTIVES

Catalysis is of vital importance for the development of society by providing a sustainable way to convert raw materials into valuable chemicals and fuels in an economical, efficient, and environmentally benign manner. Although nanoscale technology has many applications, the use of nanomaterials as catalysts is perhaps the most fascinating. There has been an increasing recent trend of the use of magnetically recoverable nanomaterials to develop more efficient and green chemical processes. In addition to their facile separation, these materials also exhibit high selectivity, activity, and stability. As compared to systems that rely on magnetic particles in microfluidic systems,<sup>205</sup> which are highly suitable for biological applications, their use and recovery in chemical reactions may not be efficient. This Review has provided an extensive overview on the applications of magnetic nanocatalysts in a wide range of catalytic processes: hydrogenation reactions, oxidation reactions, and synthetically significant carbon–carbon coupling reactions (Suzuki, Heck, Sonogashira, and Stille). This Review also discusses the use of magnetic materials as organocatalysts as well as their applications in some challenging reactions, such as hydroformylation and olefin metathesis. This Review also explores the recently emerging area of magnetic nanomaterials in environmental applications, such as for photo- and biocatalysis and for the adsorption and removal of pollutants from air and water.

These materials show great promise as enantioselective catalysts, which are used extensively for the synthesis of medicines, drugs, and other bioactive molecules. By functionalizing these materials using chiral ligands, a series of chiral nanocatalysts can be designed, offering great potential to reuse these otherwise expensive catalyst systems. However, characterization of magnetic catalysts is often a challenging task, and NMR characterization of these catalysts is difficult because the magnetic nature of the materials interferes with the magnetic field of the spectrometer. Therefore, there is a need for better characterization techniques. Also, despite the overwhelming demand for these nanocatalysts, knowledge of the mechanisms that take place at these small scales is empirical and fairly sparse.

Outlining the detailed mechanistic aspects of these catalytic processes is essential to tune and tailor new catalytic systems. One key point regarding atomically resolved knowledge of the active site is that it presents us with a platform on which we may build even better catalysts; with such knowledge, especially when

fundamental insights into the reaction and deactivation mechanisms are available, new and improved catalyst materials may be designed. The use of advanced spectroscopic techniques, such as synchrotron-based X-ray absorption (STXM), in situ synchrotron-based X-ray photoelectron spectroscopy (XPS), and IR microspectroscopy methods, can help explain the behavior of the active molecules or particles at the surface of these magnetic materials.<sup>206–208</sup> Computational studies in this field (such as those conducted in surface organometallic chemistry)<sup>209</sup> that aim to increase our understanding of the interactions of the reactive species with the magnetic material can also help to elucidate the role of these materials in the reaction mechanism and can, in turn, help to design and develop better nanocatalyst systems.

Also, considering their ease of synthesis using cheaper starting materials, these materials can outperform the alternatives in large-scale and even industrial scale applications, favorably replacing conventional materials such as silica and zeolites. However, this change will not happen soon; to achieve this goal, extensive research and development is needed to demonstrate the feasibility and productivity of these catalytic systems. At this stage, magnetically recoverable catalysts are still in their infancy; relatively easy and straightforward applications have been attempted, and we believe that it should be possible to conduct more challenging reactions. The economic and political impact of nanocatalysis is also obvious. The major environmental impact involves increased concerns about the toxicity of these materials, and more research is needed to address these concerns.

Finally, with more magnetically separable materials envisioned to be utilized for future challenges on the horizon, these systems will constitute, from our viewpoint, the future of more efficient protocols in terms of sustainability and environmental friendliness, allowing the development of active and selective materials for a wide variety of applications. It is only a matter of time before the real prospective of magnetic nanocatalysts is realized and implemented on a far-reaching scale.

## AUTHOR INFORMATION

### Corresponding Author

\*E-mail: vivek.pol@kaust.edu.sa (V.P.); jeanmarie.basset@kaust.edu.sa (J.-M.B.).

## BIOGRAPHIES

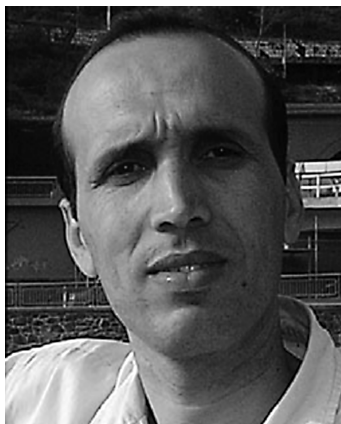


Dr. Vivek Polshettiwar was born in Mangli, India in 1979. He obtained his Ph.D. (2005) under the supervision of

Prof. M. P. Kaushik from Jiwaji University and DRDE, Gwalior. He investigated nanostructured silica for catalysis with Prof. J. J. E. Moreau in 2006 during his postdoctoral research at ENSCM, Montpellier (France). He then moved to the U.S. Environmental Protection Agency (2007-2009) to research nanocatalysis for green chemistry with Prof. R. S. Varma. Currently, he is working as senior research scientist at KAUST catalysis center directed by Prof. J. M. Basset. His research interests are in the area of advanced nanomaterials, surface organometallic chemistry, catalysis, and green chemistry. He has over 65 publications including various review articles and book chapters. He has also edited the RSC green chemistry series book. He is the recipient of the Oak Ridge Institute for Science and Education (ORISE) Research Fellowship (2007) and of the eminent Scientific and Technology Achievement Award-honorable mention by the U.S. Environmental Protection Agency (2009).



Dr. Rafael Luque became Ramon y Cajal Fellow at the Universidad de Cordoba in Spain after a 3-year postdoc at the University of York (UK) in the Green Chemistry Centre of Excellence directed by Prof. James Clark. His interests range from materials science, nanotechnology, and catalysis to biomass valorisation and biofuels. He is (co)author of more than 95 manuscripts, 15 book chapters, and 2 patents. He is currently editor of the books "Sustainable Preparation of Metal Nanoparticles" from the RSC Green Chemistry book series and "Advances in biodiesel preparation" from Woodhead Publishing as well as an Editorial Advisory Board Member of Current Organic Synthesis.



Dr. Aziz Fihri was born in Morocco in 1976. He received his Ph.D. from the Burgundy University (France), where he

studied under the guidance of Prof. J.-C. Hierro and Prof. Ph. Meunier. He focused his efforts on the synthesis of ferrocenyl-phosphines and their application in catalyzed cross-coupling reactions. He then worked as a postdoctoral fellow, first with Prof. B. Coq (ENSCM, France) and then in the group of Prof. M. Fontecave (Atomic Energy Center, France). In 2008, he became a principal research scientist at the Compiègne university, and researched on organometallic chemistry of palladium, coordination chemistry, and green chemistry. Currently, he is working at the KAUST catalysis center, on nanocatalysis by surface organometallic chemistry.



Dr. Haibo Zhu was born in Hubei, China. He obtained his bachelor degree (Chemical Engineer) and master degree (Organic Chemistry) from Hubei University. He continued his Ph.D. study at the Shanghai Jiao Tong University with Professor Zaiku Xie and obtained his Ph.D. degree in 2009. After that he joined Professor Jean-Marie Basset's group as a postdoc. From 2009 to 2010, he worked in the Laboratoire de Chimie Organométallique de Surface (CNRS-CPE, Université Lyon 1), on the metallic material for removal of pollutant from water. Currently, he is working at the KAUST catalysis center, on the heterogeneous catalysis for selective oxidation of alkane.



Dr. Mohamed Bouhrara was born in Morocco in 1981. After undergraduate studies at the Faculty of Sciences and Technologies of Settat (FSTS), he moved to the National Graduate School of Chemistry and Physics of Bordeaux (ENSCPB), where he completed his studies to obtain, in 2007, a double-degree "French Engineering Degree" and "MSc" in Material science. He then started a Ph.D. program under the supervision of

Prof. Jean-Marie Basset in the Surface Organometallic Chemistry Laboratory (LCOMS) at the Lyon School of Chemistry, Physics, and Electronics (ESCPÉ). His Ph.D. thesis was focused on the synthesis of hybrid organic–inorganic mesoporous silica-based organometallic complexes applied to heterogeneous catalysis. He is currently working as a postdoctoral fellow in the KAUST Catalysis Center (KCC) under the direction of Prof. Jean-Marie Basset and Dr. Vivek Polshettiwar, investigating the preparation of new nanomaterials for catalysis.



Prof. J. M. Basset received his doctoral and master's degrees at the University of Lyon. He served as scientific director of the school of Chemistry, Physics, and Electronics at the University of Lyon in France. He was appointed research Director at the Centre National de la Recherche Scientifique (CNRS) in 1987, and funded his laboratory of Surface Organometallic Chemistry that he has held since 1994. Dr. Basset's Lyon lab is home to 50 scientists, including Nobel Laureate Yves Chauvin. He came to CNRS in 1971 and has occupied several positions, including vice director of the Institute of Catalysis (Lyon). Dr. Basset also founded the consortium, "Actane", on alkane activation with 11 university laboratories and five companies. Since 1992, he also has served as Scientific Director of L'École Supérieure de Chimie Physique Electronique de Lyon (CPE, Lyon), which has trained 450 chemists in a 3-year scholarship program. Dr. Basset founded and serves as President of the network: Integrated Design of Catalytic Nanomaterials for a Sustainable Production (IDECAT). IDECAT is the only European Network of Excellence in Catalysis, which includes 40 laboratories and 20 companies. A Distinguished author of over 450 journal and conference papers, Dr. Basset's research interests include the relationship between homogeneous and heterogeneous catalysis. His research also includes the synthesis of single site catalysts in various fields of chemistry, petroleum, and polymers. Dr. Basset holds various professional memberships, is the recipient of several international and national awards, and is Doctor Honoris Causa of several universities. Currently, he is the Director of the KAUST Catalysis Center (KCC).

## ACKNOWLEDGMENT

We gratefully acknowledge funding and support from King Abdullah University of Science and Technology (KAUST). Thanks are also due to the KAUST communication department for designing several images for this Review.

## REFERENCES

- (1) Polshettiwar, V.; Varma, R. S. *Chem. Soc. Rev.* **2008**, 37, 1546.
- (2) Anastas, P. T.; Warner, J. C. *Green Chemistry Theory and Practice*; Oxford University Press: Oxford, 1998.
- (3) Matlack, A. S. *Introduction to Green Chemistry*; Marcel Dekker: New York, 2001.
- (4) Clark, J. H.; Macquarrie, D. J. *Handbook of Green Chemistry and Technology*; Blackwell Publishing: Abingdon, 2002.
- (5) Lancaster, M. *Green Chemistry: An Introductory Text*; RSC Editions: Cambridge, 2002.
- (6) Poliakov, M.; Fitzpatrick, J. M.; Farren, T. R.; Anastas, P. T. *Science* **2002**, 297, 807.
- (7) Polshettiwar, V.; Varma, R. S. *Aqueous Microwave Chemistry*; RSC Publishing: Cambridge, 2010.
- (8) Polshettiwar, V.; Varma, R. S. *Acc. Chem. Res.* **2008**, 41, 629.
- (9) Benaglia, M. *Recoverable and Recyclable Catalysts*; John Wiley & Sons: Chichester, 2009.
- (10) Wittmann, S.; Shätz, A.; Grass, R. N.; Stark, W. J.; Reiser, O. *Angew. Chem., Int. Ed.* **2010**, 49, 1867.
- (11) Coperet, C.; Chabanas, M.; Saint-Arroman, R. P.; Basset, J. M. *Angew. Chem., Int. Ed.* **2003**, 42, 156.
- (12) Basset, J.-M.; Coperet, C.; Soulivong, D.; Taoufik, M.; Thivolle-Cazat, J. *Acc. Chem. Res.* **2010**, 43, 323.
- (13) *Nanoparticles and Catalysis*; Astruc, D., Ed.; Wiley-VCH: Weinheim, 2008.
- (14) Somorjai, G. A.; Frei, H.; Park, J. Y. *J. Am. Chem. Soc.* **2009**, 131, 16589.
- (15) Polshettiwar, V.; Varma, R. S. *Green Chem.* **2010**, 12, 743.
- (16) Shylesh, S.; Schünemann, V.; Thiel, W. R. *Angew. Chem., Int. Ed.* **2010**, 49, 3428.
- (17) Lu, A. H.; Salabas, E. L.; Schuth, F. *Angew. Chem., Int. Ed.* **2007**, 46, 1222.
- (18) Yoon, H.; Ko, S.; Jang, J. *Chem. Commun.* **2007**, 1468.
- (19) Zhu, Y.; Zhang, L.; Schappacher, F. M.; Pöttgen, R.; Shi, J.; Kaskel, S. J. *Phys. Chem. C* **2008**, 112, 8623.
- (20) Zhu, Y.; Kockrick, E.; Kaskel, S.; Ikoma, T.; Hanagata, N. *J. Phys. Chem. C* **2009**, 113, 5998.
- (21) Kleitz, F.; Choi, S. H.; Ryoo, R. *Chem. Commun.* **2003**, 2136.
- (22) Barmatova, M. V.; Ivanchikova, I. D.; Kholdeeva, O. A.; Shmakov, A. N.; Zaikovskii, V. I.; Mel'gunov, M. S. *J. Mater. Chem.* **2009**, 19, 7332.
- (23) Barmatova, M. V.; Ivanchikova, I. D.; Kholdeeva, O. A.; Shmakov, A. N.; Zaikovskii, V. I.; Mel'gunov, M. S. *Catal. Lett.* **2009**, 127, 75.
- (24) Yoon, S. B.; Kim, J. Y.; Kim, J. H.; Park, Y. J.; Yoon, K. R.; Park, S. K.; Yu, J. S. *J. Mater. Chem.* **2007**, 17, 1758.
- (25) Wang, C.; Yin, L.; Zhang, L.; Kang, L.; Wang, X.; Gao, R. *J. Phys. Chem. C* **2009**, 113, 4008.
- (26) Xu, S.; Feng, D.; Shangguan, W. *J. Phys. Chem. C* **2009**, 113, 2463.
- (27) Hara, T.; Kaneta, T.; Mori, K.; Mitsudome, T.; Mizugaki, T.; Ebitani, K.; Kaneda, K. *Green Chem.* **2007**, 9, 1246.
- (28) Mori, K.; Hara, T.; Mizugaki, T.; Ebitani, K.; Kaneda, K. *J. Am. Chem. Soc.* **2004**, 126, 10657.
- (29) Hara, T.; Mori, K.; Mizugaki, T.; Ebitani, K.; Kaneda, K. *Tetrahedron Lett.* **2003**, 44, 6207.
- (30) Hara, T.; Kaneta, T.; Mori, K.; Mitsudome, T.; Mizugaki, T.; Ebitani, K.; Kaneda, K. *Green Chem.* **2007**, 9, 1246.
- (31) Xuan, S.; Wang, Y. X. J.; Yu, J. C.; Leung, K. C. F. *Langmuir* **2009**, 25, 11835.
- (32) Zhu, C. L.; Chou, S. W.; He, S. F.; Liao, W. N.; Chen, C. C. *Nanotechnology* **2007**, 18, 275604.
- (33) Xuan, S.; Wang, Y. X. J.; Leung, K. C. F.; Shu, K. Y. *J. Phys. Chem. C* **2008**, 112, 18804.
- (34) Panella, B.; Vargas, A.; Ferri, D.; Baiker, A. *Chem. Mater.* **2009**, 21, 4316.
- (35) Al-Hashimi, M.; Qazi, A.; Sullivan, A. C.; Wilson, J. R. H. *J. Mol. Catal. A: Chem.* **2007**, 278, 160.
- (36) Al-Hashimi, M.; Sullivan, A. C.; Wilson, J. R. H. *J. Mol. Catal. A: Chem.* **2007**, 273, 298.

- (37) Corma, A.; Garcia, H. *Top. Catal.* **2008**, *48*, 8.
- (38) Weckhuysen, B. M. *Nat. Chem.* **2009**, *1*, 690.
- (39) Hutchings, G. J. *J. Mater. Chem.* **2009**, *19*, 1222.
- (40) Lu, A.; Schmidt, W.; Matoussevitch, N.; Bönemann, H.; Spliethoff, B.; Tesche, B.; Bill, E.; Kiefer, W.; Schüth, F. *Angew. Chem., Int. Ed.* **2004**, *43*, 4303.
- (41) Tsang, S. C.; Caps, V.; Paraskevas, I.; Chadwick, D.; Thompson, D. *Angew. Chem., Int. Ed.* **2004**, *43*, 5645.
- (42) Yi, D. K.; Lee, S. S.; Ying, J. Y. *Chem. Mater.* **2006**, *18*, 2459.
- (43) Rossi, L. M.; Silva, F. P.; Vono, L. L. R.; Kiyohara, P. K.; Duarte, E. L.; Itri, R.; Landers, R.; Machado, G. *Green Chem.* **2007**, *9*, 379.
- (44) Guin, D.; Baruwati, B.; Manorama, S. V. *Org. Lett.* **2007**, *9*, 1419.
- (45) Kwon, M. S.; Park, I. S.; Jang, J. S.; Lee, J. S.; Park, J. *Org. Lett.* **2007**, *9*, 3417.
- (46) Amali, A. J.; Rana, R. K. *Green Chem.* **2009**, *11*, 1781.
- (47) Jacinto, M. J.; Landers, R.; Rossi, L. M. *Catal. Commun.* **2009**, *10*, 1971.
- (48) Mori, K.; Yoshioka, N.; Kondo, Y.; Takeuchi, T.; Yamashita, H. *Green Chem.* **2009**, *11*, 1337.
- (49) Panella, B.; Vargas, A.; Baiker, A. *J. Catal.* **2009**, *261*, 88.
- (50) Ma, Ya.; Yue, B.; Yu, L.; Wang, X.; Hu, Z.; Fan, Y.; Chen, Y. *J. Phys. Chem. C* **2008**, *112*, 472.
- (51) Baruwati, B.; Polshettiwar, V.; Varma, R. S. *Tetrahedron Lett.* **2009**, *50*, 1215.
- (52) Hu, A.; Yee, G. T.; Lin, W. J. *Am. Chem. Soc.* **2005**, *127*, 12486.
- (53) Li, J.; Zhang, Y.; Han, D.; Gao, Q.; Li, C. J. *Mol. Catal. A: Chem.* **2009**, *298*, 31.
- (54) Jacinto, M. J.; Kiyohara, P. K.; Masunaga, S. H.; Jardim, R. F.; Rossi, L. M. *Appl. Catal., A* **2008**, *338*, 52.
- (55) Ishida, T.; Haruta, M. *Angew. Chem., Int. Ed.* **2007**, *46*, 7154.
- (56) Hutchings, G. J. *Gold Bull.* **2009**, *42*, 260.
- (57) Chang, Y.; Chen, D. *J. Hazard. Mater.* **2009**, *165*, 664.
- (58) Kotani, M.; Koike, T.; Yamaguchi, K.; Mizuno, N. *Green Chem.* **2006**, *8*, 735.
- (59) Polshettiwar, V.; Varma, R. S. *Org. Biomol. Chem.* **2009**, *7*, 37.
- (60) Jacinto, M. J.; Santos, H. C. F.; Jardim, R. F.; Landers, R.; Rossi, L. M. *Appl. Catal., A* **2009**, *360*, 177.
- (61) Oliveira, R. L.; Kiyohara, P. K.; Rossi, L. M. *Green Chem.* **2010**, *12*, 144.
- (62) Arai, T.; Sato, T.; Kanoh, H.; Kaneko, K.; Oguma, K.; Yanagisawa, A. *Chem.-Eur. J.* **2008**, *14*, 882.
- (63) Ko, S.; Jang, J. *Angew. Chem., Int. Ed.* **2006**, *45*, 7564.
- (64) Baruwati, B.; Guin, D.; Manorama, S. V. *Org. Lett.* **2007**, *9*, 5377.
- (65) Mori, K.; Kondo, Y.; Morimoto, S.; Yamashita, H. *Chem. Lett.* **2007**, *36*, 1068.
- (66) Tucker-Schwartz, A.-K.; Garrell, R.-L. *Chem.-Eur. J.* **2010**, *16*, 12718.
- (67) Minisci, F.; Recupero, F.; Rodino, M.; Sala, M.; Schneider, A. *Org. Process Res. Dev.* **2003**, *7*, 794.
- (68) Anelli, P.-L.; Biffi, C.; Montanari, F.; Quici, S. *J. Org. Chem.* **1987**, *52*, 2559.
- (69) Nicolaou, K. C.; Sorensen, E. J. *Classics in Total Synthesis*; Wiley-VCH: Weinheim, 1996.
- (70) Yin, L.; Liebscher, J. *Chem. Rev.* **2007**, *107*, 133.
- (71) Polshettiwar, V.; Len, C.; Fihri, A. *Coord. Chem. Rev.* **2009**, *253*, 2599.
- (72) Miyaura, N.; Yanagi, T.; Suzuki, A. *Synth. Commun.* **1981**, *11*, 513.
- (73) Miyaura, N.; Suzuki, A. *Chem. Rev.* **1995**, *95*, 2457.
- (74) Miyaura, N. *Cross-Coupling Reactions: A Practical Guide*; Springer: New York, 2002.
- (75) Pham, N. T. S.; Van Der Sluys, M.; Jones, C. W. *Adv. Synth. Catal.* **2006**, *348*, 609.
- (76) Baudoin, O.; Cesario, M.; Guenard, D.; Gueritte, F. *J. Org. Chem.* **2002**, *67*, 1199.
- (77) Kotha, S.; Lahiri, K.; Kashinath, D. *Tetrahedron* **2002**, *58*, 9633.
- (78) Albaneze-Walker, J.; Murry, J. A.; Soheili, A.; Ceglia, S.; Springfield, S. A.; Bazalal, C.; Dormer, D. P. G.; Hughes, L. *Tetrahedron* **2005**, *61*, 6330.
- (79) Kertesz, M.; Choi, C. H.; Yang, S. *Chem. Rev.* **2005**, *105*, 3448.
- (80) Zheng, Y.; Stevens, P. D.; Gao, Y. *J. Org. Chem.* **2006**, *71*, 537.
- (81) Stevens, P. D.; Li, G.; Fan, J.; Yen, M.; Gao, Y. *Chem. Commun.* **2005**, 4435.
- (82) Stevens, P. D.; Fan, J.; Gardimalla, H. M. R.; Yen, M.; Gao, Y. *Org. Lett.* **2005**, *7*, 2085.
- (83) Jin, M.-J.; Lee, D.-H. *Angew. Chem., Int. Ed.* **2010**, *49*, 1119.
- (84) Lv, G.; Mai, W.; Jin, R.; Gao, L. *Synlett* **2008**, 1418.
- (85) Yinghuai, Z.; Peng, S. C.; Emi, A.; Zhenshun, S.; Lisa, M.; Kemp, R. A. *Adv. Synth. Catal.* **2007**, *349*, 1917.
- (86) Shylesh, S.; Wang, L.; Thiel, W. R. *Adv. Synth. Catal.* **2010**, *352*, 425.
- (87) Jung, J.-Y.; Kim, J.-B.; Taher, A.; Jin, M.-J. *Bull. Korean Chem. Soc.* **2009**, *30*, 3082.
- (88) Rosario-Amorin, D.; Wang, X.; Gaboyard, M.; Clérac, R.; Nlate, S.; Heuzé, K. *Chem.-Eur. J.* **2009**, *15*, 12636.
- (89) Wang, Z.; Xiao, P.; Shen, B.; He, N. *Colloids Surf., A* **2006**, *276*, 116.
- (90) Zhou, S.; Johnson, M.; Veinot, J. G. C. *Chem. Commun.* **2010**, 46, 2411.
- (91) Costa, N.-J.-S.; Kiyohara, P.-K.; Monteiro, A.-L.; Coppel, Y.; Philippot, K.; Rossi, L.-M. *J. Catal.* **2010**, *276*, 382.
- (92) Laska, U.; Frost, C. G.; Price, G. J.; Plucinski, P. K. *J. Catal.* **2009**, *268*, 318.
- (93) Beletskaya, I. P.; Cheprakov, A. V. *Chem. Rev.* **2000**, *100*, 3009.
- (94) Trzeciak, A. M.; Ziolkowski, J. J. *Coord. Chem. Rev.* **2005**, *249*, 2308.
- (95) Polshettiwar, V.; Molnar, A. *Tetrahedron* **2007**, *63*, 6949.
- (96) Ko, S.; Jang, J. *Angew. Chem., Int. Ed.* **2006**, *45*, 7564.
- (97) Yuan, D.; Zhang, Q.; Dou, J. *Catal. Commun.* **2010**, *11*, 606.
- (98) Tsuji, J. *Palladium Reagents and Catalysts*; John Wiley & Sons: Chichester, 1995.
- (99) Diederich, F.; Stang, P. J. *Metal-Catalyzed Cross-Coupling Reactions*; VCH: Weinheim, 1998.
- (100) Yoneda, N.; Matsuoka, S.; Miyaura, N.; Fukuhara, T.; Suzuki, A. *Bull. Chem. Soc. Jpn.* **1990**, *63*, 2124.
- (101) Liu, J.; Peng, X.; Sun, W.; Zhao, Y.; Xia, C. *Org. Lett.* **2008**, *10*, 3933.
- (102) Kim, J.; Lee, J.-E.; Lee, J.; Jang, Y.; Kim, S.-W.; An, K.; Yu, J.-H.; Hyeon, T. *Angew. Chem., Int. Ed.* **2006**, *45*, 4789.
- (103) Espinet, P.; Echavarren, A. M. *Angew. Chem., Int. Ed.* **2004**, *43*, 4704.
- (104) Stille, J. K. *Angew. Chem., Int. Ed. Engl.* **1986**, *25*, 508.
- (105) Milstein, D.; Stille, J. K. *J. Am. Chem. Soc.* **1978**, *100*, 3636.
- (106) Nicolaou, K. C.; Chakraborty, T. K.; Piscopio, A. D.; Minowa, N.; Bertinato, P. *J. Am. Chem. Soc.* **1993**, *115*, 4419.
- (107) Shair, M. D.; Yoon, T. Y.; Mosny, K. K.; Chou, T. C.; Danishefsky, S. J. *J. Am. Chem. Soc.* **1996**, *118*, 9509.
- (108) Williams, D. R.; Meyer, K. G. *J. Am. Chem. Soc.* **2001**, *123*, 765.
- (109) MacMillan, D. W. C. *Nature* **2008**, *455*, 304.
- (110) Gruttadauria, M.; Giacalone, F.; Noto, R. *Chem. Soc. Rev.* **2008**, *37*, 1666.
- (111) Karimi, B.; Biglari, A.; Clark, J. H.; Budarin, V. *Angew. Chem., Int. Ed.* **2007**, *46*, 7210.
- (112) Dalko, P. I. *Enantioselective Organocatalysis: Reactions and Experimental Procedures*; Wiley-VCH: Weinheim, 2007.
- (113) Beeson, T. D.; Mastracchio, A.; Hong, J. B.; Ashton, K.; MacMillan, D. W. C. *Science* **2007**, *316*, 582.
- (114) Bruckmann, A.; Krebs, A.; Bolm, C. *Green Chem.* **2008**, *10*, 1131.
- (115) Franzen, J.; Marigo, M.; Fielenbach, D.; Wabnitz, T. C.; Kjærsgaard, A.; Jørgensen, K. A. *J. Am. Chem. Soc.* **2005**, *127*, 18296.
- (116) Polshettiwar, V.; Baruwati, B.; Varma, R. S. *Chem. Commun.* **2009**, 1837.
- (117) Polshettiwar, V.; Varma, R. S. *Tetrahedron* **2010**, *66*, 1091.

- (118) Luque, R.; Babita, B.; Varma, R. S. *Green Chem.* **2010**, *12*, 1540.
- (119) Schätz, A.; Grass, R. N.; Stark, W. J.; Reiser, O. *Chem.-Eur. J.* **2008**, *14*, 8262.
- (120) Gleeson, O.; Tekoriute, R.; Gunko, Y. K.; Connon, S. J. *Chem.-Eur. J.* **2009**, *15*, S669.
- (121) Kuntz, E. *CHEMTECH* **1987**, *17*, 570.
- (122) Ungváry, F. *J. Organomet. Chem.* **1994**, *477*, 363.
- (123) Yan, Y.; Zhang, X.; Zhang, X. *Adv. Synth. Catal.* **2007**, *349*, 1582.
- (124) Yoon, T. J.; Lee, W.; Oh, Y. S.; Lee, J. K. *New J. Chem.* **2003**, *27*, 227.
- (125) Yoon, T. J.; Kim, J. I.; Lee, J. K. *Inorg. Chim. Acta* **2003**, *345*, 228.
- (126) Jin, J.; Iyoda, T.; Cao, C.; Song, Y.; Jiang, L.; Li, T. J.; Zhu, D. B. *Angew. Chem., Int. Ed.* **2001**, *40*, 2135.
- (127) Astruc, D.; Boisselier, E.; Ornelas, C. *Chem. Rev.* **2010**, *110*, 1857.
- (128) Abu-Reziq, R.; Alper, H.; Wang, D.; Post, M. L. *J. Am. Chem. Soc.* **2006**, *128*, S279.
- (129) Banks, R. L.; Bailey, G. C. *Ind. Eng. Chem. Prod. Res. Dev.* **1964**, *3*, 170.
- (130) Buchmeiser, M. R. *Chem. Rev.* **2009**, *109*, 303.
- (131) Ivin, K. J.; Mol, I. C. *Olefin Metathesis and Metathesis Polymerization*; Academic Press: New York, 1996.
- (132) Vougioukalakis, G. C.; Grubbs, R. H. *Chem. Rev.* **2010**, *110*, 1746.
- (133) Grubbs, R. H. *Handbook of Metathesis*; Wiley-VCH: Germany, 2003.
- (134) Kingsbury, J. S.; Harrity, J. P. A.; Bonitatebus, P. J., Jr.; Hoveyda, A. H. *J. Am. Chem. Soc.* **1999**, *121*, 791.
- (135) Schrock, R. R.; Hoveyda, A. H. *Angew. Chem., Int. Ed.* **2003**, *42*, 4592.
- (136) Schrock, R. R. *J. Mol. Catal. A: Chem.* **2004**, *213*, 21.
- (137) Trnka, T. M.; Grubbs, R. H. *Acc. Chem. Res.* **2001**, *34*, 18.
- (138) Kingsbury, J. S.; Harrity, J. P. A.; Bonitatebus, P. J.; Hoveyda, J. H. *J. Am. Chem. Soc.* **1999**, *121*, 791.
- (139) Yao, Q. W. *Angew. Chem., Int. Ed.* **2000**, *39*, 3896.
- (140) Michalek, F.; Mdge, D.; Rühle, J.; Bannwarth, W. *J. Organomet. Chem.* **2006**, *691*, S172.
- (141) Yinghuai, Z.; Kuijin, L.; Huimin, N.; Chuanzhao, L.; Stubbs, L. P.; Siong, C. F.; Muihua, T.; Peng, S. C. *Adv. Synth. Catal.* **2009**, *351*, 2650.
- (142) Che, C.; Li, W.; Lin, S.; Chen, J.; Zhang, J.; Wu, J.; Zheng, Q.; Zhang, G.; Yang, Z.; Jiang, B. *Chem. Commun.* **2009**, S990.
- (143) Shylesh, S.; Schweizer, J.; Demeshko, S.; Schünemann, V.; Ernst, S.; Thiela, W. R. *Adv. Synth. Catal.* **2009**, *351*, 1789.
- (144) Zhang, D.-H.; Li, G.-D.; Lia, J.-X.; Chen, J.-S. *Chem. Commun.* **2008**, 3414.
- (145) Mori, K.; Sugihara, K.; Kondo, Y.; Takeuchi, T.; Morimoto, S.; Yamashita, H. *J. Phys. Chem. C* **2008**, *112*, 16478.
- (146) Shokouhimehr, M.; Piao, Y.; Kim, J.; Jang, Y.; Hyeon, T. *Angew. Chem., Int. Ed.* **2007**, *46*, 7039.
- (147) Kawamura, M.; Sato, K. *Chem. Commun.* **2006**, 4718.
- (148) Kawamura, M.; Sato, K. *Chem. Commun.* **2007**, 3404.
- (149) Zheng, X.; Luo, S.; Zhang, L.; Cheng, J. *Green Chem.* **2009**, *11*, 455.
- (150) Polshettiwar, V.; Varma, R. S. *Chem.-Eur. J.* **2009**, *15*, 1582.
- (151) Fu, B.; Zhao, P.; Yu, H.; Huang, J.; Liu, J.; Ji, L. *Catal. Lett.* **2009**, *127*, 411.
- (152) Fu, B.; Zhao, P.; Yu, H.; Huang, J.; Liu, J.; Ji, L. *J. Mol. Catal. A: Chem.* **2009**, *298*, 74.
- (153) Luo, S.; Zheng, X.; Cheng, J. *Chem. Commun.* **2008**, 5719.
- (154) Claesson, E. M.; Mehendale, N. C.; Gebbink, R. J. M. K.; Koten, G. V.; Philipse, A. P. *J. Magn. Magn. Mater.* **2007**, *311*, 41.
- (155) Niu, F.; Zhang, L.; Luo, S.-Z.; Song, W.-G. *Chem. Commun.* **2010**, *46*, 1109.
- (156) Phan, N. T. S.; Jones, C. W. *J. Mol. Catal. A: Chem.* **2006**, *253*, 123.
- (157) Schätz, A.; Hager, M.; Reiser, O. *Adv. Funct. Mater.* **2009**, *19*, 2109.
- (158) Martinez, R.; Ramon, D. J.; Yus, M. *Org. Biomol. Chem.* **2009**, *7*, 2176.
- (159) Hirakawa, T.; Tanaka, S.; Usuki, N.; Kanzaki, H.; Kishimoto, M.; Kitamura, M. *Eur. J. Org. Chem.* **2009**, *6*, 789.
- (160) Yan, J.-M.; Zhang, X.-B.; Akita, T.; Haruta, M.; Xu, Q. *J. Am. Chem. Soc.* **2010**, *132*, S326.
- (161) Gonzalez-Arellano, C.; Yoshida, K.; Luque, R.; Gai, P.-L. *Green Chem.* **2010**, *12*, 1281.
- (162) Mahmoudi, M.; Simchi, A.; Imani, M. *J. Phys. Chem. C* **2009**, *113*, 9573.
- (163) Alexiou, C.; Jurgons, R.; Seliger, C.; Iro, H. *J. Nanosci. Nanotechnol.* **2006**, *6*, 2762.
- (164) Watson, S.; Beydoun, D.; Amal, R. *J. Photochem. Photobiol., A* **2002**, *148*, 303.
- (165) Kostedt, W. L.; Drwiega, J.; Mazzyck, D. W.; Lee, S. W.; Sigmund, W.; Wu, C. Y.; Chadik, P. *Environ. Sci. Technol.* **2005**, *39*, 8052.
- (166) Beydoun, D.; Amal, R.; Lowb, G.; McEvoy, S. *J. Mol. Catal. A: Chem.* **2002**, *180*, 193.
- (167) Xu, S.; Feng, D.; Shangguan, W. *J. Phys. Chem. C* **2009**, *113*, 2463.
- (168) Belessi, V.; Lambropoulou, D.; Konstantinou, I.; Zboril, R.; Tucek, J.; Jancik, D.; Albanis, T.; Petridis, D. *Appl. Catal., B* **2009**, *87*, 181.
- (169) Beydoun, D.; Amal, R.; Low, G. K. C.; McEvoy, S. *J. Phys. Chem. B* **2000**, *104*, 4387.
- (170) Gao, Y.; Chen, B.; Li, H.; Ma, Y. *Mater. Chem. Phys.* **2003**, *80*, 348.
- (171) Asahi, R.; Morikawa, T.; Ohwaki, T. *Science* **2001**, *293*, 269.
- (172) Ao, Y.; Xu, J.; Shen, X.; Fu, D.; Yuan, C. *Sep. Purif. Technol.* **2008**, *61*, 436.
- (173) Ao, Y.; Xu, J.; Zhang, S.; Fu, D. *J. Phys. Chem. Solids* **2009**, *70*, 1042.
- (174) Ye, M.; Zhang, Q.; Hu, Y.; Ge, J.; Lu, Z.; He, L.; Chen, Z.; Yadong, Y. *Chem.-Eur. J.* **2010**, *16*, 6243.
- (175) Pitcher, W. H., Jr. *Catal. Rev.* **1975**, *12*, 37.
- (176) Blaser, H. U.; Pugin, B.; Studer, M. *Chiral Catalyst Immobilization and Recycling*; Wiley-VCH: Weinheim, 2000.
- (177) Wu, C. W.; Lee, J. G.; Lee, W. C. *Biotechnol. Appl. Biochem.* **1988**, *27*, 225.
- (178) Bommarius, A. S.; Riebel, B. R. *Biocatalysis*; Wiley-VCH: Weinheim, 2004.
- (179) Braehler, M.; Georgieva, R.; Buske, N.; Mueller, A.; Mueller, S.; Pinkernelle, J.; Teichgraber, U.; Voigt, A.; Baeumler, H. *Nano Lett.* **2006**, *6*, 2505.
- (180) Gao, L.; Zhuang, J.; Nie, L.; Zhang, J.; Zhang, Y.; Gu, N.; Wang, T.; Feng, J.; Yang, D.; Perret, S.; Yan, X. *Nat. Nanotechnol.* **2007**, *2*, 577.
- (181) Reetz, M. T.; Zonta, A.; Vijayakrishnan, V.; Schimossek, K. *J. Mol. Catal. A: Chem.* **1998**, *134*, 251.
- (182) Reetz, M. T.; Zonta, A.; Simpelkamp, J. *Angew. Chem., Int. Ed.* **1995**, *34*, 301.
- (183) Reetz, M. T.; Zonta, A.; Vijayakrishnan, V.; Schimossek, K. *J. Mol. Catal. A: Chem.* **1998**, *134*, 251.
- (184) Jaeger, K. E.; Liebeton, K.; Zonta, A.; Schimossek, K.; Reetz, M. T. *Appl. Microbiol. Biotechnol.* **1996**, *46*, 99.
- (185) Sen, T.; Bruce, I.-J.; Mercer, T. *Chem. Commun.* **2010**, *46*, 6807.
- (186) Gao, L.; Zhuang, J.; Nie, L.; Zhang, J.; Zhang, Y.; Gu, N.; Wang, T.; Feng, J.; Yang, D.; Perret, S.; Yan, X. *Nat. Nanotechnol.* **2007**, *2*, 577.
- (187) Yang, H. H.; Zhang, S. Q.; Chen, X. L.; Zhuang, Z. X.; Xu, J. G.; Wang, X. R. *Anal. Chem.* **2004**, *76*, 1316.
- (188) Yang, Z.; Si, S.; Zhang, C. *Biochem. Biophys. Res. Commun.* **2008**, *367*, 169.
- (189) Palmer, T. *Understanding Enzymes*; Prentice Hall: New York, 1995.
- (190) Lee, J.; Lee, D.; Oh, E.; Kim, J.; Kim, Y. P.; Jin, S.; Kim, H. S.; Hwang, Y.; Kwak, J. H.; Park, J. G.; Shin, C. H.; Kim, J.; Hyeon, T. *Angew. Chem., Int. Ed.* **2005**, *44*, 7427.

- (191) Wang, W.; Xu, Y.; Wang, D. I. C.; Li, Z. *J. Am. Chem. Soc.* **2009**, *131*, 12892.
- (192) Van de Velde, F.; Lourenço, N.; Bakker, M.; Van Rantwijk, F.; Sheldon, R. *Biotechnol. Bioeng.* **2000**, *69*, 286.
- (193) Bayramoglu, G.; Kiralp, S.; Yilmaz, M.; Toppare, L.; Arica, M. *Biochem. Eng. J.* **2008**, *38*, 180.
- (194) Trevisan, V.; Signoretto, M.; Colonna, S.; Pironti, V.; Strukul, G. *Angew. Chem., Int. Ed.* **2004**, *43*, 4097.
- (195) Wang, X.; Dou, P.; Zhao, P.; Zhao, C.; Ding, Y.; Xu, P. *ChemSusChem* **2009**, *2*, 947.
- (196) Nouredini, H.; Gao, X.; Philkana, R. S. *Bioresour. Technol.* **2005**, *96*, 769.
- (197) Chen, Y. Z.; Yang, C. T.; Ching, C. B.; Xu, R. *Langmuir* **2008**, *24*, 8877.
- (198) Lee, K. S.; Woo, M. H.; Kim, H. S.; Lee, E. Y.; Lee, I. S. *Chem. Commun.* **2009**, 3780.
- (199) Zhu, H.; Pan, J.; Hu, B.; Yu, H. L.; Xu, J. H. *J. Mol. Catal. B: Enzym.* **2009**, *61*, 174.
- (200) Guo, L.; Cui, X.; Li, Y.; He, Q.; Zhang, L.; Bu, W.; Shi, J. *Chem. Asian J.* **2009**, *4*, 1480.
- (201) Sen, T.; Bruce, I. J. *Microporous Mesoporous Mater.* **2009**, *120*, 246.
- (202) Shin, S.; Jang, J. *Chem. Commun.* **2007**, 4230.
- (203) Brar, S. K.; Verma, M.; Tyagi, R. D.; Surampalli, R. Y. *Waste Manage.* **2010**, *30*, 504.
- (204) Li, M.; Huang, C. P. *Water Environ. Res.* **2009**, *81*, 1817.
- (205) Gijs, M. A. M.; Lacharme, F.; Lehmann, U. *Chem. Rev.* **2010**, *110*, 1518.
- (206) de Smit, E.; Swart, I.; Creemer, J. F.; Hoveling, G. H.; Gilles, M. K.; Tylliszczak, T.; Kooyman, P. J.; Zandbergen, H. W.; Morin, C.; Weckhuysen, B. M.; de Groot, F. M. F. *Nature* **2008**, *456*, 222.
- (207) de Smit, E.; Swart, I.; Creemer, J. F.; Karunakaran, C.; Bertwistle, D.; Zandbergen, H. W.; de Groot, F. M. F.; Weckhuysen, B. M. *Angew. Chem., Int. Ed.* **2009**, *48*, 3632–3636.
- (208) Kweskin, S. J.; Rioux, R. M.; Habas, S. E.; Komvopoulos, K.; Yang, P.; Somorjai, G. A. *J. Phys. Chem. B* **2006**, *110*, 15920.
- (209) Sautet, P.; Delbecq, F. *Chem. Rev.* **2010**, *110*, 1788.